รายงานวิจัยฉบับสมบูรณ์

โครงการ

การรู้จำสัญญาณคลื่นไฟฟ้ากล้ามเนื้อจากการเคลื่อนที่ของนิ้ว

Recognition of surface electromyography signals from finger movements

โดย รองศาสตราจารย์ ดร. พรชัย พฤกษ์ภัทรานนต์

เดือน ปี ที่เสร็จโครงการ มิถุนายน 2561

สัญญาเลขที่ RSA5980049

รายงานวิจัยฉบับสมบูรณ์

โครงการ

การรู้จำสัญญาณคลื่นไฟฟ้ากล้ามเนื้อจากการเคลื่อนที่ของนิ้ว

Recognition of surface electromyography signals from finger movements

โดย รองศาสตราจารย์ ดร. พรชัย พฤกษ์ภัทรานนต์

ภาควิชาวิศวกรรมไฟฟ้า คณะวิศวกรรมศาสตร์ มหาวิทยาลัยสงขลานครินทร์

สนับสนุนโดยสำนักงานกองทุนสนับสนุนการวิจัยและมหาวิทยาลัยสงขลานครินทร์

กิตติกรรมประกาศ

ทางคณะผู้วิจัยขอขอบคุณสำนักงานกองทุนสนับสนุนการวิจัย (สกว.) คณะวิศวกรรมศาสตร์ มหาวิทยาลัยสงขลานครินทร์ และมหาวิทยาลัยสงขลานครินทร์เป็นอย่างสูง ที่ร่วมกันให้ทุนสนับสนุนการวิจัยครั้งนี้

พรชัย พฤกษ์ภัทรานนต์

บทคัดย่อ

รหัสโครงการ: RSA5980049

ชื่อโครงการ: การรู้จำสัญญาณคลื่นไฟฟ้ากล้ามเนื้อจากการเคลื่อนที่ของนิ้ว

ชื่อนักวิจัย: รองศาสตราจารย์ ดร. พรชัย พฤกษ์ภัทรานนต์

E-mail Address: pornchai.p@psu.ac.th

ระยะเวลาโครงการ: 2 ปี

บทคัดย่อ :

สัญญาณคลื่นไฟฟ้ากล้ามเนื้อถูกนำมาใช้ในการควบคุมแขนเทียมหรืออุปกรณ์ช่วยเหลือแบบสวมใส่ การนำมาใช้ดังกล่าวจะต้องผ่านการประมวลผลสำคัญ คือ การสกัดคุณลักษณะและการจำแนก โครงการวิจัยนี้ศึกษาการสกัดคุณลักษณะ 6 เทคนิคและการจำแนก 7 เทคนิค เพื่อประยุกต์ใช้ในการรู้จำการเคลื่อนที่ของนิ้วและการจำแนกแรง การสกัดคุณลักษณะ 6 เทคนิค ได้แก่ (1) principal component analysis (PCA) (2) linear discriminant analysis (LDA) (3) uncorrelated linear discriminant analysis (ULDA) (4) orthogonal fuzzy neighbourhood discriminant analysis (OFNDA) (5) spectral regression linear discriminant analysis (SRDA) และ (6) spectral regression extreme learning machine (SRELM) ส่วนการจำแนก 7 เทคนิคที่ทำการศึกษา คือ (1) support vector machine (SVM) (2) linear classifier (LC) (3) Naive Bayes (NB) (4) k-nearest neighbours (KNN) (5) radial basis function extreme learning machine (RBF-ELM) (6) adaptive wavelet extreme learning machine (AW-ELM) และ (7) neural network (NN) ผลการศึกษาการรู้จำการเคลื่อนที่ของนิ้ว 14 รูปแบบ ด้วยสัญญาณคลื่นไฟฟ้ากล้ามเนื้อ 6 ช่อง พบว่าคู่ของ SRELM และ NN ให้ค่าความถูกต้องสูงที่สุดถึง 99% ซึ่งสูงกว่าคู่ของเทคนิคอื่นอย่างมีนัยสำคัญ ส่วนการศึกษาการจำแนกแรงด้วยสัญญาณคลื่นไฟฟ้ากล้ามเนื้อ 12 ช่องพบว่าคู่ของ SRELM และ NN ก็ยังคงให้ค่าความถูกต้องสูงที่สุดถึง 98%

คำหลัก : สัญญาณคลื่นไฟฟ้ากล้ามเนื้อ (อีเอ็มจี) การสกัดคุณลักษณะ การจำแนก การเคลื่อนที่ของนิ้ว ระดับแรง

Abstract

Project Code: RSA5980049

Project Title: Recognition of surface electromyography signals from finger movements

Investigator: Associate Professor Dr. Pornchai Phukpattaranont

E-mail Address: pornchai.p@psu.ac.th

Project Period: 2 years

Abstract:

Electromyography (EMG) in bio-driven system is used as a control signal, for driving a hand prosthesis or other wearable assistive devices. Processing to get informative drive signals involves 2 main modules: feature extraction and classification. We explored 6 feature extraction techniques and 7 classifiers applied for (1) finger movement recognition and (2) force classification in this research project. While the 6 feature extraction techniques consist of (1) principal component analysis (PCA), (2) linear discriminant analysis (LDA), (3) uncorrelated linear discriminant analysis (ULDA), (4) orthogonal fuzzy neighbourhood discriminant analysis (OFNDA), (5) spectral regression linear discriminant analysis (SRDA), and (6) spectral regression extreme learning machine (SRELM), the 7 classifiers are composed of (1) support vector machine (SVM), (2) linear classifier (LC), (3) Naive Bayes (NB), (4) k-nearest neighbours (KNN), (5) radial basis function extreme learning machine (RBF-ELM), (6) adaptive wavelet extreme learning machine (AW-ELM), and (7) neural network (NN). For finger movement recognition, we classified a 6-channel EMG signal from 14 finger movements. Results showed that the combination of SRELM and NN yielded the best classification accuracy of 99%, which was significantly higher than those from the other combinations tested. For force classification, we classified a 12-channel EMG signal from 5 force levels. Results showed that the combination of SRELM and NN also yielded the best classification accuracy of 98%,

Keywords: Electromyography (EMG), feature extraction, classification, Finger movement, Force level

Contents

LIST OF FIGURES

LIST OF FIGURES (CONT.)

LIST OF FIGURES (CONT.)

LIST OF TABLES

LIST OF TABLES (CONT.)

CHAPTER 1 Introduction

1.1 Research problem and its significance

The loss of finger functions is a major disability that limits everyday capabilities and interactions [1]. Hence, myoelectric control based devices using residual muscles, such as the muscles of the shoulder and/or arm, are used for improving the quality of life for people with physical disabilities [2], [3]. Surface electromyography (EMG) observes electrical activities of the muscles by detection with surface electrodes [4]. The EMG signal contains useful information related to muscular activity, neuromuscular disease, and movements intended [5]. It can be used for controlling a prosthetic arm or hand, as well as with other devices such as a wheelchair, a mouse, and a keyboard. This requires that the pattern of an EMG signal is classified into a predefined class that is matched with the command for controlling the device [6], [7].

Myoelectric control of active hand prosthesis can be realized in two different categories, i.e. finger movement based on motion and finger movement based on object [8]. Details of each category are as follows.

- The first category is classification of the movement of each finger based on motion consisting of flexion/extension of five individual fingers and combined 2-5 fingers, finger joint angle, and finger force. Figure 1.1, Figure 1.2, and Figure 1.3 show the examples of experiment setup from finger flexion/extension, finger joint angle, and finger force researches, respectively.
- The second category is classification of the intended grasping (based on object) consisting of various object shapes (e.g. sphere, cylinder, cone, pyramid, cube, and parallelepiped), object sizes, and object positions. Figure 1.4 shows the example of six hand grasp postures from the previous publication [9].

The objective of this study is to classify finger movements using surface EMG signal measured from hand and forearm muscles to classify the combination of two different categories of finger movements presented above, which has not been proposed in literature. In order to improve the performance and response time of the

system, it is necessary to optimize the feature extraction, dimensionality reduction and classification method.

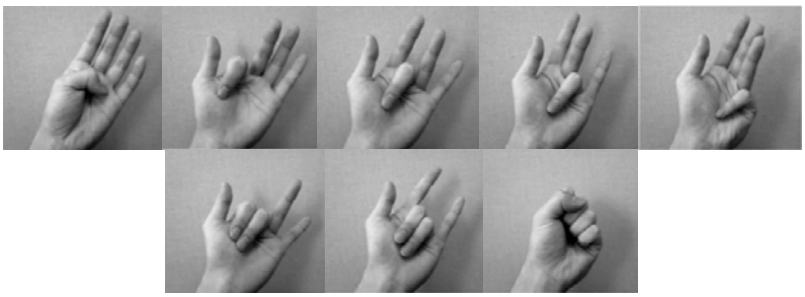

Figure 1.1 Individual and combined fingers flexion.

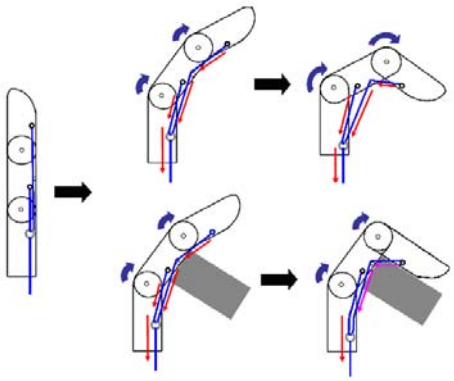

Figure 1.2 Finger joint angle for grasping object [10].

Figure 1.3 Finger pushing on piano keyboard [11].

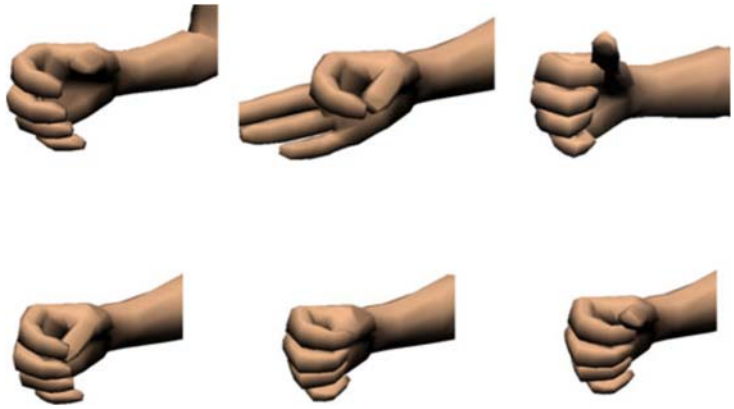

Figure 1.4 Six hand grasp postures: from top left (clockwise) are cylindrical, tip/fine pinch, hook, palmar, thumb enclosed, and lateral grasps [9].

1.2 Literature review

Figure 1.5 shows the procedure of myoelectric control system. Myoelectric control system can be divided into three main modules including EMG signal acquisition and preprocessing, EMG pattern recognition, and EMG control system [2, 4]. Details of each module are as follows.

EMG signal acquisition and preprocessing can be divided into three sub-modules including amplifying, filtering, and sampling. Firstly, surface EMG signals are detected by surface electrodes placed on the skin. To provide the suitable EMG amplitude for processing, the EMG signal must be amplified by EMG amplifier circuit. Secondly, the filter is applied for removing noise contaminated with the raw EMG signals. Finally, the continuous EMG signals are sampled using an analog to digital convertor. As a result, the EMG signals are already used for processing in the next module.

EMG pattern recognition can be divided into three sub-modules consisting of feature extraction, dimensionality reduction and classification method. Firstly, the feature extraction methods are used to extract the useful information and discard the un-wanted part of EMG signal. The raw EMG signals can be transformed into feature sets. Secondly, the high dimension feature vectors should be reduced using dimensionality reduction techniques before sending them to the next sub-module. Finally, the patterns of EMG signals for different motions are classified.

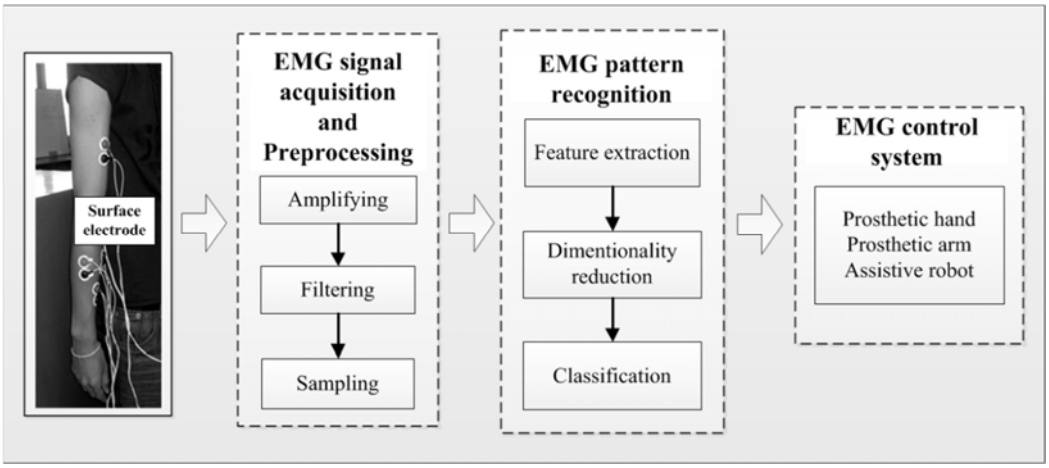

Figure 1.5 The procedure of myoelectric control system.

In EMG control system module, the control commands produced from the classification stage are sent to control the devices, such as prosthetic hand, prosthetic arm, electric wheelchair, electric bed, and assistive devices while also utilized for other applications including computer games.

The rest of this section presents the details of the procedure of myoelectric control system based on a literature review of classification of finger movements using surface EMG signals to indicate the gaps, which will cause further research. The papers related to the classification of finger movement based on motion can be separated into 3 groups including finger flexion/extension [12, 13, 14-32], finger joint angle [10, 33-34, 35-39], and finger force [11, 40-43]. Most publications are from classification of finger flexion/extension. On the other hand, a few studies have proposed the classification of finger joint angle and finger force.

In this proposal, all modules of the myoelectric control system have been proposed for only the classification of finger movement based on motion, since it requires highly advanced methods more than the classification of finger movement based on object. Thus, only a review of experiment setup module for the classification of finger movement based on object is presented.

1.2.1 EMG signal acquisition and pre-processing

Figure 1.6 shows the examples of EMG signal in time domain and frequency domain. EMG signal represents neuromuscular activity, which can be used to express movement intent for assistive device control and to detect abnormalities for ergonomic assessment or neuromuscular diagnosis. In general, the frequency of EMG signal is between 0 to 500 Hz with the dominant energy being in the 10-150 Hz range and the amplitude of EMG signal is between 50 μV to 100 mV. Since the amplitude of EMG signal is very low, an appropriate amplifier and a noise removal filter in a data acquisition system are needed.

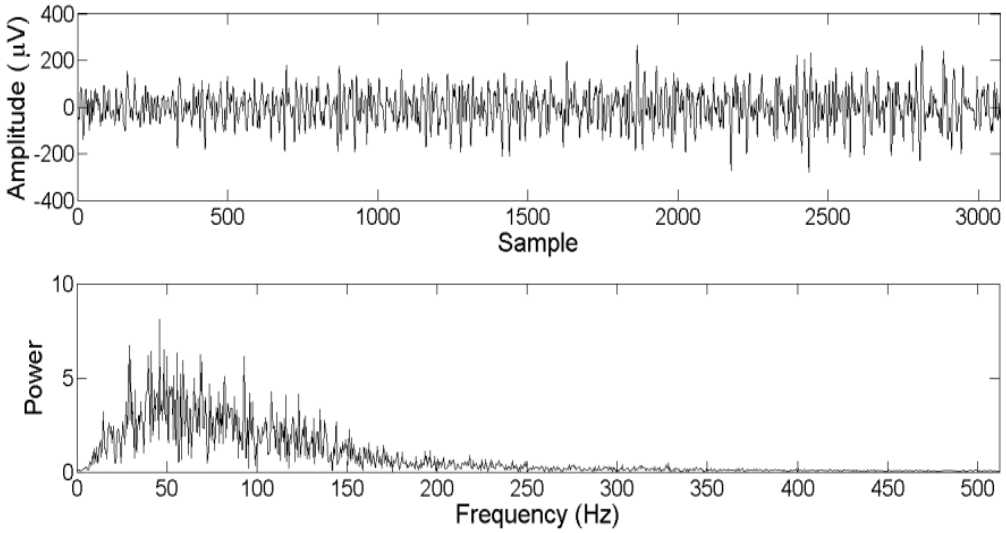

Figure 1.6 Examples of EMG signal in time domain (top) and frequency domain (bottom).

1.2.1.1 Data acquisition and experiment setup

1) Finger movement based on motion

- Surface electrode

Surface electrode is used to measure the voltage fluctuations resulting from ion changes in the muscle fibers. The electrode materials, electrode shape, and inter-electrode distance (IED) should be reported for surface EMG recording. The Ag/AgCl electrode is commonly electrode material used for EMG signal detection, which is robust and has excellent long term stability. Electrode shape is defined as the shape of the conductive area. The circular electrode is widely used for EMG recording. IED is defined as the center to center distance between the conductive areas of electrodes. Since the bipolar electrodes configuration is frequently used for EMG recording, so the IED is important. The IED of 20 mm is recommended by Surface ElectroMyoGraphy for the Non-Invasive Assessment of Muscles project (SENIAM project) [44]. However, for the small muscles, IED should not exceed 1/4 of the muscle fiber length. In addition, the skin should be cleaned with alcohol for stability of electrode placement.

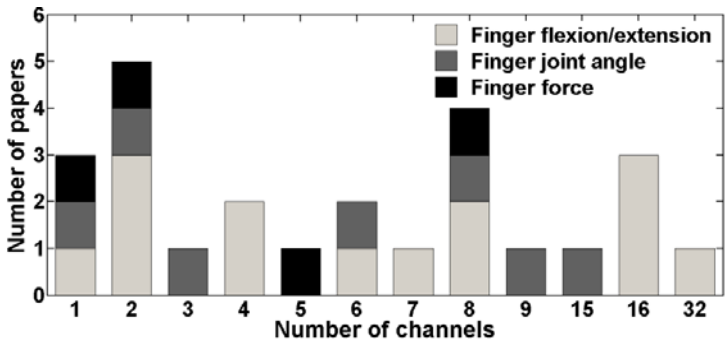

Figure 1.7 Summary of number of channels used in acquiring EMG signals.

- Number of channels and electrode locations

Figure 1.7 shows the summary of number of channels used in acquiring EMG signals. One, two, three, four, five, six, seven, eight, nine, sixteen, and thirty two channels were used in the literature. Most researchers used two channels to reduce computational complexity. In contrast, some studies [20, 45] used thirty two channels to increase the classification accuracy. In order to reduce the number of channel, some researchers investigated the optimal electrode placements that yielded high classification accuracy while maintaining a low computational load and processing time [1, 12].

Figure 1.8 and Figure 1.9 show the summary of electrode locations and forearm muscles positions, respectively. The electrode location is one of issue for the successful identification of motions [47]. From a literature review, there are two ways to place the electrode locations. Firstly, the electrode location can be exactly placed on the muscle. Secondly, the electrode location can be placed on the forearm such as approximately 5 cm from elbow and around the forearm. Flexor digitorum superficialis (FDS) is the most popular muscle used in a literature. In addition, Extensor digitorum (ED), Flexor carpi radialis (FCR), flexor carpi ulnaris (FCU), brachioradialis (BR), palmaris longus (PL), flexor pollicis longus (FPL), and extensor indicispropius (EP) muscles are usually used.

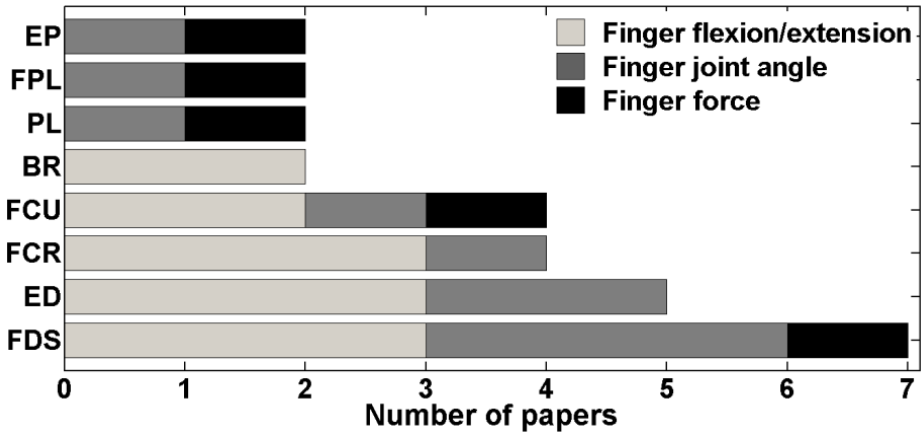

Figure 1.8 Summary of electrode locations.

Note: FDS = Flexor digitorum superficialis, ED = Extensor digitorum, FCR = Flexor carpi radialis, FCU = Flexor carpi ulnaris, BR = Brachioradialis, PL = Palmaris longus, FPL = Flexor pollicis longus, EP = Extensor indicis propius

In order to acquire EMG signals from hand and finger movements, the electrodes need to be placed on all the corresponding muscle groups. However, users typically do not have knowledge about muscle positions. In medical application, the placement of electrodes on the muscle is time consuming and requires some levels of expertise. Additionally, some muscles closely locate together, so it is impossible to acquire the EMG signal from a single muscle [46]. In order to solve these problems, recent studies [13, 33-34, 40] designed and developed the multi-channel sensor rings, which can be placed around forearm and wrist, so it is easy to set up the system.

(a)

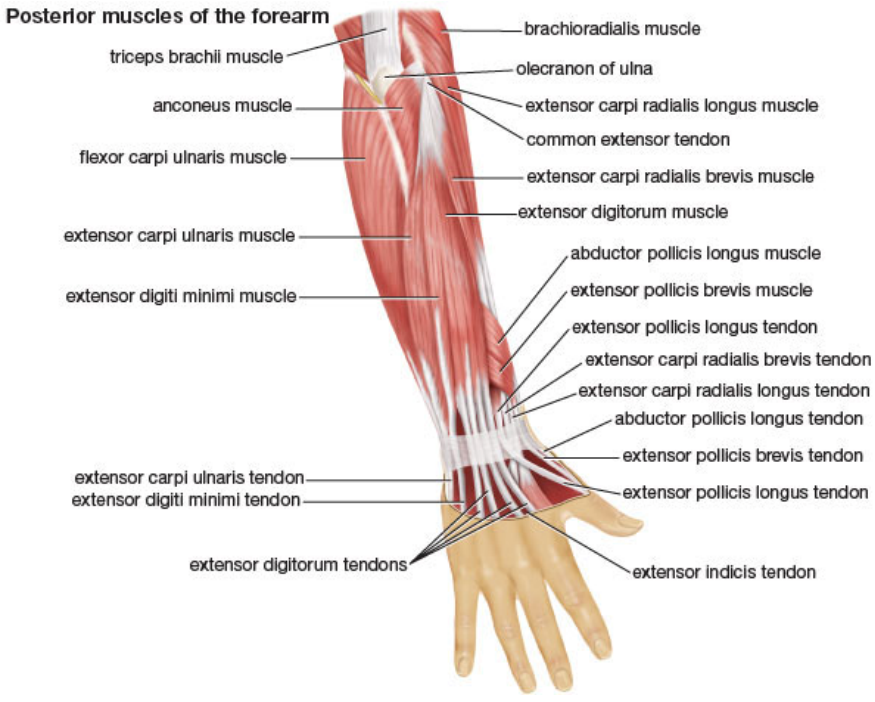

(b)

Figure 1.9 Forearm muscles positions (a) anterior forearm muscles (b) posterior forearm muscles [48]

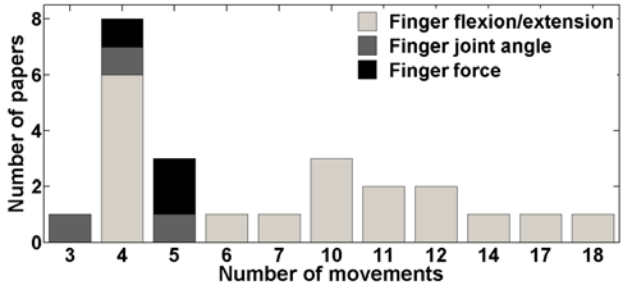

Figure 1.10 Summary of number of movements.

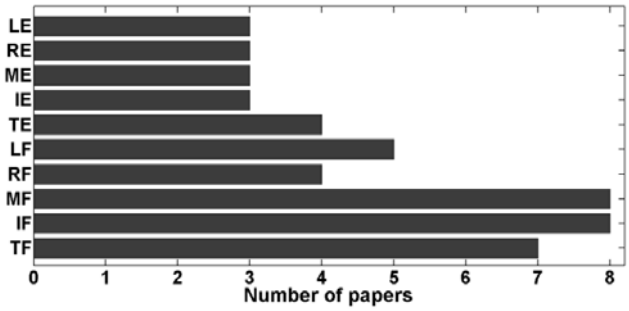

(a)

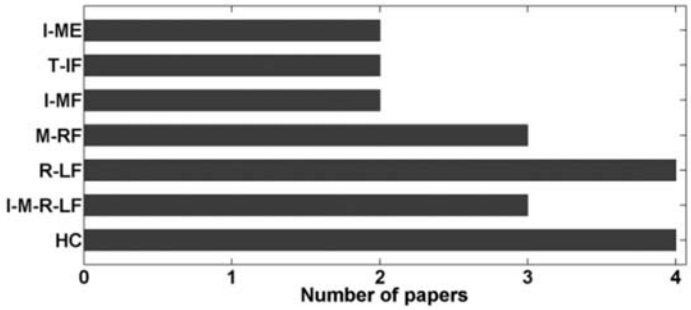

(b)

Figure 1.11 Summary of movement types. (a) individual finger. (b) combined fingers.

Note: Thumb flexion = TF, Index flexion = IF, Middle flexion = MF, Ring flexion = RF, Little flexion = LF, Thumb extension = TE, Index extension = IE, Middle extension = ME, Ring extension = RE, Little extension = LE, Hand close = HC, Index-middle-ring-little flexion = I-M-R-LF, Ring-little flexion = R-LF, middle-ring flexion = M-RF, index-middle flexion = I-MF, thumb-index flexion = T-IF, index-middle extension = I-ME

- Number of movements and movement types

Figure 1.10 and Figure 1.11 show the summary of number of movements and the summary of movement types, respectively. Many researchers have proposed the classification of different finger movement types applied for prosthesis hand control.

The highest number of movement and the most popular number of movement are 18 [37] and 4 motions, respectively. For individual finger motion, index flexion (IF) and middle finger flexion (MF) are most popular motions. For combined fingers motion, ring-little flexion (R-LF) and all fingers flexion or hand close (HC) are most popular motions.

- Number of subjects

Figure 1.12 shows the summary of number of subjects. The most popular number of subject is one subject. Since some factors (i.e. gender, age,) affect the variation of EMG signal between subjects, the system should be evaluated using more subjects. Healthy subjects participated in the experiment for most studies.

2) Finger movement based on object

The finger movement based on object has been extensively studied and gain high interest [8-9, 49-63]. The finger movement based on object can be classified using surface EMG signal or dataglove information. Dataglove resembles a glove worn on the hand, which is equipped with sensors that detect the hand and finger gestures. The sensor information can be used as an input for classification of finger and hand movements. In addition, materials, locations, and number of sensors of the dataglove depend on manufacturers [64]. However, the classification of finger movement using dataglove information is suitable to apply with healthy or maybe disabled users but it is limited to users who do not have a hand. Thus, the system based on EMG signal is suitable for most trans-radial amputees and healthy users [28].

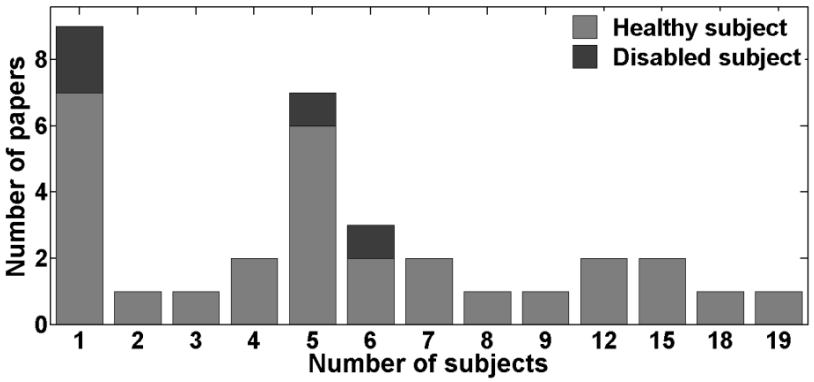

Figure 1.12 Summary of number of subjects.

The objects used in daily life are different in sizes and shapes. The hand and finger gesture depends on shapes, sizes, and other properties of object, especially during the reach-to-grasp movement [65] and applying forces to maintain a stable grasp [66]. Therefore, the finger joint angle, number of fingers and positions finger to contact point on the object surface should be considered. Moreover, it has different gestures for grasping the same object. In general, the objects grasping can be divided into two types consisting of power grasp and precision grasp [67]. A power grasp is performed using the all fingers and the palm of the hand, such as ball and glass grasping, whereas a precision grasp is performed using some fingers or fingertips, such as key and pen grasping. In addition, Schlesinger [68] divided grasping types into six different gestures including cylindrical, spherical, tip, hook, palmar, and lateral, as can be seen in Figure 1.13. The example of each grasping type is given below.

(1) Cylindrical used for grasping a glass and a bottle
(2) Spherical used for grasping a ball
(3) Tip used for grasping a pen and a pencil
(4) Hook used for grasping a suitcase handle
(5) Palmar used for grasping a book
(6) Lateral used for grasping a key

The summary of basic object shapes linked with the objects used in daily life and their corresponding grasping types is shown in Table 1.1. Many studies have proposed the basic object shapes and objects used in daily life. In addition, reach-to-grasp object at one position or various positions were examined.

Figure 1.13 Six different grasping types divided by Schlesinger. [69]

Table 1.1 Summary of simple object shapes linked with the objects used in daily life and their corresponding grasping types

Shape	Object	Grasp type
Cylinder	Paper roll, plastic cup, plastic cylinder, sponge, glue bottle, spray, twine roll, bottle, coke tin, torch, CDs pack, electric adapter plug, dumbbell	cylindrical
	Boxes seal tape	cylindrical/Palmar
	Pen, pencil	tip
	Suitcase handle	hook
Sphere	Plastic sphere, fabric ball, tennis ball, styrofoam sphere, golf ball, soft rubber ball	spherical
Cube	Plastic cube	palmar
Circular	CD	lateral
Parallelepiped	Cigarette pack, card box, paperclips pack, Audio-cassette case, post-it notes package	lateral/palmar
Rectangular	Business card, single CD case, pad-per-hole perfboard	lateral

1.2.1.2 Pre-processing

- Amplifying

The amplitude of EMG signal is between 50 μV to 100 mV. Thus, it is necessary to amplify EMG signal amplitude. In order to reject the 50 Hz/60 Hz power line interference, the difference amplifier is widely used. The suitable amplifier should have the following properties:

- The common mode rejection ratio and input impedance of amplifier should be high.

- The gain of amplifier should be set more than 1000 times.

- Frequency responses of amplifier must match frequency spectrum of the EMG signal.

- Filtering

The power density function of the EMG signals is between 0 to 500 Hz. Thus, the movement artifacts (< 20 Hz) and high frequency noises (> 500 Hz) should be removed. In addition, notch filter 50/60 Hz should be used to eliminate the power line noise.

- Sampling

After amplifying and filtering, the raw EMG signal is sampled to store in the computer for digital processing. The minimal acceptable sampling is at least twice the highest frequency cutoff of the band-pass filter. For example, if a band-pass filter of 10 to 400 Hz was used, the minimal sampling rate should be at least 800 Hz (400 x 2), as dictated by Nyquist theorem [70].

1.2.2 EMG pattern recognition

To achieve high performance in EMG pattern recognition, two important factors are considered including computational time and accuracy. Details of each factor are as follows.

For EMG pattern recognition that must be processed for real-time application, the system must respond immediately after the input is applied. In order to provide a real-time application, the EMG signal should be segmented before calculating feature values. The EMG data segments should be equal or less than 300 ms [2] while the popular segments are between 200 to 250 ms which contain enough information of gestures [71]. Although, EMG data segment smaller than 250 ms could reduce computational time, it leads to the increase in the variation of feature estimation. On the other hand, EMG data segments larger than 250 ms could decrease the variance of feature estimation, while it leads to increase the computational load [72]. In addition, EMG data segmentation can be divided in two types, i.e., disjoint and overlapped segmentations [71].

To achieve the performance in EMG pattern recognition accuracy, three sub-modules consisting of feature extraction, dimensionality reduction, and classification must be optimized [73]. Details of feature extraction, dimensionality reduction, and

classification method used for classification of finger flexion/extension, finger joint angle, and finger force from literature review are given as follows.

1.2.2.1 Feature extraction

Feature extraction is important issue to achieve high classification performance on myoelectric control systems. It is a technique to transform raw EMG data into a reduced representation set of features. The suitable feature vector should contain the useful information and remove the unwanted EMG parts and interferences [74]. Features used for EMG signals are categorized by the computational techniques. In other words, they can be determined in time domain, frequency domain, time and frequency domain, high-order statistics (HOS), and multiple features, which are the feature combination of two or more categories. Details of features in each category are as follows.

Feature extraction methods based on time domain are the most popular in EMG classification. Time domain features are extracted based on raw EMG time series, which do not need any transformation, thus they are quick and easy to implement [3, 6]. They indicate the signal energy, duration, and force during activation of the muscle. Three well-known time domain features are root mean square (RMS), mean absolute value (MAV) and integrated EMG (IEMG) [6]. From a literature review, RMS, MAV and IEMG are usually used for classification of finger movement. RMS, MAV, and IEMG are defined as the following equations:

$$RMS = \sqrt{\frac{1}{N}\sum_{n=1}^{N} x_n^2} \tag{1}$$

$$MAV = \frac{1}{N}\sum_{n=1}^{N} |x_n| \tag{2}$$

$$IEMG = \sum_{n=1}^{N} |x_n| \tag{3}$$

where x_n represents the n^{th} EMG amplitude sample and N denotes a length of analysis data window.

Naik et al. [27-31] applied independent component analysis (ICA) before calculating RMS of EMG signal. The accuracy of the classification is approximately 96-99%. Some studies [35-36] showed that there are high linear relationship between RMS values and finger joint angle and finger force. Many researchers [11, 16, 22, 24] used MAV for classification of finger motion and finger force that achieved the classification accuracy more than 80%. Moreover, time domain features, such as zero crossing (ZC), slope sign change SSC), willison amplitude (WAMP), waveform length (WL), mean absolute value slope (MAVS), and histogram have been proposed for hand movement classification [3, 6, 75-76]. However, time domain features are calculated based on the mathematical assumption of signal stationarity. Hence, the variation of feature estimation may be largely obtained when testing on the EMG signals measured during dynamic contraction. Additionally, time domain features are calculated based on EMG amplitude. They should be used for classification in low noise environments [77].

Feature extraction methods based on frequency domain are usually used to investigate the fatigue and the recruitment of motor unit of the muscle [6]. The different contractions level and different motions correspond to different motor unit recruitments, hence frequency domain features are also used to recognize hand and finger gestures [78]. Power spectral density (PSD) becomes a major analysis in frequency domain features. Two characteristic variables of the PSD, mean frequency (MNF) and median frequency (MDF) are commonly used in EMG classification [6]. There are other characteristic variables, such as peak frequency, mean power, and total power [77]. Fast Fourier transform (FFT) has been proposed for classification of four finger motions consisting of thumb flexion, index flexion, middle flexion, and all fingers flexion that yielded the accuracy more than 80% [14-15]. In addition, FFT can be used for classification of finger force [10]. However, features in frequency domain require the computational complexity more than features in time domain. Moreover, Fourier transform loses time domain information of the signal that leads to lose the information of signal change over time. Hence, frequency domain features are suitable for stationary signals [6].

Feature extraction methods based on time and frequency domain, such as, short-time Fourier transform (STFT), wavelet transform (WT), and wavelet packet

transform (WPT) are designed to solve the limitation of time domain and frequency domain features when testing on the non-stationary signals. Time-frequency features require the computational complexity of implementations more than features in time domain and features in frequency domain [79]. However, they cannot be directly used to extract the EMG signal by themselves [73]. Because, time-frequency features vector have high dimension, their dimensions should be reduced before classification. Some studies have proposed time domain features for EMG classification, because the classification accuracy achieved with time domain features is higher than the classification accuracy achieved with time-frequency domain features using a linear discriminant classifier [72, 77]. Moreover, a single time-frequency feature has not been proposed in previous studies.

Feature extraction methods based on HOS, such as kurtosis, skewness, and bispectrum have been proposed in recent studies [5, 12, 43, 72-73, 80]. Nazapour et al. [43] investigated the relationship between finger force and kurtosis and bicoherence of EMG signals acquired during control computer cursors. Kurtosis and bicoherence are defined as the following equations:

$$kurtosis = \frac{E\{x^4\}}{[E\{x^2\}]^2} - 3 \tag{4}$$

where x is EMG data and $E\{.\}$ is the statistical expectation operator.

$$S^x = \sum_{w_1, w_2} \left| Bic^x(w_1, w_2) \right|^2 \tag{5}$$

where S^x is mean bicoherence power and $Bic^x(w_1,w_2)$ is the normalized bispectrum of x at frequency w.

In order to improve the classification accuracy, multiple features have been proposed. There are many proposed multiple features in previous publication. Examples include G1 (MAV, WAMP, VAR, and WL), G2 (IEMG, WL, VAR, ZC, SSC, and WAMP), G3 (WL, RMS, and 4th autoregressive coefficient), G4 (SSC, ZC, WL, HTD and skewness), G5 (WL and MAV), and G6 (Binary feature, AR11, and DFT). The most popular multiple features used in finger movement classification is G1 consisting of

MAV, WAMP, VAR, and WL. Although many studies have proposed the feature extraction method for myoelectric control system, there is no work which make quantitative comparison for feature quality. Overall, a high quality feature space should have the following properties:

1) Maximum class separability: A high quality feature space must achieve high classification accuracy as possible. There are two ways to evaluate a quality feature space. Firstly, it is evaluated from classification error rate. It has disadvantage that the result depends on the classifier types. In order to avoid the disadvantage presented above, the evaluation by statistical criteria such as the ratio of a Euclidean distance to a standard deviation index (RES index) is proposed [81].

2) Robustness: The selected feature space should be implemented in a noisy environment.

3) Complexity: The selected feature should require a low computational complexity that can be implemented with reasonable hardware and in a real-time manner.

1.2.2.2 Dimensionality reduction

It is necessary to reduce the dimension of feature vectors for the studies that used the multiple EMG features or time-frequency domain feature because it would bring data redundancy and increase the computational time [78]. High dimension of an original feature vector must be reduced by keeping the most discriminative information and removing the irrelevant information [72]. There are two main strategies of dimensionality reduction, i.e., feature projection and feature selection. Details on literature review of each strategy are as follows.

1) Feature projection: This strategy tries to determine the best combination of the original features vector to form a new feature set which is generally smaller than the original one [80]. Principal component analysis (PCA) and linear discriminant analysis (LDA) are two main methods used for feature projection [6]. From a literature review, the most popular feature projection method is PCA. However, feature projection methods, such as combination of PCA and self-organizing feature map

(SOFM) [82] and nonlinear discriminant analysis (NLDA) [79] have not been proposed for finger movement classification.

2) Feature selection: This strategy chooses the best subset of the original feature vector that yield the maximum classification accuracy. Genetic algorithm (GA) is the most popular feature selection method. However, some methods have not been proposed for finger movement classification, such as tabu search (TS), simulated annealing (SA), particle swarm optimization (PSO) and ant colony optimization (ACO) [83].

1.2.2.3 Classification method

It is necessary to distinguish different categories of the features sets using a classifier before sending them to the control system. Thus, it is important to select the suitable classifier which is able to cope with varying patterns and prevent over fitting. In addition, it must be fast enough to implement for real-time constraints [84]. There are several techniques applied for EMG classification and neural network (NN) is becoming one of the most useful method [61].

Many studies used back-propagation neural network (BPNN) for classification of finger flexion and extension that yield the accuracy from 80 to 90% [14-17, 20-21]. Naik et al. used BPNN to identify hand and finger gestures and achieved relatively high classification accuracy (96-99%) [27-31]. NN was mostly used for classification of finger joint angle. In addition, NN was used to classify EMG signal acquired during pressing piano. Support vector machine (SVM) and K-nearest neighbor (KNN) are also popularly used. SVM and KNN were applied to distinguish EMG signals from finger flexion and extension [12, 47, 24-25, 32, 37]. KNN was used for classification of finger pushing [41]. Recently, LDA was used to classify finger flexion. In addition, some classifiers have not been proposed for classification finger movement, such as log-linearized Gaussian mixture network (LL-GMN), probabilistic NN (PNN), fuzzy mean max NN (FMMNN), and radial basis function artificial NN (RBFNN), hidden Markov model, and Bayes classifier.

1.2.3 Control system

The output commands produced in the classification are fed to this stage for control the devices, such as prosthetic devices and assistive robot. In order to improve performance of the control system, post-processing should be performed. Majority voting is applied as a post-processing to manage excessive classified output regarding continuous segmentation. It can improve the quality of system and make a smooth and reliable of class decisions [6, 85]. In addition, the feedback may need to improve the quality of system [6].

1.3 Objectives

- To develop the experimental setup and the algorithm for classifying surface electromyography signals from finger movements.

1.4 Methodology

The classification of finger movement based on a literature review indicates the gaps for future research as the details presented below.

1.4.1 Electrode location and experimental setup

Three novel methods of electrode placement and experimental setup will be carried out. Details on each method are as follows.

1.4.1.1 Finger flexion/extension

The novel method of electrode placement for finger flexion/extension will be designed. The new design will use the multi-channel sensor rings with unequal distance of placement for each electrode. In other words, each electrode in the ring will be placed as closely as possible to the corresponding muscle so that the maximum EMG signal to noise ratio will be obtained. For example, six bipolar electrodes are placed around the forearm on FCR, PL, FCU, extensor carpi radialis longus (ECRL), ED, and extensor carpi ulnaris (ECU) muscles and four bipolar electrodes are placed around the wrist on FPL, FDS, abductor pollicis longus (ABL), and extensor pollicis brevis (EPB) muscles. This method is capable of combining the easiness of use from multi-channel sensor rings with EMG signal quality from the exact placement of the electrode on the muscle. In addition, EMG signals from all

possible finger flexion/extension (14 cases) will be acquired so that we can have completed analysis of EMG signals from finger flexion/extension movement in all aspects.

1.4.1.2 Finger force

The literature has mainly proposed the classification of finger flexion/extension and finger joint angle, whereas a few studies classified the finger force. Thus, another study direction is to collect the EMG signal acquired during individual and combined finger flexion and/or finger force. To achieve better understanding on correlation between force and EMG signals from various muscles, the novel experimental setup for finger force movement will be conducted to obtain surface EMG and force data during thump-index pinch on five different boxes: 45, 60, 75, 90, and 105 mm, three wrist postures: neutral, flexion, and extension, and five force levels: 10, 30, 50, 70, and 100% of maximum voluntary contraction. Twelve channels of EMG signals will be recorded from 3 muscle regions on the right arm including hand muscles, lower and upper forearm muscles for analysis.

1.4.2 EMG pattern recognition

EMG pattern recognition can be divided into three stages consisting of feature extraction, dimensionality reduction, and classification. The study directions for EMG pattern recognition are presented below.

- The first study direction is to examine feature extraction, dimensionality reduction, and classification methods that have not been proposed in literature, as can be summarized in

Table 1.2.

- The second study direction is to investigate the optimal feature extraction, dimensionality reduction, and classification methods used for finger movement recognition.

Table 1.2 Summary of gaps for future research based on a literature review of feature extraction, dimensionality reduction, and classification methods.

Procedure	Literature review	Study direction
Feature extraction	- Single time domain features: MAV, IEMG, RMS, and HOS - Single frequency domain features: FFT - Multiple features: MAV+WAMP+VAR+WL, IEMG+WL+VAR+ZC+SSC+WAMP, WL+RMS+AR4, SSC+ZC, WL+HTD+skewness, WL+MAV, and binary feature+AR11+ DFT	- Time domain features: MAV, IEMG, RMS, HOS, WL, WAMP, VAR, SSC, ZC, MAVS, and AR - Frequency domain features: FFT, MNF, and MDF - Time and frequency features: STFT and wavelet transform - Novel set of multiple features
Dimensionality reduction	- Feature projections: PCA and LDA - Feature selections: GA	- Feature projections: PCA, LDA, SOFM, and NLDA - Feature selections: GA, TS, SA, PSO, and ACO
Classification	- Classifiers: NN, KNN, SVM, and LDA	- Classifiers: NN, KNN, SVM, LDA, HMM, GMM, LL-GMN, PNN, RBFNN, and Bayes classifier

1.5 Scope of research

- The experimental setup and the algorithm for classifying EMG signals will be developed from the following movements: Finger flexion/extension, finger force, and finger movement based on object.

1.6 Expected benefits

The recognition of EMG signals from finger movements is very challenging because the strength of muscle contraction from the electrodes is quite weak. In addition, the problem will be more difficult if the EMG signal from each pair of electrode is the combination from multiple active muscles. Therefore, the understanding of basic knowledge on EMG signals from finger movements resulting from this research is very important because it may open an opportunity for developing a practical and efficient EMG-based human computer interface system. The potential applications include upper limb prosthesis control, game control, and rehabilitation system.

CHAPTER 2 Flexion EMG data

2.1 Introduction

Fligge et al. reported that myoelectric control of active hand prosthesis can be realized in two different fashions [8]. While one is based on a movement such as finger flexion/extension and finger joint angle, the other is based on an object, such as for grasping objects with different shapes, sizes, and positions [8]. The classification based on the movement requires a more complicated algorithm than that based on the object, because it has to classify the movement of each finger in each of its movement directions. Moreover, an accurate prediction algorithm for the movement of each finger is highly required by marketed prosthetic hands. In previous studies [12, 14-16, 24, 86-87], no more than 10 movements were proposed in a finger movement classification system. In order to obtain a multifunctional myoelectric control system, we classify 14 finger movements involving individual and combined finger flexion, in this paper.

To achieve high classification rate, the algorithms for feature extraction, dimensionality reduction, and classification should be optimized [73]. In the literature, we found that the classification rate was below 90% when a single feature was used. The classification accuracy from mean absolute value (MAV) was 85-89% [16, 24]. The feature based on fast Fourier transform was employed for analyzing EMG patterns in [15] and [14]. Uchida et al. [15] reported that the classification accuracy with the feature based on power spectral density was 86%. In addition, in hand movement classification, performance of many features both in time and frequency domains were evaluated by Phinyomark et al. [77, 88]. They found that most classification accuracies were 80-90%.

Multiple features have been proposed by combining time domain, frequency domain, and/or statistical features to improve the classification rate. Multiple features can have redundancy and add to the computational complexity of classification. Therefore, various dimensionality reduction techniques were proposed to reduce the redundancy and computational complexity [80]. There are two main strategies of dimensionality reduction, i.e., feature projection and feature selection. While feature

projection tries to determine the best combinations of the original features to form a new feature set, feature selection chooses the best subset of the original feature set. Previous studies applied various feature projection methods in EMG classification including principal component analysis (PCA) [45], [89], linear discriminant analysis (LDA) [12], [90], uncorrelated linear discriminant analysis (ULDA) [88], orthogonal fuzzy neighborhood discriminant analysis (OFNDA) [91], and spectral regression linear discriminant analysis (SRDA) [92]. Classification accuracies greater than 90% were reported.

Our previous study [87] proposed a new feature projection, namely spectral regression extreme learning machine (SRELM), and evaluated its performance along with other feature projection techniques, including SRDA, ULDA, OFNDA, and PCA. Moreover, in [87] five classifiers including adaptive wavelet ELM (AW-ELM) [93], radial basis function ELM (RBF-ELM), support vector machine (SVM), k-nearest neighbors (KNN), and linear classifier (LC) were evaluated for their performances in classifying two channels of EMG signals from 10 hand and finger movements. We reported that SRELM gave the best performance. Moreover, we found that the classification accuracy depended on the classifier. In other words, while SREML provided the best performance when the KNN classifier was used, ULDA gave the best performance with the SVM classifier. These results indicated that the pairing of a feature projection technique with a type of classifier affects the classification accuracy. Therefore, another effective classifier, neural network (NN), which was not used in [87], was investigated in this current study.

2.2 Theory

2.2.1 Feature extraction

Feature extraction is a technique to transform EMG data into a reduced representation of features, which are usually extracted from EMG in the time domain and/or the frequency domain [6]. Recent studies have proposed further features based on statistical methods. In this paper, we used Hudgins's feature set: MAV [2-3, 26, 86, 89], waveform length (WL) [2-3, 20, 25-26, 87], zero crossing (ZC) [2-3, 12, 26, 88], and slope sign change (SSC) [2-3, 12, 26, 87], which are popular time domain

features used in previous studies. In addition, we also used the fourth order autoregressive coefficient (AR) for representing information on the prediction model [32, 86-87, 89], mean frequency (MNF) for representing information on the power spectral density [75, 77], kurtosis (KURT) for representing information on peakedness of distribution [86], and skewness (SKW) for representing information on the symmetry of distribution in the EMG signal [12, 87]. The total number of features used in this paper is 11. The detailed mathematical definition of each feature is as follows.

(1) Mean absolute value (MAV) represents the signal energy, which is frequently used for detecting the onset of an EMG signal. MAV feature is the average of absolute value of transformed EMG signal. It can be defined as [2]

$$\mathrm{MAV} = \frac{1}{N}\sum_{i=1}^{N} | x_i | \tag{1}$$

where x_i is the amplitude of the EMG signal at sample i and N is the length of the EMG signal.

(2) Waveform length (WL) is the cumulative length of the EMG waveform over the segment, and is indicative of the complexity of the EMG signal. It can be expressed as [2]

$$\mathrm{WL} = \sum_{i=1}^{N-1} | x_{i+1} - x_i | \tag{2}$$

(3) Zero crossing (ZC) is the number of times that the EMG signal amplitude crosses zero. In other words, it is the number of times that the signal amplitude changes its sign. A threshold must be set to reduce the noise (i.e., threshold was set to 10 μV). It can be defined as [2]

$$\mathrm{ZC} = \sum_{i=1}^{N-1} \left[f(x_i \times x_{i+1}) \cap \left| x_i - x_{i+1} \right| \geq 10 \right] \tag{3}$$

$$f(x) = \begin{cases} 1, & \text{if } x < 0 \\ 0, & \text{otherwise} \end{cases} \tag{4}$$

(4) Slope sign change (SSC) is the number of times that the slope of the EMG signal changes sign. It is defined as [2]

$$\mathrm{SSC}=\sum_{i=2}^{N}\left[s\left\{(x_i-x_{i-1})(x_i-x_{i+1})\right\}\cap\left\{\left|x_i-x_{i-1}\right|\geq 10\cup\left|x_i-x_{i+1}\right|\geq 10\right\}\right] \tag{5}$$

$$s(x)=\begin{cases}1, & \text{if } x>0\\ 0, & \text{otherwise}\end{cases} \tag{6}$$

(5) Autoregressive coefficient (AR) describes each sample of the EMG signal as a linear combination of the previous sample plus a white noise error term, which can be defined as [32]

$$x_i=\sum_{p=1}^{P}a_p x_{i-p}+w_i \tag{7}$$

where a_p is the coefficient in the AR model. P is the order of the AR model and w_i is white noise or error sequence. In this paper, P is set to four.

(6) Mean frequency (MNF) is the average frequency. It is defined as the sum of product of power spectrum and frequency divided by the total spectrum intensity, which can be expressed as [77]

$$\mathrm{MNF}=\sum_{j=1}^{M}f_j P_j \Big/ \sum_{j=1}^{M}P_j \tag{8}$$

where f_j is the frequency of spectrum at frequency bin j. P_j is the EMG power spectrum at frequency bin j and M is the number of bins.

(7) Kurtosis (KURT) is a classical higher-order statistical characteristic indicating non-Gaussianity, and is used to quantify the peakedness of a distribution. It is the fourth-order cumulant of the data, which can be defined as [86]

$$\mathrm{KURT}=\left[\frac{1}{N}\sum_{i=1}^{N}y_i^4 \Big/ \left(\frac{1}{N}\sum_{i=1}^{N}y_i^2\right)^2\right]-3 \tag{9}$$

where y_i represents the ith normalized EMG amplitude, which has zero mean and unit variance. N denotes the total number of the normalized EMG samples. Kurtosis can be either positive or negative.

(8) Skewness (SKW) is a measure used for characterizing the degree of asymmetry of the distribution of a random variable *y*. It is the third-order cumulant of the data, which can be defined as [12]

$$\mathrm{SKW} = \frac{1}{N}\sum_{i=1}^{N}(y_i - \bar{y})^3 \Bigg/ \left(\sqrt{\frac{1}{N}\sum_{i=1}^{N}(y_i - \bar{y})^2}\right)^3 \tag{10}$$

2.2.2 Feature projection

Six feature projection techniques are evaluated in this paper including PCA, LDA, ULDA, OFNDA, SRDA, and SRELM. It should be noted that the number of reduced features from each feature projection technique except PCA was set 13, matching the total number of movements minus one. The number of reduced features from PCA was 14. The brief details on each technique are as follows.

- PCA tries to find a set of orthogonal basis vectors that captures maximum information from the original dimensions. PCA decomposes the covariance structure of the original dimensions by calculating the eigenvalues and eigenvectors of the data. The components, i.e., eigenvalues and eigenvectors, are ranked according to their variance to the principal axes ranging from the highest contribution to the lowest.
- LDA tries to find an optimal transformation vector by maximizing the ratio of the between-class distance to the within-class distance, so that the maximum class discrimination is achieved.
- ULDA is an extension of classical LDA, such that the features in the transformed space are uncorrelated, so the redundancy in the transformed space could be reduced. The objective of ULDA is to find the optimal discriminant vectors.
- OFNDA minimizes the distances within the classes and maximizes the distances between the centers of different classes, while taking into account the contribution of the samples to the different classes and to efficiently overcome the singularity problems of classical LDA by employing the QR-decomposition.

- SRDA combines the spectral analysis of the graph matrix and regression techniques, and is essentially developed from LC [94]. A set of linear regression problems is solved to obtain the transformation vectors.
- SRELM was proposed in our previous study [87]. It is integrated from extreme learning machine (ELM) and spectral regression (SR), which utilizes the obtained eigenvector to project the hidden layer output to the output layer. The hidden layer weights are determined randomly. The output weight is computed using SR. There are two parameters in optimizing SRELM performance: number of hidden nodes and alpha. In order to evaluate the optimal parameters in this paper, the number of hidden nodes was varied from 100 to 1,500 nodes with an increment of 100 nodes and alpha was varied from 1 to 20 with an increment of 1.

2.2.3 Feature evaluation

In this paper, we applied the statistical criteria, namely, the ratio of a Euclidean distance to a standard deviation (RES) index, to evaluate class separation performance of the projected feature obtained from each feature projection technique. The advantage of the RES index is that its result is independent of any classifier. The RES index can be defined as [81]

$$\text{RES index} = \frac{\overline{ED}}{\overline{\sigma}} \tag{11}$$

$\overline{ED}$ is the distance between coordinates of a pair of clusters p and q in n-dimensional Euclidean space, which can be defined as

$$\overline{ED} = \frac{2}{K(K-1)} \sum_{p=1}^{K-1} \sum_{q=p+1}^{K} \sqrt{(\overline{m}_1^p - \overline{m}_1^q)^2 + (\overline{m}_2^p - \overline{m}_2^q)^2} \tag{12}$$

where m is the average value of feature. p and q are indexes representing the movements. K is the total number of movements. ($1 \le k \le K$, $K = 14$)

$\overline{\sigma}$ is dispersion of clusters p and q, which can be expressed as

$$\overline{\sigma_i} = \frac{1}{IK} \sum_{i=1}^{I} \sum_{k=1}^{K} s_{ik} \tag{13}$$

where s is a standard deviation of a feature and I is the length of feature vector ($1 \leq i \leq I$, I = 13 or 14). The RES index increases when the class separation performance of EMG features increases.

2.2.4 Classification

Seven classifiers are tested and compared in this paper, i.e., SVM, LC, NB, KNN, RBF-ELM, AW-ELM, and NN. Brief details of each classifier and its corresponding parameters used are as follows.

- SVM uses a discriminant hyperplane to separate the classes. SVM aims to find the optimal hyperplane that maximizes the margins between the points of different classes. The margins are the distances between the hyperplane and the nearest training points. In this study, SVM type was *C*-support vector classification. Kernel type was radial basis function. Gamma in kernel function was set to 1/number of features and cost was set to 1.

- LC was implemented using a simple max gate function as a classification rule [95]. It is assumed that the vector of feature variables has multivariate normal distribution with mean vector and common covariance matrix.

- NB classifier aims to reach the best hypothesis through a given training dataset. Bayes theorem provides a way to calculate the probability of a hypothesis based on its prior probability of both the data found and the total data.

- KNN is a process to assign a feature vector to a class according to the k training samples, which are the nearest neighbors to the test sample. Subsequently, it is classified to the category that has the largest category probability [95]. In this paper, k was set to 14.

- RBF-ELM is a variant of ELM classifier, which is single layer feed-forward network with radial basis function. It employs randomized method to initialize the centers and widths of RBF kernels and the output weights of RBF network

are calculated analytically [96]. In order to select the optimal parameter, the kernel parameter was varied and tested at 0.1, 0.5, 1, 5, 10, 15, and 20.

- AW-ELM proposed by Anam and Al-Jumaily [93] is the combination of ELM with wavelet neural network. It utilizes a wavelet function as the activation function in the hidden node. The function is adjusted according to changes in the input. In order to select the optimal parameter, the number of hidden nodes was varied from 25 to 500 nodes with an increment of 25 nodes

- NN is a multilayer perceptron, which is composed of several layers: one input layer, one or several hidden layers and output layers. Each neuron in each layer is connected with the output of the previous one. In this paper, we designed three layered feed-forward back-propagation neural networks consisting of input layer, tan-sigmoid hidden layer and linear output layer [76]. The number of neurons in hidden layer was 10, 20, or 30, with the best alternative selected for obtaining maximal accuracy.

2.3 Materials and methods

2.3.1 EMG data acquisition

Figure 2.1 shows the electrode placements on 6 forearm muscles used for EMG data acquisition. While the first group of muscles, namely, extensor carpi ulnaris (CH6), extensor carpi radialis longus (CH5), and extensor digitorum (CH4), are located on the posterior compartment of the forearm to perform extension at the fingers, the second group of muscles, namely, flexor carpi ulnaris (CH3), palmaris longus (CH2), and flexor carpi radialis (CH1) are located on the anterior compartment of the forearm to produce flexion at the fingers. EMG signals from all muscles were recorded using bipolar disposable Ag/AgCl electrodes (H124SG, Kendel ARBO) with an inter-electrode distance of 20 mm. All EMG data were recorded by a commercial EMG measurement system (Mobi6-6b, TMS International B.V.). The EMG signals were amplified with a gain factor of 19.5 and the bandwidth was from 20 Hz to 500 Hz, while the sampling rate was 1024 Hz.

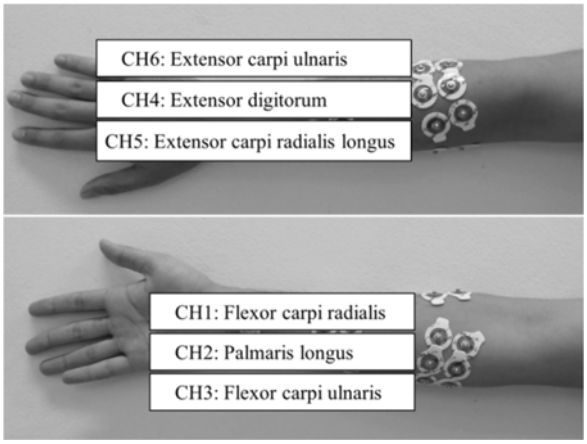

(a)

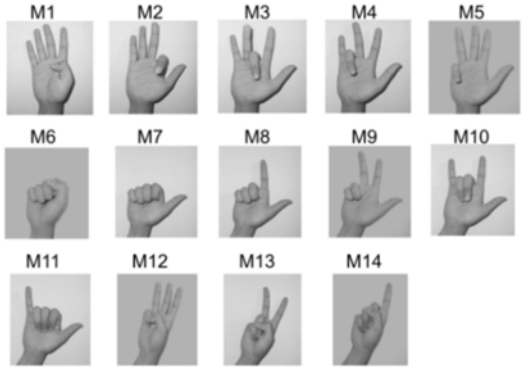

(b)

Figure 2.1 The electrode locations on forearm muscles (a) The fourteen finger movements (b).

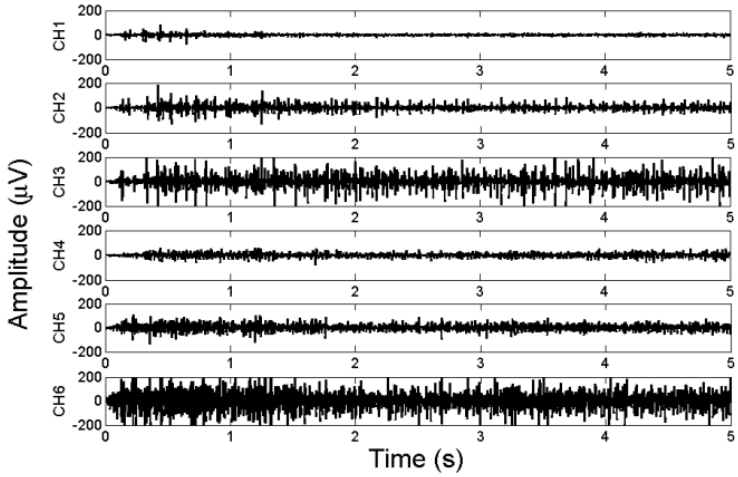

Figure 2.2 Example of the six-channel EMG signal from thumb flexion (M1).

Ten able-bodied subjects participated in the experiment. Each subject performed 14 different finger movements as shown in Figure 2.1 (Right) consisting of

thumb flexion (M1), index flexion (M2), middle flexion (M3), ring flexion (M4), little flexion (M5), hand close (M6), index-middle-ring-little flexion (M7), middle-ring-little flexion (M8), ring-little fingers flexion (M9), middle-ring flexion (M10), index-middle-ring flexion (M11), thumb-little flexion (M12), thumb-ring-little flexion (M13), and thumb-middle-ring-little flexion (M14). Each movement was recorded for 5 s in duration for each trial and was repeated for 5 times. Figure 2.2 shows an example of EMG signals obtained from six muscles during thumb flexion (M1).

2.3.2 Methods

Figure 2.3 shows the method for evaluating feature projection techniques and classifiers used in recognizing the EMG signals from finger movements in this research. After 6 channels of EMG signals from 14 hand and finger movements were acquired, they were processed using the analytical method consisting of 5 steps, i.e., (1) Data collection and segmentation, (2) Feature extraction, (3) Feature projection (FP), (4) Performance evaluation with RES index, and (5) Performance evaluation with classifiers. The details on each analytical step are as follows.

Step 1) Segmentation: In this step, EMG data with a length of 5120 samples was segmented by the disjoint windowing technique with a window length of 256 samples (250 ms) resulting in 20 segmented EMG data for each trail of each EMG channel.

Step 2) Feature extraction: In this step, the eleven features described in Section 2.2.1 including MAV, WL, ZC, SSC, MNF, L-KURT, SKW, and 4 coefficients from AR were calculated for each EMG segment. The total EMG feature data had 1,400 rows (20 segments × 5 trials × 14 movements) and 66 columns (11 features × 6 channels).

Step 3) Feature projection: In this step, the six feature projection techniques described in Section 2.2.2 including SRLEM, LDA, ULDA, OFNDA, SRDA, and PCA were applied to the features extracted in Step 2). As a result, the total number of features, which was 66 from Step 2), was reduced to 14 for PCA and 13 for the others in this step.

Step 4) Performance evaluation with RES index: In this step, the performance on class separation ability of the projected features resulting from Step 3) was evaluated with the RES index.

Step 5) Performance evaluation with classifiers: In this step, the projected features from Step 3) were used as the inputs of 7 classifiers, which were briefly described in Section 2.2.4. The performance (classification accuracy) using the projected features resulting from Step 3) was evaluated and compared.

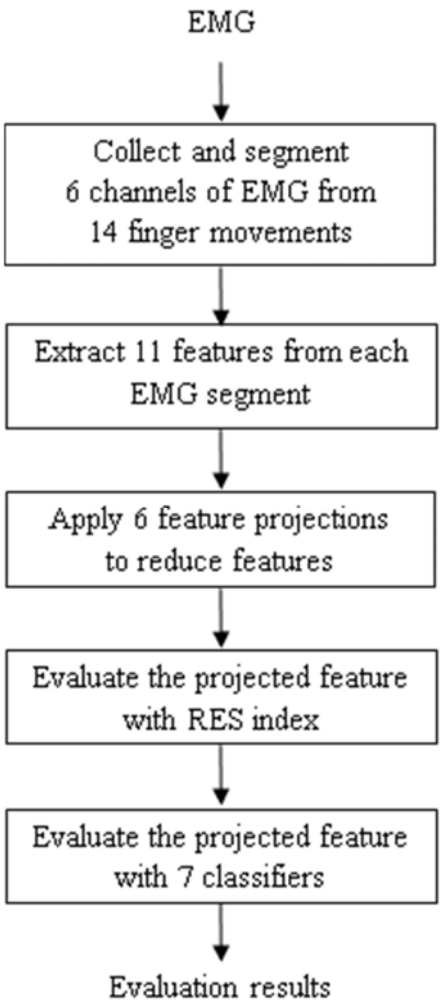

Figure 2.3 EMG acquisition and analytical method.

Note that, the projected features were classified with a 10-fold cross-validation. In other words, the projected features were randomly partitioned into 10 subsets. The classifier training was performed using 9 subsets and the remaining

subset was used for classifier testing. This process was repeated 10 times such that each of the 10 subsets was used as the testing data. Finally, the performance of each pairing of the projected feature with the classifier was evaluated and compared using mean and standard deviation of classification accuracies.

2.4 Results and discussion

2.4.1 Characteristics of the projected features

Figure 2.4 shows as an example the scatter plot between two projected features from each feature projection technique. The result shows that the projected features by SRELM provided better separation than those from other feature projection techniques, while the projected features from LDA, ULDA, OFNDA, and SRDA are quite overlapped. In addition, PCA provided projected features that had the worst performance in separating finger movements.

Figure 2.5 shows the RES index calculated from projected features by each feature projection technique. The RES index of projected features by SRELM is higher than that of other feature projection techniques. In other words, SRELM provides the projected features that have the best performance in separating finger movements. The RES indexes of projected features from SRDA, OFNDA, LDA, and ULDA are quite similar, while the projected features from PCA give the lowest RES index. We can clearly see that the RES index of projected features in Figure 2.5 is consistent with the scatter plot of projected features in Figure 2.4.

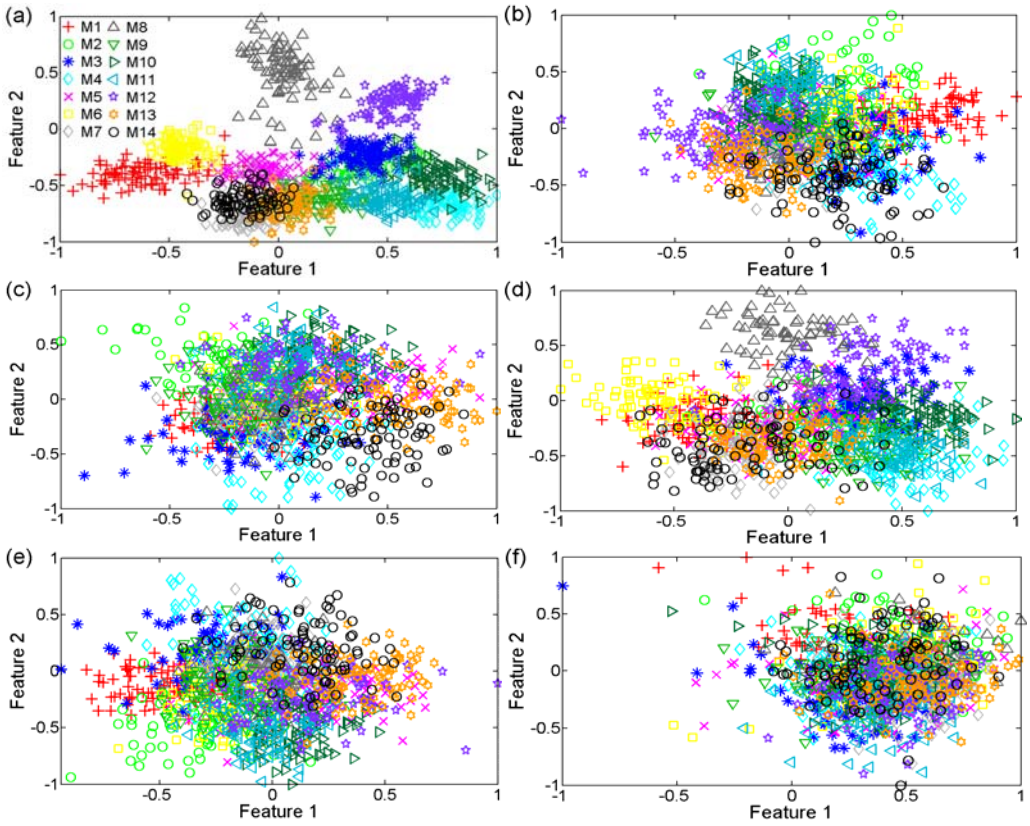

Figure 2.4 Scatter plots of the two top ranked projected features when using (a) SRELM, (b) LDA, (c) ULDA, (d) SRDA, (e) OFNDA, and (f) PCA.

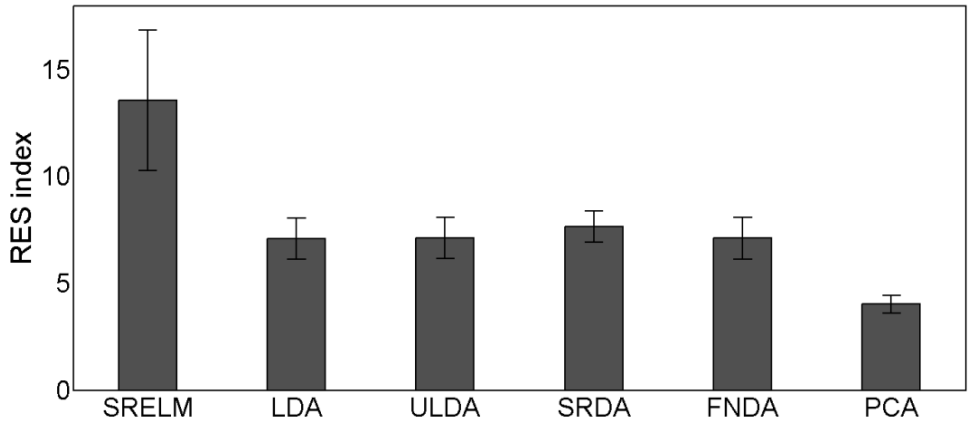

Figure 2.5 RES index of the projected features from different feature projection techniques.

2.4.2 Classification accuracy

Table 2.1 presents the classification accuracy using various feature projection techniques paired with different classifiers. While the best classification accuracies from LC, KNN, AW-ELM, and NN are obtained with the projected features from SRELM, the best classification accuracies from SVM and RBF-ELM are obtained with the projected feature from SRDA. However, for each feature projection technique, we can observe that NN with 10 nodes in the hidden layer provides the highest classification accuracy. Moreover, the combination of SRELM and NN gives the maximum classification accuracy at 99.09%.

Anam and Al-Jumaily [87] reported that SRELM is an extreme learning machine (ELM) for supervised feature projection with consideration of the class label. The aim of the training is to produce output that is very close to the output target. In other words, the training tries to minimize the error between the actual output and target. As a result, the projected features from SRELM show better performance in separating fourteen finger movements than those from other feature projections. In addition, LDA considers also class label in the projection step (i.e., supervised feature projection) and ULDA is developed to solve the limitation of LDA by producing a set of uncorrelated discriminant features employing the singular value decomposition [90]. In contrast, as Chu et al. [97] reported the PCA does not consider the class labels in the projection process (i.e., it performs unsupervised feature projection). Therefore, the output is another representation of the features and its performance is lower than with other feature projection techniques.

Table 2.1 Mean and standard deviation of classification accuracies for 14 movements obtained with various pairs of feature projection (FP) and classifier.

FP	SVM	LC	NB	KNN	RBF-ELM	AW-ELM	NN
SRELM	92.9±4.4	***93.6±4.0***	90.0±4.6	***93.0±4.1***	93.2±3.9	***92.1±4.3***	***99.1±0.8***
LDA	93.3±3.9	92.4±3.7	***90.4±4.4***	92.3±4.4	93.3±4.1	91.1±4.6	95.5±2.7
ULDA	93.0±3.9	92.3±3.8	90.0±4.3	92.2±4.5	93.1±4.1	90.8±5.0	95.6±2.8
SRDA	***93.7±3.6***	92.1±3.9	89.8±4.4	93.0±3.7	***93.9±3.5***	92.1±4.2	95.1±3.1
OFNDA	93.1±4.0	92.3±3.8	90.3±4.2	92.1±4.3	93.3±3.9	90.8±4.7	95.6±2.8
PCA	84.0±6.9	83.2±6.5	72.6±7.3	79.5±7.8	81.9±8.3	75.5±7.7	85.6±6.6

Table 2.2 presents the classification accuracies for 14 movements obtained from the NN classifier with different numbers of nodes in hidden layer, i.e. 10, 20, or 30 neurons. When we increase the number of neurons in hidden layer from 10 to 20 and to 30, the classification accuracy changes slightly for each feature projection technique. Results show that 20 neurons in hidden layer gives the best accuracy at 99.57% among all combinations of feature projection techniques and classifiers, when the projected features from SRELM are used.

Table 2.3 presents classification accuracies with channel reduction. The subset of channels was optimized by considering the classification accuracies obtained from all combinations of each channel set. Firstly, all possible combinations of five channels out of the six totals were trialled for classification. Only the set of five channels providing the highest classification accuracy was selected. Secondly, all possible combinations of four channels out of the five total from the first step, were trialled for classification. For instance, the accuracies from all combinations of five channels are shown in the second row to the seventh row in Table 2.3. We can see that the combination of CH2, CH3, CH4, CH5, and CH6 provides the highest classification accuracy, so this channel set was selected as the best combination of five channels. Then, all possible combinations of four channels out of the five selected channels from the first step were trialled. As a result, the combination of CH2, CH3, CH5, and CH6 provides the best classification accuracy and it was chosen as the optimal set of four channels. The procedure was repeated for three, two and one channels, respectively. The results show that the classification accuracy decreases from 99.57 to 58.95% when the number of channels decreases from 6 to 1. Results show that to obtain a high classification accuracy, EMG signals from the muscles located on the anterior and posterior compartments of the forearm are needed. For example, the maximum classification accuracy from two EMG channels at 85.38% can be obtained from the combination of flexor carpi radialis (CH3) and extensor carpi ulnaris (CH6), which are located on the anterior and posterior compartments of the forearm, respectively.

Table 2.2 Mean and standard deviation of classification accuracies for 14 movements obtained from the NN classifier with three alternative sizes of the hidden layer.

FP	10 neurons	20 neurons	30 neurons
SRELM	***99.09±0.83***	***99.57±0.42***	***99.54±0.46***
LDA	95.51±2.74	96.61±2.45	96.84±2.25
ULDA	95.58±2.82	96.68±2.34	96.83±2.21
SRDA	95.12±3.08	96.37±2.33	96.49±2.40
OFNDA	95.59±2.76	96.47±2.56	96.86±2.25
PCA	85.59±6.58	87.87±6.21	88.47±6.01

Table 2.3 Mean and standard deviation (SD) of classification accuracies for 14 movements obtained from the SRELM feature projection and the NN classifier as the number of available EMG channels is reduced step by step.

Channel combination	Mean±SD	Note
CH1-CH2-CH3-CH4-CH5-CH6	***99.57±0.52***	6 channels
CH2-CH3-CH4-CH5-CH6	***99.24±0.51***	Remove CH1
CH1-CH2-CH3-CH4-CH5	98.71±1.12	
CH1-CH2-CH3-CH4-CH6	98.90±0.90	
CH1-CH2-CH3-CH5-CH6	99.05±1.00	
CH1-CH2-CH4-CH5-CH6	98.90±1.60	
CH1-CH3-CH4-CH5-CH6	98.86±1.31	
CH2-CH3-CH5-CH6	***97.95±1.52***	Remove CH1 and CH4
CH2-CH3-CH4-CH5	97.33±1.70	
CH2-CH3-CH4-CH6	97.90±1.06	
CH2-CH4-CH5-CH6	96.95±2.24	
CH3-CH4-CH5-CH6	97.90±1.29	
CH3-CH5-CH6	***93.71±3.94***	Remove CH1, CH4, and CH2
CH2-CH3-CH5	93.38±2.68	
CH2-CH3-CH6	92.81±3.79	
CH2-CH5-CH6	92.90±3.32	
CH3-CH6	***85.38±4.55***	Remove CH1, CH4, CH2, and CH5
CH3-CH5	84.76±4.92	
CH5-CH6	80.19±5.67	
CH3	***58.95±8.49***	Remove CH1, CH4, CH2, CH5, and CH6
CH6	56.24±9.45	

Table 2.4 presents classification accuracies from movement reduction using 2 channels of EMG signals, namely, CH3 and CH6, which selection was guided by Table 2.3. The subset of finger movements was optimized by considering classification accuracy of each movement. All EMG signals from 14 finger movements were firstly classified, and then the classification accuracy was individually investigated for each movement from the confusion matrix [98]. The movement providing the lowest classification accuracy was removed from the movement set. The procedure was repeated until the number of movements decreased to two movements. The results show that the classification accuracy increases from 87.14 to 100% when the number of movements decreases from 14 to 10 movements. Increasing the number of movements increases the complexity of classification, resulting in decreased classification accuracy.

2.4.3 Performance comparisons

Table 2.5 presents the performance comparisons of the proposed method with those from previous publications. When a single feature is used, such as MAV [16] and fast Fourier transform [15] in classifying EMG signals from 8 and movements, respectively, the feature projection is necessary. The classification accuracies are in the range of 85%-86%. The classifier used in this group is NN. When the number of movements increases to 10 {A}, [12, 25-26, 32, 87, 89], and {B} the number of features increases for providing more information to a classifier and feature projection is needed for reducing the dimension of a feature vector. The accuracy of our proposed technique for classification of 10 movements from 2-channel EMG signals achieves 100% {A}. Note that, in [87], the features were extracted from two EMG channels plus one channel formed from summation of the two channels. Moreover, Bayesian fusion was applied as a post processing in [12]. Comparison between {A} and [87] indicates that the classifier has a significant effect on the classification accuracy. Another way to increase classification accuracy is to increase in the number of EMG channels as shown in [26, 32, 45, 89], and {B}. Results show that our proposed technique give good accuracy of for classifying 14 movements from 4-channel EMG signals at 99.60%.

Table 2.4 Mean and standard deviation of classification accuracies for movement reduction obtained from the SRELM feature projection and the NN classifier using the EMG signals from CH3 and CH6**.**

# movements	Mean±SD	Movement removal
14	87.14±4.92	-
13	99.08±0.68	M7
12	99.28±0.59	M7 and M13
11	99.94±0.19	M7, M13, and M6
10	100.00±0.00	M7, M13, M6, and M14

Table 2.5 Performance comparisons with other techniques from previous publications sorted with the number of movements.

Ref.	**#Ch**	**#M**	**Features**	**#TF**	**FP**	**Classifiers**	**Acc. (%)**
{B}	6	14	4^{th}-order AR, MAV, WL, ZC, SSC, MNF, KURT, SKW	66	SRELM	NN	99.60
[89]	6	15	6^{th}-order AR, RMS, WL, ZC, IEMG, SSC	66	OFNDA	LDA	98.25
[32]	4	15	4^{th}-order AR, WL, RMS	28	-	SVM	97.60
[45]	32	12	WL	32	PCA	NN	94.30
[26]	7	11	IEMG, WL, VAR, ZC, SSC, WAMP	42	-	NN	93.90
{A}	2	10	4^{th}-order AR, MAV, WL, ZC, SSC, MNF, KURT, SKW	22	SRELM	NN	100.00
[12]	2	10	7^{th}-order AR, SSC, ZC, WL, HTD, SKW		LDA	SVM	≈92.00
[87]	2+1	10	6^{th}-order AR, MAV, ZC, WL, SSC, SKW, HTD	42	SRELM	AW-ELM	86.73
[15]	2	5	FFT	8	-	NN	86.00
[16]	2	8	MAV	2	-	NN	85.10

#Ch: The number of channels, #M: The number of movements, #TF: The total number of features extracted, FP: Feature projection, Acc: Accuracy, VAR: variance of EMG, FFT: fast Fourier transform, HTD: Hjorth time domain,

2.5 Conclusions

In the study of flexion EMG data, the system for classifying 14 finger movements, involving individual and combined finger flexion observed by 6 channels of EMG signals is proposed. Six feature projection techniques were evaluated including principal component analysis (PCA), linear discriminant analysis (LDA), uncorrelated linear discriminant analysis (ULDA), orthogonal fuzzy neighborhood discriminant analysis (OFNDA), spectral regression linear discriminant analysis (SRDA), and spectral regression extreme learning machine (SRELM). The results show that the projected features from SRELM give the best performance in terms of feature separation among these feature projection techniques. In addition, the best feature separation ability obtained with SRELM was confirmed by a quantitative measure, namely the RES index. Subsequently, seven classifiers were validated, namely, support vector machine (SVM), linear classifier (LC), Naive Bayes (NB), *k*-nearest neighbors (KNN), radial basis function extreme learning machine (RBF-ELM), adaptive wavelet extreme learning machine (AW-ELM), and neural network (NN). The results show that NN provides the best performance in separating 6-channel EMG signals to identify 14 finger movements. Classification accuracy of up to 99% was reached when using SRELM and NN in combination.

CHAPTER 3 Pinch EMG data

3.1 Introduction

The study of pinch EMG data is rationally structured into four sections involving this introduction section and other sections as follows:

Section of materials and methods presents in detail of EMG data and evaluation of pattern recognition techniques, which are applied to this study. It directs the two main outlines: (1) EMG data acquisition is described, such as posture testing, electrode placements, measurement system, and experimental procedure (2) the evaluation of pattern recognition techniques is explained including the step of experiment and the applied methods.

Section of results and discussion presents from the experiments explained in previous section. They can be divided into two outlines following the experiments. Firstly, the results from feature projection using SRELM method are shown. The effect of force data is presented. The performance results of seven classifiers, namely DT, LDA, QDA, SVM, KNN, Naïve Bayes, and NN, are also compared. Then, six feature projection methods, namely PCA, LDA, ULDA, OFNDA, SRDA, and SRELM, are compared and discussed.

Section of conclusion reviews the methods and experiments and summarizes the achievements of the study.

3.2 Materials and methods

3.2.1 EMG data acquisition

The experiment was conducted to obtain surface EMG and force data during thump-index pinch on five different boxes: 45, 60, 75, 90, and 105 mm width, in three wrist postures: neutral, flexion, and extension. The electrode placements of hand, lower forearm, and upper forearm muscles are shown in Figure 3.1, Figure 3.2, and Figure 3.3. Twelve channels of EMG signals were recorded from 3 muscle regions on the right arm including hand muscles, lower and upper forearm muscles as shown in Table 3.1. EMG signals from 3 hand muscles consisting of adductor pollicis (AP),

abductor pollicis brevis (APB), and first dorsal interosseous (FDI), were collected from bipolar Ag/AgCl electrodes (EL254S, BIOPAC) at an inter-electrode distance 10 mm. Two muscles from lower forearm: flexor pollicis longus (FPL) and extensor pollicis longus (EPL) were recorded from bipolar Ag/AgCl electrodes (H124SG, Kendel ARBO) at an inter-electrode distance 20 mm. Seven pair of electrodes were placed around upper forearm without specific muscle positions at approximately one third of the forearm length from the head of the ulna. The distances between adjacent electrodes (*d*) were approximately equal. For each subject, *d* was calculated from the distance around the forearm circumference divided by seven (Total number of electrodes). The first pair of electrode was placed at a distance of *d*/2 from ulnar. EMG data were acquired using the same electrode configuration as lower forearm muscles.

All EMG data were acquired by a commercial EMG measurement system (MP150, BIOPAC system). The EMG signals were amplified with a gain of 1000 times and bandwidths of 10 Hz to 500 Hz. EMG data were sampled at a rate of 1000 Hz. Force sensor (KISTLER 9017B) was used to measure force data during thumb-index pinch. Force data were recorded synchronously with EMG data by BIOPAC MP150 acquisition system and were sampled at a rate of 1000 Hz.

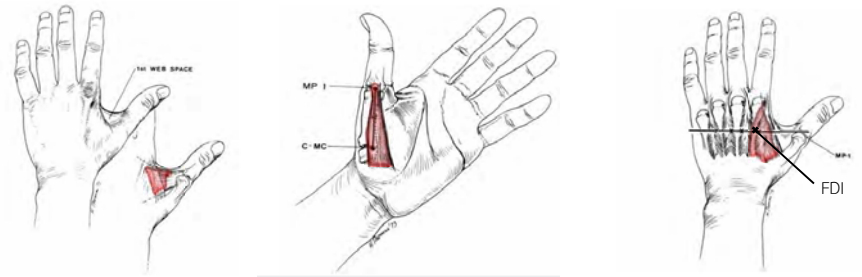

(a) (b) (c)

Figure 3.1 Three hand muscles (a) AP (b) APB (c) FDI [99]

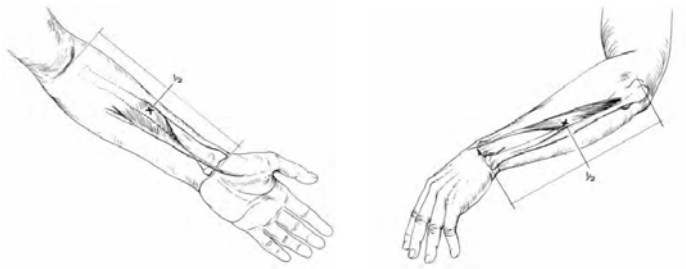

(a) (b)

Figure 3.2 Two lower forearm muscles (a) FPL (b) EPL [99]

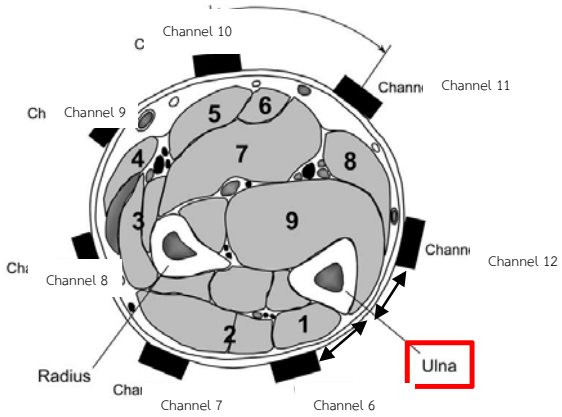

Figure 3.3 Cross-section of the right forearm indicating approximate electrode locations. Muscles are as follows: (1) extensor carpi ulnaris (ECU), (2) extensor digitorum communis (EDC) and extensor digiti minimi (EDM), (3) extensor carpi radialis longus (ECRL) and extensor carpi radialis brevis (ECRB), (4) brachioradialis (BR), (5) fexor carpi radialis (FCR), (6) palmaris longus (PL), (7) fexor digitorum superficialis (FDS), (8) fexor carpi ulnaris (FCU), and (9) fexor digitorum profundus (FDP) [100].

Table 3.1 Summary of electrode placements and manual muscle testing

Location	Number of channel	Muscle or related muscle channels	Manual muscle testing
Hand	3	AP, APB, FDI	AP, APB, FDI
Lower forearm	2	FPL, EPL	FPL, EPL
Upper forearm	7	ECU, EDC, EDM, ECRL, ECRB, BR, FCR, PL, FDS, FCU, FDP	-

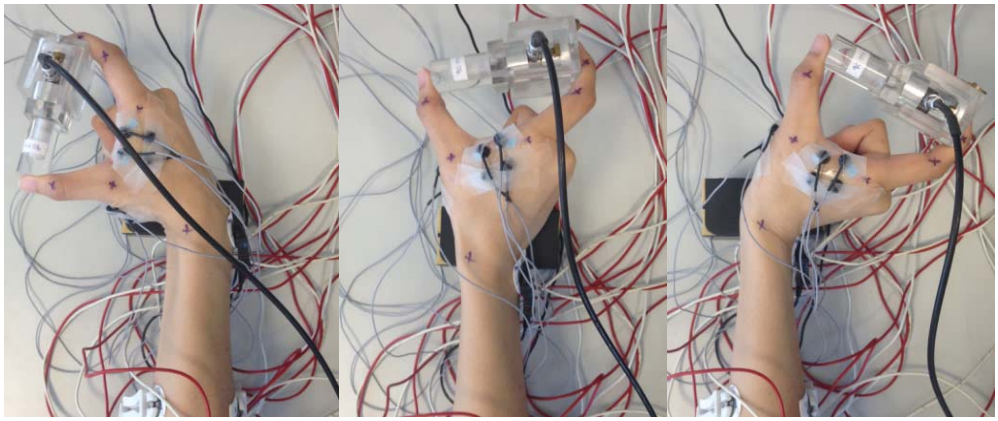

(a) (b) (c)

Figure 3.4 Thumb-index pinch at three wrist postures (a) flexion (b) neutral (c) extension

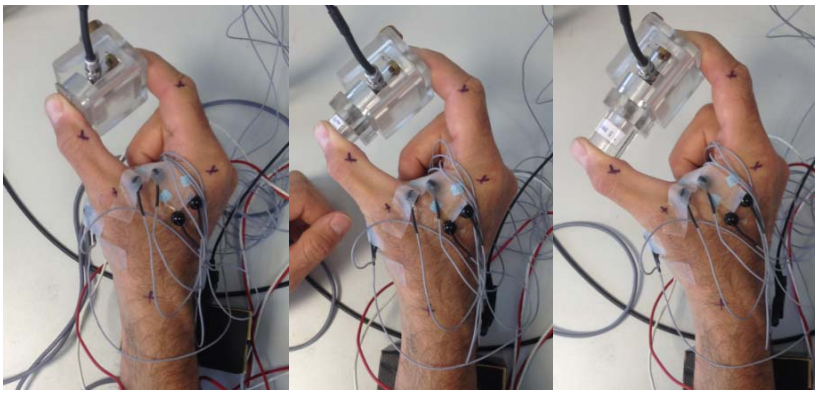

(a) (b) (c)

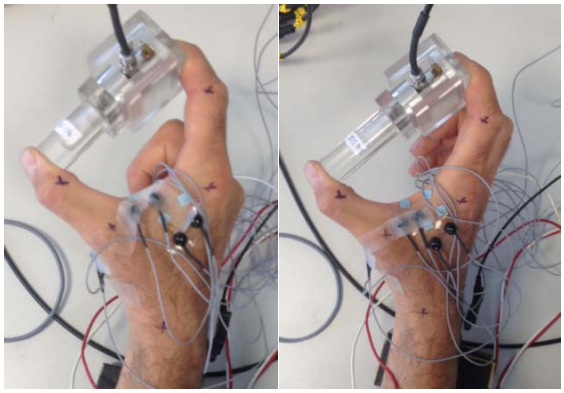

(d) (e)

Figure 3.5 Thumb-index pinch on the boxes with five different widths (a) 45 mm (b) 60 mm (c) 75 mm (d) 90 mm (e) 105 mm

Figure 3.4 shows thumb-index pinch on object at three wrist postures: flexion, neutral, and extension. Figure 3.5 shows thumb-index pinch on the boxes with five different widths: 45, 60, 75, 90, and 105 mm. The experimental procedure can be described by following:

(1) Maximal voluntary contractions (MVCs) of five specific muscles: AP, APB, FDI, FPL, and EPL were obtained using manual muscle testing as described by Kendall et al. [101]. The subjects were asked to maintain MVCs with duration of 3 s and repeat three times. For each subject, a total of 15 data sets were collected (5 muscles × 3 trials).

(2) The maximal pinch force (F_{max}) was performed. The subjects seated in a chair with the elbow flexed at 90° and the lower forearm resting in the horizontal plane. The subjects were asked to pinch the object with maximal force with 3 s in duration. The maximum contraction was repeated 3 times with at least 30 s of rest between the trials for each wrist posture and object width. The order of wrist posture/object width combinations was randomized. For each subject, a total of 45 data sets were collected (3 wrist postures × 5 object width × 3 trials).

(3) The subjects performed 4 static levels of contraction: 10, 30, 50, and 70% F_{max} for 4 s in duration and repeat the contraction 3 times. The order of wrist posture and object width combinations was randomized. For each subject, a total of 180 data sets were collected (3 wrist postures × 5 object widths × 4 force levels × 3 trials).

In addition, 21 anthropometric variables: (1) body mass, (2) standing height, (3) hand length, (4) hand breadth, (5) bicep circumference, (6) shoulder breadth, (7) forearm circumference, (8) wrist circumference, (9) elbow circumference, (10) hand circumference, (11) max hand circumference, (12) hand width, (13) elbow-fingertip length, (14) shoulder-elbow length, (15) thumb length, (16) index finger length, (17) index finger circumference (metacarpophalangeal joint, MCP), (18) index finger circumference (proximal interphalangeal joint, PIP), (19) index finger circumference (distal interphalangeal joint, DIP), (20) thumb circumference (MCP), and (21) thumb circumference (interphalangeal joint, IP), were measured from the right arm of all subjects.

3.2.2 Evaluation of pattern recognition techniques

Figure 3.6 showed the flowchart of the experiment starting with the filtered EMG signal and force signal by notch filter. The comparison between before and after signal filtering was shown in Figure 3.7 and examples of filtered EMG in each channel were shown in Figure 3.8. Then, the filtered EMG was segmented using a 250-ms analysis window with 50% overlapping, so 14 segments were prepared for next step, feature extraction. In this study, 12 features in time domain were extracted from each segment and each channel of EMG. The names and equations of each method were presented in Table 3.2. In total, 156 columns (12 features × (12 channels + 1 force data)) and 3,150 rows (14 segments × 3 trials × 3 postures × 5 force levels × 5 box widths) were obtained for each feature extraction method.

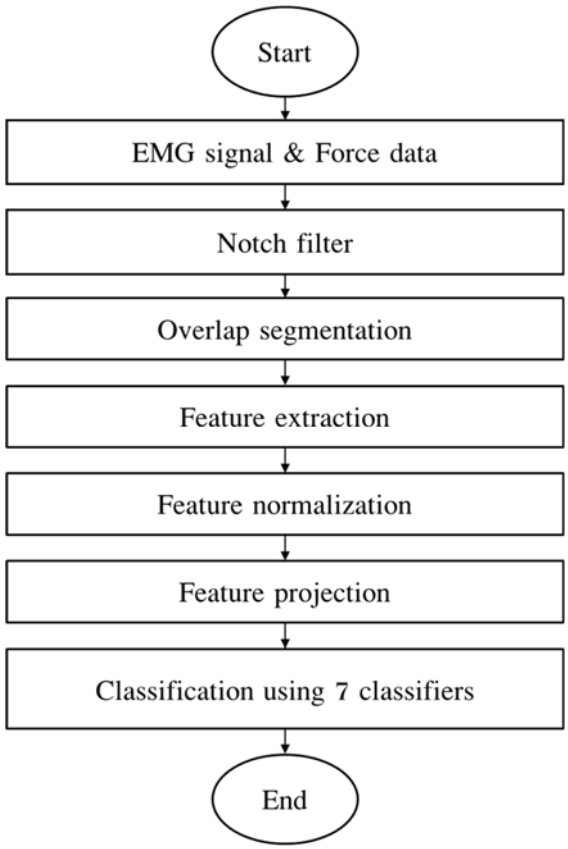

Figure 3.6 Flowchart of the experiment.

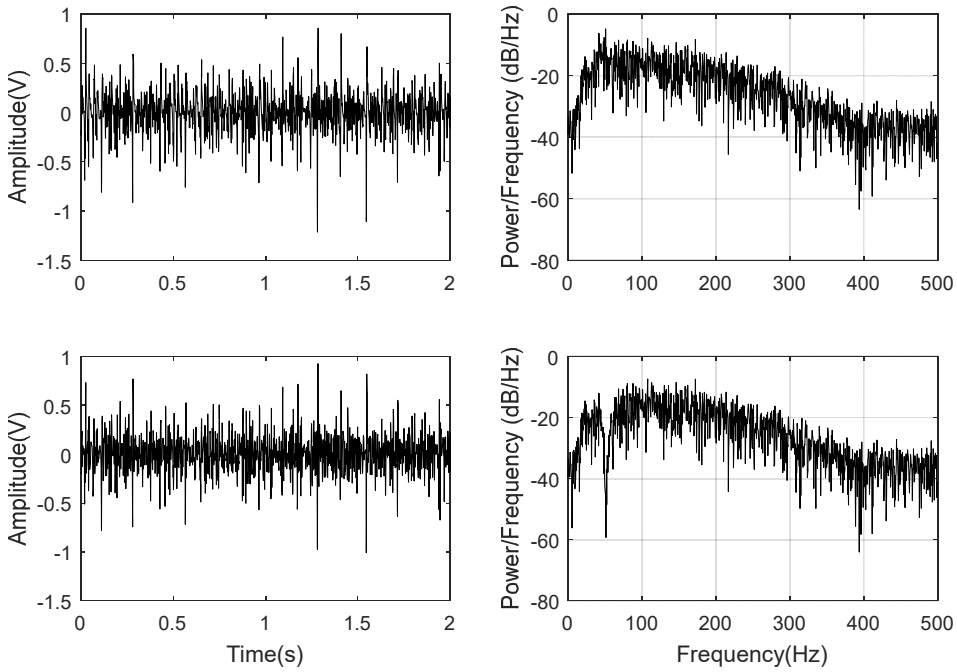

Figure 3.7 Example of EMG signal plots in time domain (left) and frequency domain (right) before filtering (top) and after filtering (bottom).

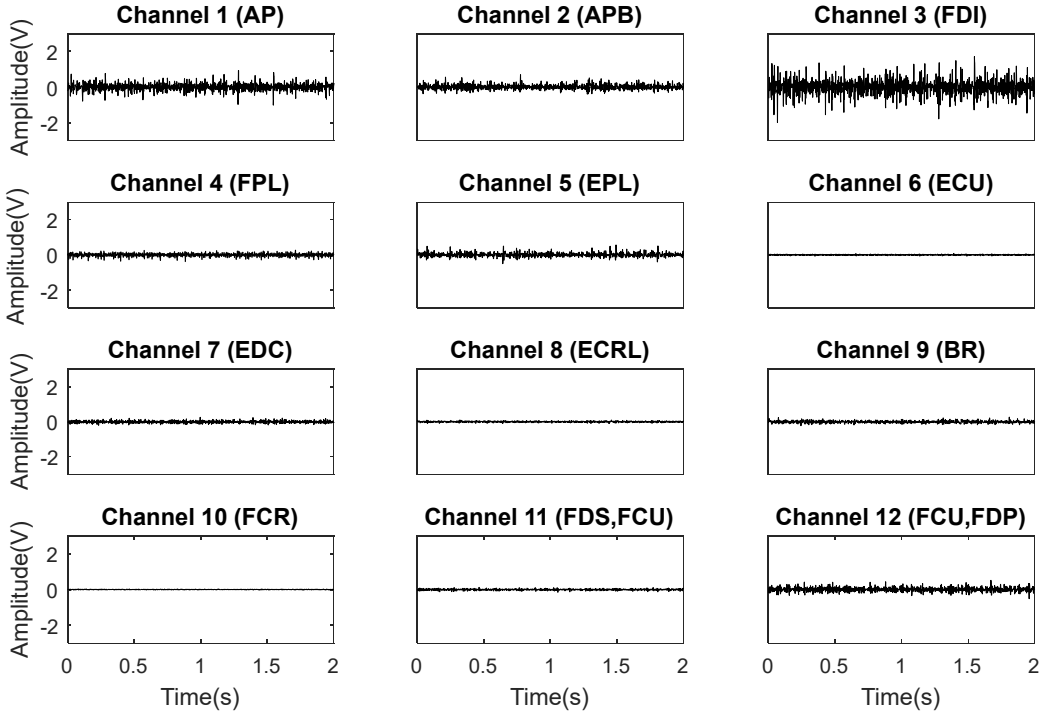

Figure 3.8 Example of 12-channel EMG data after filtering.

Table 3.2 List of time domain features used in this study

Feature name	Equation
1) Difference Absolute Standard Deviation Value	$\mathrm{DASDV} = \sqrt{\frac{1}{N-1}\sum_{i=1}^{N-1}(x_{i+1}-x_i)^2}$
2) Log Detector	$\mathrm{LOG} = e^{\frac{1}{N}\sum_{i=1}^{N}\log(\lvert x_i\rvert)}$
3) Modified Mean Absolute Value 1	$\mathrm{MAV1} = \frac{1}{N}\sum_{i=1}^{N} w_i \lvert x_i \rvert$ $w_i = \begin{cases} 1, & \text{if } 0.25N \le i \le 0.75N \\ 0.5, & \text{otherwise} \end{cases}$
4) Modified Mean Absolute Value 2	$\mathrm{MAV2} = \frac{1}{N}\sum_{i=1}^{N} w_i \lvert x_i \rvert$ $w_i = \begin{cases} 1, & \text{if } 0.25N \le i \le 0.75N \\ 4i/N, & \text{elseif } i < 0.25N \\ 4(i-N)/N, & \text{otherwise} \end{cases}$
5) Mean Absolute Value (MAV)	$\mathrm{MAV} = \frac{1}{N}\sum_{i=1}^{N} \lvert x_i \rvert$
6) Maximum Fractal Length (MFL)	$\mathrm{L}_m(k) = \frac{\left\{\left(\sum_{i=1}^{\left\lfloor\frac{N-m}{k}\right\rfloor}\left\lvert X\left(m+ik\right)-X\left(m+(i-1).k\right)\right\rvert\right)\frac{N-1}{\left\lfloor\frac{N-m}{k}\right\rfloor.k}\right\}}{k}$
7) Root Mean Square	$\mathrm{RMS} = \sqrt{\frac{1}{N}\sum_{i=1}^{N} x_i^2}$
8) Third Temporal Moment	$3^{rd}TM = \left\lvert\frac{1}{N}\sum_{i=1}^{N} x_i^3\right\rvert$
9) Forth Temporal Moment	$4^{th}TM = \left\lvert\frac{1}{N}\sum_{i=1}^{N} x_i^4\right\rvert$
10) Fifth Temporal Moment	$5^{th}TM = \left\lvert\frac{1}{N}\sum_{i=1}^{N} x_i^5\right\rvert$
11) Variance of EMG	$\mathrm{VAR} = \frac{1}{N-1}\sum_{i=1}^{N} x_i^2$
12) Waveform Length	$\mathrm{WL} = \sum_{i=1}^{N-1} \lvert x_{i+1} - x_i \rvert$

Figure 3.9 to Figure 3.11 shows examples of averaged EMG and boxplot of averaged force data of three times of trial from subject 2 in a) and b), respectively. Figure 3.9 represents them in each posture estimated from 45 mm box width and 10% force level. Figure 3.10 appears the EMG and force data in force classification obtained from flexion posture and 45 mm box width. Figure 3.11 shows them in each box width of flexion posture and 10% force level.

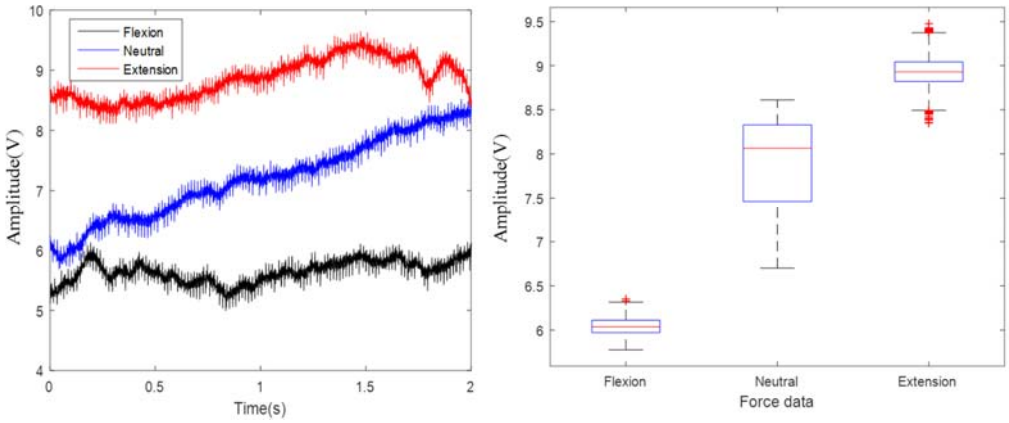

(a) (b)

Figure 3.9 Example of force data (a) and boxplot of its average (b) obtained from three times of trial in each posture from 45 mm box width and 10% force level.

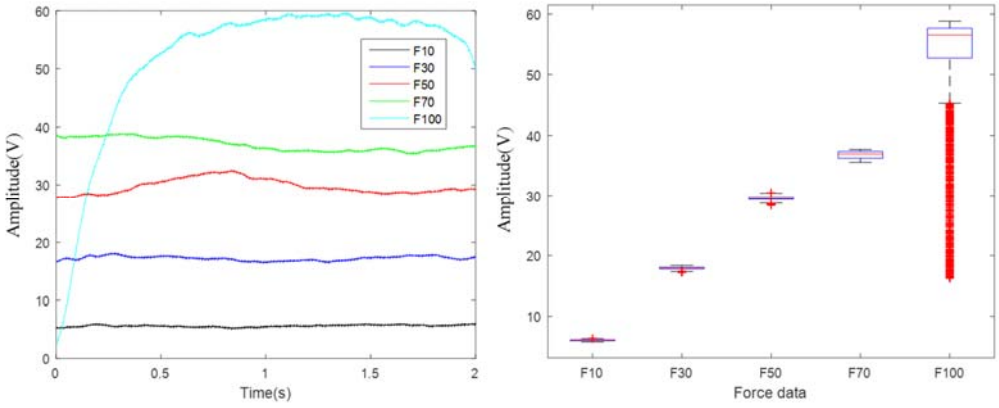

(a) (b)

Figure 3.10 Example of force data (a) and boxplot of its average (b) obtained using three times of trial on five different forces from flexion posture and 45 mm box width.

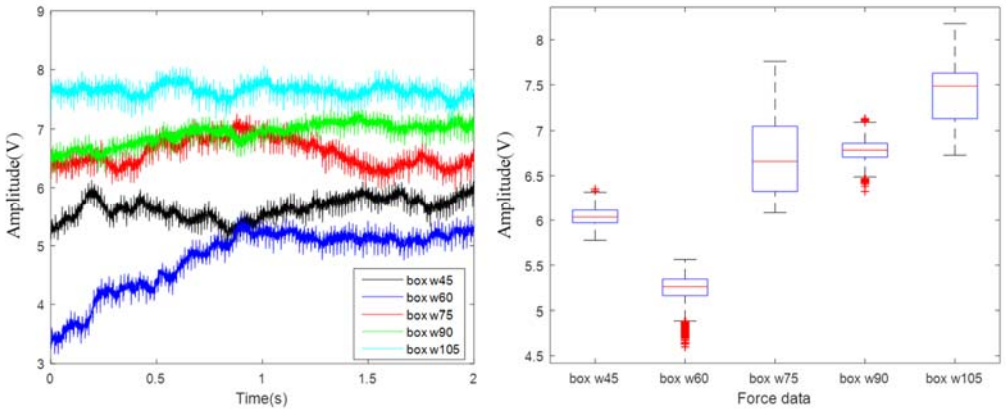

(a) (b)

Figure 3.11 Example of force data (a) and boxplot of averaged its average (b) obtained using three times of trial on five different box widths from flexion posture and 10% force level.

Then, each column of feature values was normalized using the min–max normalization method, resulting in the range of value from -1 to 1 before entering to the feature projection step. The dimension of EMG features was reduced using six methods of feature projection described in Section 2.2.2 including SRLEM, LDA, ULDA, OFNDA, SRDA, and PCA. Finally, reduced features set were classified using 7 classifiers, namely decision tree (DT), linear discriminant analysis (LDA), quadratic discriminant analysis (QDA), support vector machine (SVM), k-nearest neighbour (KNN), Naïve Bayes and neural network (NN). The parameters in all classifiers were defined as default. For example, the DT was no pruning and purity binary splitting criterion, the LDA and QDA were no regularization, the SVM was defined the radial basis function as the kernel function, the number of k in KNN classifier was randomly selected based accuracy, the Naïve Bayes was 10 bins and the architecture of NN was the feed-forward network and trained by the Levenberg-Marquardt, the number of neurons in one hidden layer was compared between 10, 20 and 30, and the number of iterations to train was 50. The 10-fold cross-validation was applied for the performance evaluation from each classifier during the training.

The evaluation of pattern recognition techniques is divided into 2 experiments. Both of them focus on the step after feature extraction which is reduction of the complexity and time of processing called feature projection.

1) Feature projection using SRELM method

In this experiment, the SRELM method is applied to the data to test the performance of feature projection step and to compare between with and without force data in the classification. However, the data estimated from three subjects are tested in this study.

2) Feature projection comparison

In this experiment, six feature projection techniques are used with the extracted feature data of subject 2. The comparison performance obtained from seven classifiers is studied. Moreover, the different number of neurons in hidden layer of neural network classifier (10, 20, 30 neurons) are compared.

3.3 Results and discussion

The results can be divided into 3 patterns of classification including postures, force levels and box widths. The postures are grouped into 3 types: flexion, neutral and extension. The force levels are grouped into 5 classes: 10, 30, 50, 70, 100 percent of the maximum force. The box widths are divided into 5 groups including 45, 60, 75, 90, 105 mm.

3.3.1 Feature projection using SRELM method

Figure 3.12 shows the EMG signal from channel 1 in each posture at 45 mm box width and 10% force level. The EMG in flexion posture gives the highest amplitude, whereas the neutral posture is the lowest. Figure 3.13 shows the boxplot of averaged MAV values in each posture from all box widths and all force levels. It is found that their mean values are comparable. However, the SRELM projection method is able to classify them as shown in Figure 3.14. Figure 3.14 (a) shows scatter plots of normal MAV feature from 2 channels, whereas Figure 3.14 (b) shows scatter plot after using SRELM method. The results show that the SRELM is clearly classified three postures. Table 3.3 shows the accuracies from SRELM method and each

classifier compared between with and without force data in subject 1, 2 and 3. They show that the accuracies obtained from force data is slightly increased from them without force data in all subjects. Although the accuracies obtained from QDA, KNN and NN are higher accuracy than others, the accuracies are quite high (>95%) in all classifiers.

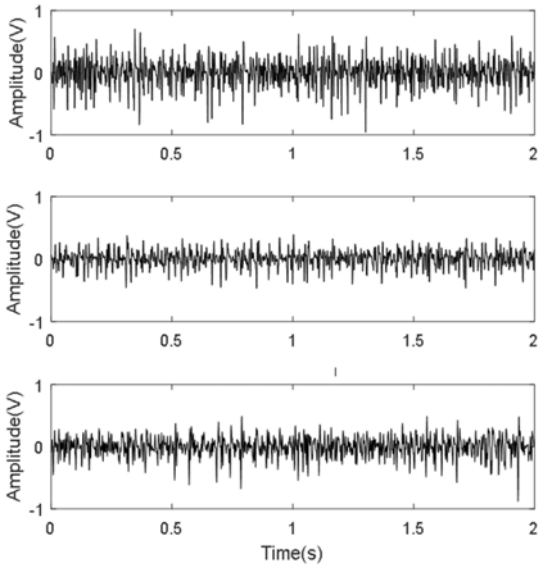

Figure 3.12 Example of EMG signal from channel 1 in three postures, 45 mm box width, 10% force level and 1st trial. Top, middle, and bottom panels represent posture of flexion, neutral and extension, respectively.

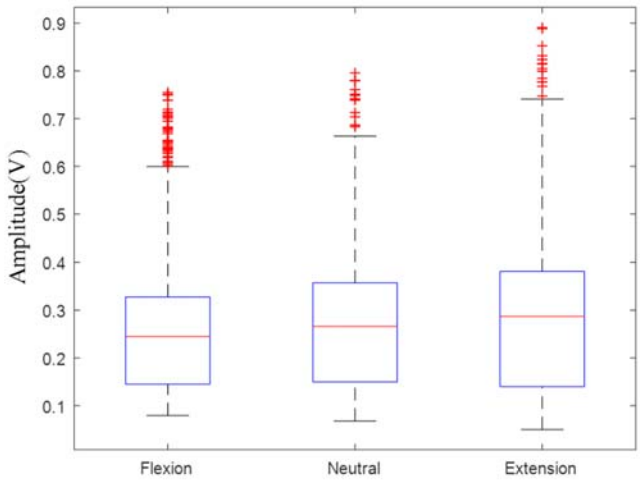

Figure 3.13 Boxplot of MAV values in each posture from channel 1 that are averaged from all box widths, all force levels and all trials.

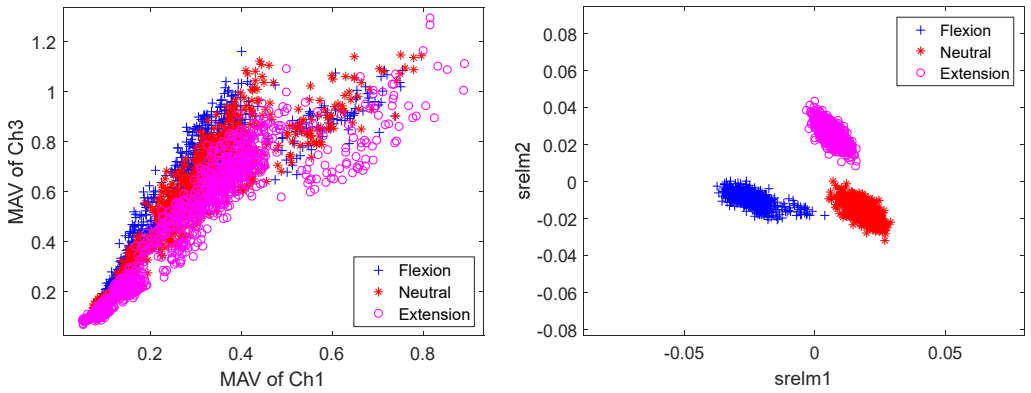

(a) (b)

Figure 3.14 Scatter plot from MAV features (ch1 and ch3) (a) and from the feature projection (SRELM) (b) in posture classification of subject 2, all box widths, all force levels and all trials.

Table 3.3 Accuracies from each classifier compared between with and without force data in subject 1, 2 and 3 using SRELM as feature projection in posture classification.

Classifiers	Subject 1		Subject 2		Subject 3	
	With force data	Without force data	With force data	Without force data	With force data	Without force data
DT	98.06±0.71	97.37±0.98	99.75±0.33	99.43±0.42	96.28±1.27	93.40±1.97
LDA	98.86±0.54	98.22±0.60	99.84±0.34	99.71±0.32	97.91±0.49	97.30±0.54
QDA	99.02±0.48	98.51±0.45	99.97±0.10	99.90±0.15	98.34±0.78	97.30±0.69
SVM	98.73±0.75	97.78±0.85	99.71±0.48	99.52±0.46	98.09±0.65	97.60±0.76
KNN	98.79±0.59	98.38±0.51	99.94±0.13	99.94±0.13	98.14±0.68	97.50±0.72
Naïve Bayes	98.03±0.94	97.27±1.05	99.37±0.63	99.40±0.51	97.42±0.94	96.80±0.70
NN	98.83±0.50	98.19±0.67	99.94±0.13	99.90±0.15	97.88±0.81	97.60±0.81

Figure 3.15 shows the EMG signal from channel 1 in each force level at flexion posture and 45 mm box width. The amplitude of EMG is consistent with the level of force. In other words, a higher force level means the higher amplitude. Figure 3.16 shows the boxplot of averaged MAV values in each force level from all postures and all box widths. The boxplot shows that their mean values are separated. Moreover, the scatter plots of MAV values from 2 channels and from SRELM method are shown in Figure 3.17 and Figure 3.18, respectively. The scatter plot from MAV feature is quite clear despite the fact that the force level of 70 has some overlap with force level of 50 and 100. The scatter plot obtained from SRELM method is shown in 6 panels

because the type resulted from the method is reduced from 5 to 4. They show that the force levels are separated with some overlap like Figure 3.17. However, the accuracies are high when used with the classifiers as shown in Table 3.4. It is also the comparison between with and without force data. The results show that both are slightly different with the higher found in force data like in posture classification.

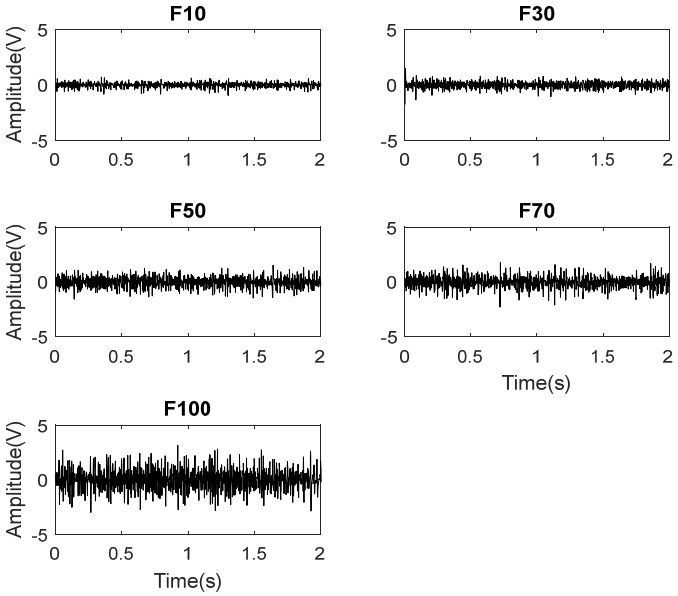

Figure 3.15 Example of EMG signal from channel 1 in five forces, flexion posture and 45 mm box width.

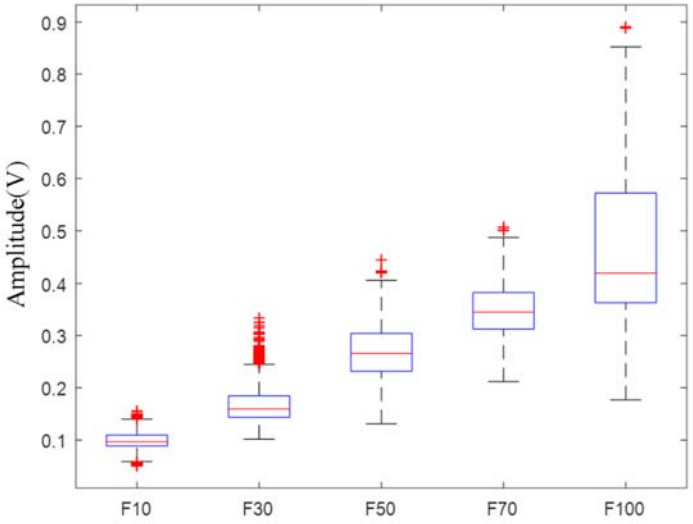

Figure 3.16 Boxplot of MAV value in each force level from channel 1 that are averaged from all postures all box widths and all trials.

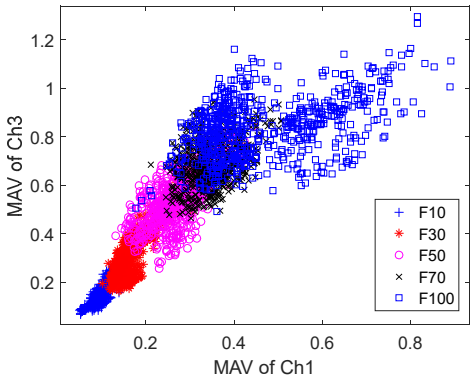

Figure 3.17 Scatter plot from MAV features (ch1 and ch3) in force classification, all postures, all box widths and all trials.

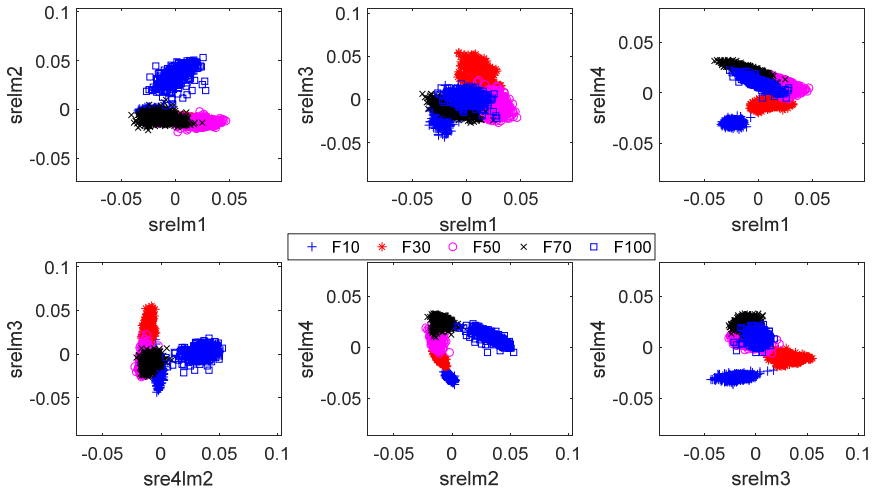

Figure 3.18 Scatter plot from the feature projection (SRELM) in force classification from all postures, all box widths and all trials.

Table 3.4 Accuracies from each classifier compared between with and without force data in subject 1, 2 and 3 using SRELM as feature projection in force classification.

Classifiers	Subject 1		Subject 2		Subject 3	
	With force data	Without force data	With force data	Without force data	With force data	Without force data
DT	96.95±1.11	93.65±1.12	96.98±0.94	96.35±0.89	97.46±1.34	91.40±1.17
LDA	98.38±0.71	95.87±1.06	98.25±0.71	98.00±0.86	99.17±043	93.40±1.58
QDA	98.25±0.81	95.59±1.33	98.10±0.76	97.84±1.22	99.37±0.42	93.11±1.28
SVM	95.90±1.04	94.79±1.25	97.11±0.57	96.35±1.13	97.75±0.94	92.41±1.26
KNN	98.22±0.72	96.16±1.06	98.25±0.74	97.43±1.08	99.33±0.35	93.84±1.15
Naïve Bayes	97.30±0.78	95.43±1.15	96.63±0.71	96.00±0.98	97.84±0.79	91.52±1.62
NN	98.67±0.82	96.73±1.04	98.41±0.65	97.68±0.70	99.17±0.45	93.90±1.51

Figure 3.19 shows the EMG signal from channel 1 in each box width at flexion posture and 10% force level and Figure 3.20 shows the boxplot of averaged MAV values in each box width from all postures and all force levels. The boxplot indicates that their mean values are not different and not significant in each box width. Figure 3.21 shows the scatter plots of MAV values from 2 channels that are quite difficult to separate each group. Figure 3.22 shows the scatter plots from SRELM method in 6 panels. They show that the box width separation is better than that before entering the process. Table 3.5 represents the accuracies obtained from each classifier that the best accuracy is from KNN classifier. However, they are high in all classifiers, especially when obtaining with force data.

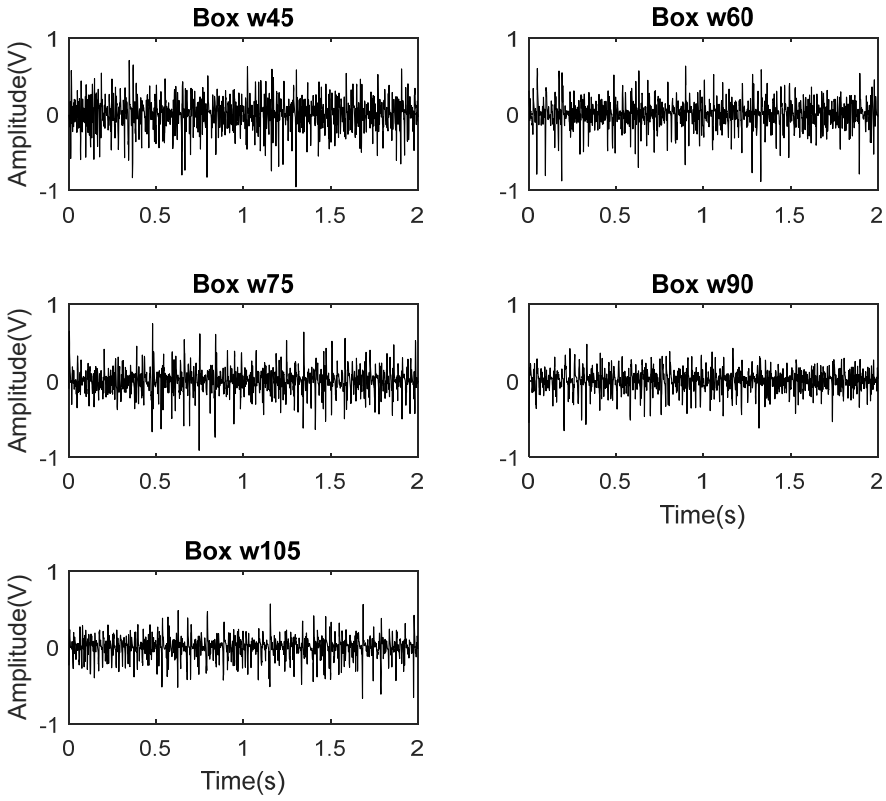

Figure 3.19 Example of EMG signal from channel 1 in five box width, flexion posture and 10% force level.

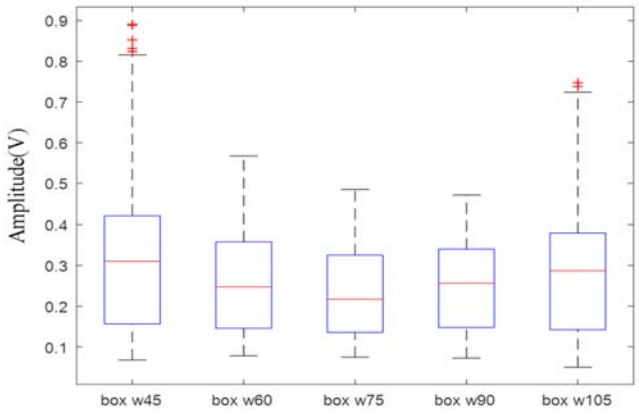

Figure 3.20 Boxplot of MAV value in each box width from channel 1 that are averaged from all postures all force levels and all trials.

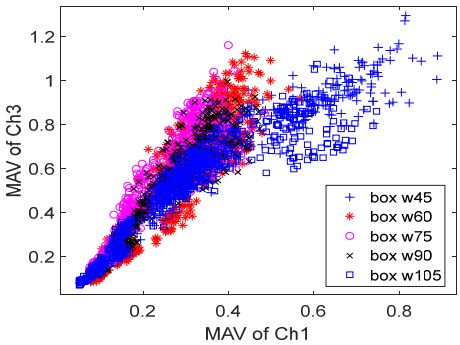

Figure 3.21 Scatter plot from MAV features (ch1 and ch3) in box width classification from all postures, all force levels and all trials.

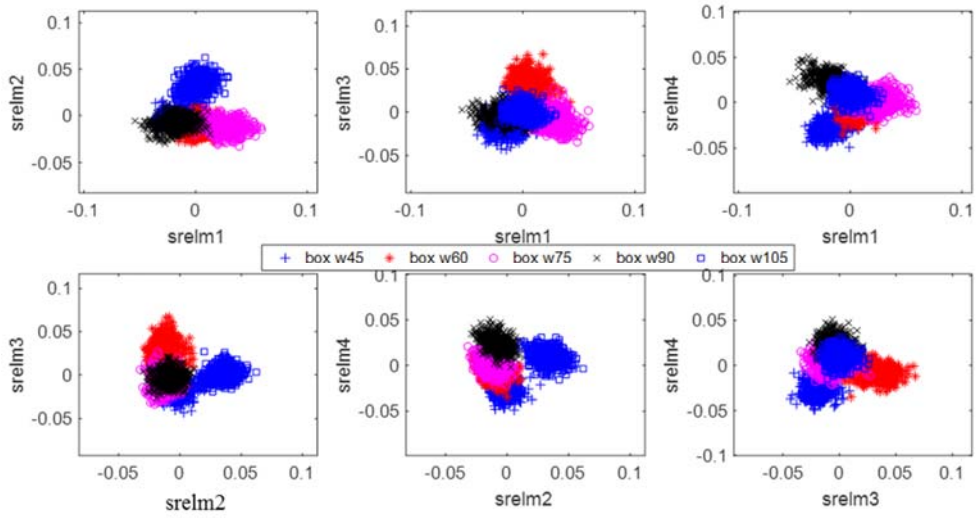

Figure 3.22 Scatter plot from the feature projection (SRELM) in box width classification from all postures, all force levels and all trials.

Table 3.5 Accuracies from each classifier compared between with and without force data in 1, 2 and 3 using SRELM as feature projection in box width classification.

Classifiers	Subject 1		Subject 2		Subject 3	
	With force data	Without force data	With force data	Without force data	With force data	Without force data
DT	91.43±2.01	88.10±1.69	91.33±1.96	90.67±1.51	96.51±1.76	94.79±1.53
LDA	94.92±1.03	92.19±1.38	94.76±1.63	94.79±1.67	98.60±0.51	96.87±0.84
QDA	94.95±1.26	92.32±1.23	95.40±1.41	95.05±1.53	98.73±0.73	97.11±0.61
SVM	94.13±1.27	91.97±1.23	94.16±1.99	94.48±1.53	98.44±0.80	96.19±1.22
KNN	94.95±1.15	92.76±1.62	95.87±1.50	95.49±1.14	98.92±0.67	97.08±0.96
Naïve Bayes	93.84±1.30	90.67±1.86	92.98±1.78	93.75±1.40	98.32±0.52	95.56±1.19
NN	94.86±1.25	92.73±1.38	94.86±1.58	94.95±1.02	98.70±0.66	97.02±0.58

3.3.2 Feature projection method comparison

The accuracies obtained from the methods of feature projection and classifiers in classifying postures, force levels, and box widths are shown in Table 3.6, Table 3.7, and Table 3.8, respectively. The highest accuracy in each feature projection method is given in bold typeface and that in each classifier is given in *slanted* typeface. The best of all in the classification is filled in yellow shading.

In posture classification (Table 3.6), most high accuracies are from QDA classifier that works together with the feature projection of SRELM, ULDA and FNPAQR method. They give the accuracies at 99.97%, 99.81%, and 100%, respectively. The highest accuracy in each classifier is found in different methods of feature projection. However, all classifiers give the high performance in all feature projection methods, except in PCA, that is only found in KNN classifier (94.10%).

In force classification (Table 3.7), most high accuracies are from KNN classifier that works together with the feature projection of LDA, PCA and SRDA method. They give the accuracies at 96.38%, 98.10%, and 95.75%, respectively. All highest accuracies in each classifier are from SRELM method that the best (98.41%) is found in NN classifier with 10 neurons. However, all classifiers give the high performance in all feature projection methods.

Table 3.6 Accuracies performance (%) obtained from the posture classification in Subject 2.

	SRELM	LDA	PCA	SRDA	ULDA	FNPAQR
DT	99.75±0.33	*99.75±0.20*	89.68±1.30	99.75±0.25	99.49±0.37	99.68±0.30
LDA	99.84±0.34	99.71±0.38	81.05±1.94	99.43±0.54	99.62±0.29	*99.84±0.22*
QDA	**99.97±0.10**	99.81±0.31	79.27±1.70	99.81±0.31	**99.81±0.27**	***100.00***
SVM	*99.71±0.48*	99.68±0.30	88.41±6.79	99.30±0.75	99.46±0.40	99.68±0.40
KNN	*99.94±0.13*	99.87±0.22	**94.10±1.13**	99.87±0.16	99.75±0.25	*99.94±0.13*
Naïve Bayes	99.37±0.63	*99.75±0.39*	72.16±3.73	98.79±0.73	99.71±0.23	99.71±0.32
NN (10)	99.94±0.13	99.68±0.42	87.49±1.65	99.84±0.22	99.75±0.25	*99.97±0.10*
NN (20)	99.90±0.21	99.87±0.22	87.97±2.36	**99.90±0.15**	99.78±0.26	*99.94±0.13*
NN (30)	99.90±0.15	**99.87±0.16**	87.27±2.32	99.87±0.16	99.68±0.30	*99.97±0.10*

Table 3.7 Accuracies performance (%) obtained from the force classification in Subject 2.

	SRELM	LDA	PCA	SRDA	ULDA	FNPAQR
DT	*96.98±0.94*	94.79±1.70	92.44±1.87	91.43±1.70	95.21±1.01	95.11±1.51
LDA	*98.25±0.71*	95.24±1.22	87.40±1.30	93.37±1.42	95.71±0.97	96.06±1.47
QDA	*98.10±0.76*	95.40±1.04	91.46±1.11	94.29±1.20	96.22±0.94	96.19±0.81
SVM	*97.11±0.57*	93.71±1.41	96.48±1.13	91.94±1.20	91.68±1.00	91.94±2.25
KNN	*98.25±0.74*	**96.38±0.94**	**98.10±0.76**	**95.75±1.10**	95.84±0.83	95.40±1.39
Naïve Bayes	*96.63±0.71*	93.33±2.11	81.81±1.61	90.67±1.03	95.46±0.75	95.56±1.19
NN (10)	***98.41±0.65***	96.13±1.55	94.06±1.41	95.14±0.81	96.41±0.91	96.44±1.22
NN (20)	*98.41±0.71*	94.25±6.19	95.56±0.88	95.11±1.19	**96.51±1.16**	96.51±1.00
NN (30)	*98.32±0.76*	96.03±1.72	95.08±1.59	95.27±1.03	96.48±0.78	**96.98±1.13**

In force classification (Table 3.8), most high accuracies are from KNN classifier that works together with the feature projection of LDA, PCA, SRDA, and FNPAQR method. They give the accuracies at 90.83%, 91.59%, 87.87%, and 90.35%, respectively. All highest accuracies in each classifier are from SRELM method that the best (97.27%) is found in NN classifier with 30 neurons in hidden layer. However, all classifiers give the high performance in all feature projection methods.

Table 3.8 Accuracies performance (%) obtained from the box-width classification in Subject 2.

	SRELM	LDA	PCA	SRDA	ULDA	FNPAQR
DT	*91.33±1.96*	84.29±2.41	77.05±2.41	79.87±2.30	85.05±2.18	84.22±2.47
LDA	*94.76±1.63*	88±2.01	31.33±3.08	81.27±1.63	90±1.55	89.78±1.58
QDA	*95.39±1.41*	88±2.36	35.24±2.98	82.92±1.21	89.56±1.45	90±1.32
SVM	*94.15±1.99*	84.73±3.08	86.98±2.87	79.37±2.29	87.90±1.72	87.87±1.40
KNN	*95.87±1.50*	**90.83±2.07**	**91.59±2.00**	**87.87±1.80**	89.84±1.82	**90.35±1.48**
Naïve Bayes	*92.98±1.78*	86.06±1.61	34.06±2.84	79.90±2.17	87.81±1.99	88.19±1.21
NN (10)	*97.24±1.17*	87.87±6.35	60.63±3.95	84.95±1.66	90.1±2.01	90.06±1.67
NN (20)	*97.05±1.44*	88.89±1.90	71.59±4.33	86.98±1.37	**91.43±1.11**	88.89±1.90
NN (30)	***97.27±1.38***	88.57±6.09	76.83±5.18	86.51±1.67	90.16±0.90	88.57±6.09

Figure 3.23 shows the RES index calculated from projected features by each feature projection method. The RES index of projected features by PCA is lower than that of other feature projection techniques in all classifications. Conversely, the SRELM is the highest RES index except in force classification that the baseline and LDA give the better results. The RES indexes of projected features from SRDA, ULDA, and FNPAQR are extremely similar. Moreover, the results showed that the classification of five box widths gives the lowest value in all feature projection methods. In other words, the box width classification is more difficult to categorize than other classifications.

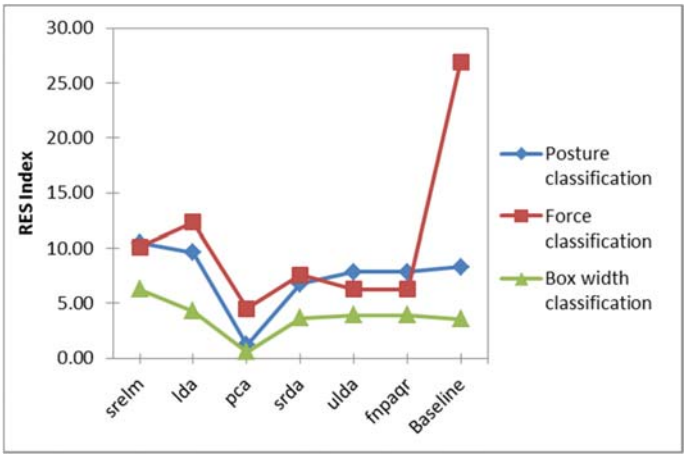

Figure 3.23 RES Index in feature projection method comparing with baseline feature in posture classification, force classification and box width classification.

3.4 Conclusions

In the study of pinch EMG data, the system for three classifications including postures, force levels and box widths observed by 12 channels of EMG signals and force signal is proposed. Twelve time domain features are extracted from data. Six feature projection techniques are evaluated like in flexion data. Firstly, the effect of force data from the force sensor is also studied by comparing results between with and without force data in the classifications by using the SRELM technique for projecting the features. Then, the performances obtained from seven classifiers are compared. The result of the effect of force data shows that the performance from EMG with force data can slightly increase that from only EMG data. The results from the comparison of feature projection methods show that the SRELM gives the best performance in force and box width classifications. However, the RES index obtained from SRELM show that is the best feature separation ability in posture and box width classification and is less than the results from baseline and LDA in force classification. The results of classifier comparison show that KNN provides the valuable performance in force and box width classification, especially when using with the feature projection of LDA, PCA, and SRDA. Nevertheless, the best accuracy is from NN when working together with SRELM in force and box width classification, whereas the classification accuracy of up to 100% is from the combination of QDA classifier and FNPAQR feature projection in posture classification.

CHAPTER 4 Conclusions and recommendations for future work

4.1 Conclusions

In this study, six feature projection techniques were evaluated including PCA, LDA, ULDA, OFNDA, SRDA, and SRELM. Seven classifiers were validated, namely, SVM, LC, NB, KNN, RBF-ELM, AW-ELM, and NN.

In flexion EMG data, the system for classifying 14 finger movements, involving individual and combined finger flexion observed by 6 channels of EMG signals is proposed. The results of feature projection comparison show that the projected features from SRELM give the best performance in terms of feature separation among these feature projection techniques. The results of classifier comparison show that NN provides the best performance in separating 6-channel EMG signals to identify 14 finger movements. Classification accuracy of up to 99% was reached when using SRELM and NN in combination.

In pinch EMG data, the system for three classifications including postures, force levels and box widths observed by 12 channels of EMG signals and force signal is proposed. The results from the comparison of feature projection methods show that the SRELM gives the best performance in force and box width classifications. However, the RES index obtained from SRELM show that is the best feature separation ability in posture and box width classification and is less than the results from baseline and LDA in force classification. The results of classifier comparison show that KNN provides the valuable performance in force and box width classification, especially when using with the feature projection of LDA, PCA, and SRDA. Nevertheless, the best accuracy is from NN when working together with SRELM in force and box width classification, whereas the classification accuracy of up to 100% is from the combination of QDA classifier and FNPAQR feature projection in posture classification. However, the effect of force data from the force sensor is also studied by comparing results between with and without force data in the classifications by using the SRELM technique for projecting the features. The result of the effect of force data shows that the performance from EMG with force data can slightly increase that from only EMG data.

In summary, the classification accuracies are quite high when using the feature projection methods with the optimal classifiers. Moreover, the processing time of using feature projection is less than using all features and all EMG channels to be input of classifiers.

4.2 Recommendations for future study

In the future, the other algorithms in pattern recognition, e.g., other features of time domain and frequency domain, or feature selection technique, or combining the classifier, will be applied to improve the performance of the EMG classification. Moreover, the posture, force level, and box width classifications will be concluded to predict the data immediately.

References

[1] T. A. Kuiken, G. Li, B. A. Lock, R. D. Lipschutz, L. A. Miller, K. A. Stubblefield, and K. Englehart, "Targeted muscle reinnervation for real-time myoelectric control of multifunction artificial arms," *J. Am. Med*. Assoc., vol. 301, no. 6, pp. 619–628, Feb. 2009.

[2] K. Englehart and B. Hudgins, "A robust, real-time control scheme for multifunction myoelectric control," *IEEE Trans. Biomed. Eng*., vol. 50, no. 7, pp. 848–854, Jul. 2003.

[3] B. Hudgins, P. Parker, and R. N. Scott, "A new strategy for multifunction myoelectric control," *IEEE Trans. Biomed. Eng*, vol. 40, no. 1, pp. 82–94, Jan. 1993.

[4] C. J. De Luca, "Physiology and mathematics of myoelectric signals," *IEEE Trans. Biomed. Eng*., vol. 26, no. 6, pp. 313–325, Jun. 1979.

[5] E. C. Orosco, N. M. Lopez, and F. di Sciascio, "Bispectrum-based features classification for myoelectric control," *Biomed. Signal Process. Control*, vol. 8, no. 2, pp. 153–168, Mar. 2013.

[6] M. A.Oskoei and H. Hu, "Myoelectric control systems—A survey," *Biomed. Signal Process. Control*, vol. 2, no. 4, pp. 275–294, Oct. 2007.

[7] P. Parker, K. Englehart, and B. Hudgins, "Myoelectric signal processing for control of powered limb prostheses," *J. Electromyogr. Kinesiol.*, vol. 16, no. 6, pp. 541–548, Dec. 2006.

[8] N. Fligge, H. Urbanek, and P. van der Smagt, "Relation between object properties and EMG during reaching to grasp," *J. Electromyogr. Kinesiol.*, vol. 23, no. 2, pp. 402–410, Apr. 2013.

[9] J. A. Birdwell, L. J. Hargrove, R. F. ff. Weir, and T. A. Kuiken, "Extrinsic finger and thumb muscles command a virtual hand to allow individual finger and grasp control," *IEEE Trans. Biomed. Eng*., vol. 62, no. 1, pp. 218–226, Jan. 2015.

[10] A. Harada, T. Nakakuki, M. Hikita, and C. Ishii, "Robot finger design for myoelectric prosthetic hand and recognition of finger motions via surface EMG," in *Proc.* IEEE International Conference on Automation and Logistics, 2010, pp. 273–278.

[11] G. Kondo, R. Kato, H. Yokoi, and T. Arai, “Classification of individual finger motions hybridizing electromyogram in transient and converged states,” in *Proc.* IEEE International Conference on Robotics and Automation, 2010, pp. 2909 –2915.

[12] R. N. Khushaba, S. Kodagoda, M. Takruri, and G. Dissanayake, “Toward improved control of prosthetic fingers using surface electromyogram (EMG) signals,” *Expert Sys. Appl.*, vol. 39, no. 12, pp. 10731–10738, 2012.

[13] X. Tang, Y. Liu, C. Lv, and D. Sun, “Hand motion classification using a multi-channel surface electromyography sensor,” *Sensors*, vol. 12, no. 2, pp. 1130–1147, Jan 2012.

[14] A. Hiraiwa, K. Shimohara, and Y. Tokunaga, “EMG pattern analysis and classification by neural network,” in *Proc.* IEEE International Conference on Systems, Man and Cybernetics, 1989, pp. 1113 –1115.

[15] N. Uchida, A. Hiraiwa, N. Sonehara, and K. Shimohara, “EMG pattern recognition by neural networks for multi fingers control,” in *Proc.* 14th Annual International Conference of the IEEE Engineering in Medicine and Biology, 1992, pp. 1016–1018.

[16] D. Nishikawa, W. Yu, H. Yokoi, and Y. Kakazu, “EMG prosthetic hand controller using real-time learning method,” in *Proc.* IEEE International Conference on Systems, Man and Cybernetics, 1999, pp. 153–158.

[17] F. C. P. Sebelius, B. N. Rosén, and G. N. Lundborg, “Refined myoelectric control in below-elbow amputees using artificial neural networks and a data glove,” *J. Hand Surg.*, vol. 30, no. 4, pp. 780–789, 2005.

[18] K. Nagata, K. Adno, M. Yamada, and K. Magatani, “A classification method of hand movements using multichannel electrode,” in *Proc.* 27th Annual International Conference of the IEEE Engineering in Medicine and Biology, 2005, pp. 2375–2378.

[19] K. Nagata, K. Ando, K. Magatani, and M. Yamada, “Development of the hand motion recognition system based on surface EMG using suitable measurement channels for pattern recognition,” in *Proc.* 29th Annual International Conference of the IEEE Engineering in Medicine and Biology. Soc., 2007, pp. 5214 –5217.

[20] F. Tenore, A. Ramos, A. Fahmy, S. Acharya, R. Etienne-Cummings, and N. V. Thakor, “Towards the control of individual Fingers of a prosthetic hand using surface EMG signals,” in *Proc.* 29th Annual International Conference of the IEEE Engineering in Medicine and Biology, 2007, pp. 6145–6148.

[21] F. V. G. Tenore, A. Ramos, A. Fahmy, S. Acharya, R. Etienne-Cummings, and N. V. Thakor, “Decoding of individuated finger movements using surface electromyography,” *IEEE Trans. Biomed. Eng.*, vol. 56, no. 5, pp. 1427 –1434, May. 2009.

[22] C. Antfolk, C. Cipriani, M. Controzzi, M. C. Carrozza, G. Lundborg, B. Rosén, and F. Sebelius, “Using EMG for real-time prediction of joint angles to control a prosthetic hand equipped with a sensory feedback system,” *J. Med. Biol. Eng.*, vol. 30, no. 6, pp. 399–406, 2010.

[23] C. Cipriani, C. Antfolk, C. Balkenius, B. Rosen, G. Lundborg, M. C. Carrozza, and F. Sebelius, “A novel concept for a prosthetic hand with a bidirectional interface: A feasibility study,” *IEEE Trans. Biomed. Eng.*, vol. 56, no. 11, pp. 2739–2743, Nov. 2009.

[24] C. Cipriani, C. Antfolk, M. Controzzi, G. Lundborg, B. Rosen, M. C. Carrozza, and F. Sebelius, “Online myoelectric control of a dexterous hand prosthesis by transradial amputees,” *IEEE Trans. Neural Syst. Rehabil. Eng.*, vol. 19, no. 3, pp. 260–270, Jun. 2011.

[25] G. R. Kanitz, C. Antfolk, C. Cipriani, F. Sebelius, and M. C. Carrozza, “Decoding of individuated finger movements using surface EMG and input optimization applying a genetic algorithm,” in *Proc.* 33rd Annual International Conference of the IEEE Engineering in Medicine and Biology, 2011, pp. 1608–1611.

[26] Y.-C. Du, C.-H. Lin, L.-Y. Shyu, and T. Chen, “Portable hand motion classifier for multi-channel surface electromyography recognition using grey relational analysis,” *Expert Sys. Appl.*, vol. 37, no. 6, pp. 4283–4291, 2010.

[27] G. R. Naik and D. K. Kumar, “Hybrid feature selection for myoelectric signal classification using MICA,” *J. Elec. Eng.*, vol. 61, no. 2, pp. 93–99, Mar. 2010.

[28] G. R. Naik and D. K. Kumar, “Identification of hand and finger movements using multi run ICA of surface electromyogram,” *J. Med. Sys.*, vol. 36, no. 2, pp. 841–851, Apr. 2012.

[29] G. R. Naik, D. K. Kumar, and M. Palaniswami, "Classification of low level surface electromyogram using independent component analysis," *IET Sig. Process*., vol. 4, no. 5, pp. 479 –487, Oct. 2010.

[30] G. R. Naik and D. K. Kumar, "Subtle Electromyographic pattern recognition for finger movements: A pilot study using BSS techniques," *J. Mech. Med. Biol.*, vol. 12, no. 04, p. 1250078, Sep. 2012.

[31] G. R. Naik, D. K. Kumar, and M. Palaniswami, "Signal processing evaluation of myoelectric sensor placement in low-level gestures: sensitivity analysis using independent component analysis," *Expert Syst*., 2012.

[32] M. Tavakolan, Z. G. Xiao, and C. Menon, "A preliminary investigation assessing the viability of classifying hand postures in seniors," *Biomed. Eng. Online*, vol. 10, p. 79, Sep. 2011.

[33] R. J. Smith, F. Tenore, D. Huberdeau, R. Etienne-Cummings, and N. V. Thakor, "Continuous decoding of finger position from surface EMG signals for the control of powered prostheses," in *Proc.* 30th Annual International Conference of the IEEE Engineering in Medicine and Biology, 2008, pp. 197–200.

[34] R. J. Smith, D. Huberdeau, F. Tenore, and N. V. Thakor, "Real-time myoelectric decoding of individual finger movements for a virtual target task," in *Proc.* 31st Annual International Conference of the IEEE Engineering in Medicine and Biology, 2009, pp. 2376–2379.

[35] N. P. Reddy and V. Gupta, "Toward direct biocontrol using surface EMG signals: Control of finger and wrist joint models," *Med. Eng. & Phys*., vol. 29, no. 3, pp. 398–403, 2007.

[36] N. Shrirao, N. Reddy, and D. Kosuri, "Neural network committees for finger joint angle estimation from surface EMG signals," *Biomed. Eng. Online*, vol. 8, no. 1, p. 2, Jan. 2009.

[37] D. Yang, J. Zhao, Y. Gu, X. Wang, N. Li, L. Jiang, H. Liu, H. Huang, and D. Zhao, "An anthropomorphic robot hand developed based on underactuated mechanism and controlled by EMG signals," *J. Bionic Eng*., vol. 6, no. 3, pp. 255–263, 2009.

[38] P. Kumar, A. Sebastian, C. Potluri, A. Ilyas, M. Anugolu, A. Urfer, and M. P. Schoen, "Adaptive finger angle estimation from sEMG data with multiple

linear and nonlinear model data fusion," in *Proc.* 10th World Scientific and Engineering Academy and Society (WSEAS) International Conference on Dynamical Systems and Control, 2011, pp. 154–159.

[39] A. Fassih, D. S. Naidu, S. Chiu, and P. Kumar, "Robust control of a prosthetic hand based on a hybrid adaptive finger angle estimation," in *Proc.* 11th international conference on Applications of Electrical and Computer Engineering, 2012, pp. 70–76.

[40] A. Andrews, E. Morin, and L. McLean, "Optimal electrode configurations for finger movement classification using EMG," in *Proc.* 31st Annual International Conference of the IEEE Engineering in Medicine and Biology, 2009, pp. 2987–2990.

[41] D. Peleg, E. Braiman, E. Yom-Tov, and G. F. Inbar, "Classification of finger activation for use in a roboticprosthesis arm," *IEEE Trans. Neural Syst. Rehabil. Eng.*, vol. 10, no. 4, pp. 290–293, Dec. 2002.

[42] G. Naik, D. Kumar, and S. Arjunan, "Pattern classification of myo-electrical signal during different maximum voluntary contractions: A study using BSS techniques," *Measure. Sci. Rev.*, vol. 10, no. 1, pp. 1–6, Jan. 2010.

[43] K. Nazarpour, A. H. Al-Timemy, G. Bugmann, and A. Jackson, "A note on the probability distribution function of the surface electromyogram signal," *Brain Res. Bull.*, vol. 90, pp. 88–91, Jan. 2013.

[44] Recommendations for sensor locations on individual muscles. [Online]. Available: http://www.seniam.org/ [Accessed: July 26, 2013].

[45] F. V. G. Tenore, A. Ramos, A. Fahmy, S. Acharya, R. Etienne-Cummings, and N. V. Thakor, "Decoding of individuated finger movements using surface electromyography," *IEEE Trans. Biomed. Eng.*, vol. 56, no. 5, pp. 1427 –1434, May. 2009.

[46] T. S. Saponas, D. S. Tan, D. Morris, and R. Balakrishnan, "Demonstrating the feasibility of using forearm electromyography for muscle-computer interfaces," *in Proc. of the SIGCHI Conference on Human Factors in Computing Systems*, 2008, pp. 515–524.

[47] L. Y. Shyu, J. Y. Chen, R. W. Tatn, and W. Hu, "A new electrode system for hand action discrimination,". *J. Med. Biol. Eng.*, vol. 22, no. 4, pp. 211-217, 2002

[48] Introduction to Targeted Forearm Muscle Training. [Online]. Avaiable: http://www.bisonstrength.com/blog/2010/04/introduction-to-targeted-forearm-muscle-training/ [Accessed: July 26, 2013].

[49] K. A. Farry, I. D. Walker and R. G. Baraniuk "Myoelectric teleoperation of a complex robotic hand", *IEEE Trans. on Robot. Auto.*, vol. 12, no. 5, pp.775 - 788 1996

[50] H. P. Huang, Y. H. Liu, L. W. Liu, and C.-S. Wong, "EMG classification for prehensile postures using cascaded architecture of neural networks with self-organizing maps," in *Proc.* IEEE International Conference on Robotics and Automation, 2003, pp. 1497 –1502.

[51] A. BoluAjiboye and R.F.Weir, "Fuzzy c-means clustering analysis of the EMG patterns of six major hand grasps," in *Proc.* 9th International Conference on Rehabilitation Robotics, 2005, pp. 49-52.

[52] C. Martelloni, J. Carpaneto, and S. Micera, "Characterization of EMG patterns from proximal arm muscles during object- and orientation-specific grasps," *IEEE Trans. Biomed. Eng*, vol. 56, no. 10, pp. 2529–2536, Oct. 2009.

[53] S. H. Walbran, E. P. Calius, G. Dunlop, and I. A. Anderson, "A technique for optimizing electrode placement for electromyographic control of prostheses," in 31st Annual International Conference of the IEEE Engineering in Medicine and Biology, 2009, pp. 1331–1334.

[54] Y. Y. Huang, K. H. Low, and H. B. Lim, "Objective and quantitative assessment methodology of hand functions for rehabilitation," in *Proc.* IEEE International Conference on Robotics and Biomimetics, pp. 846-851, 2009.

[55] G. C. Matrone, C. Cipriani, E. L. Secco, G. Magenes, and M. C. Carrozza, "Principal components analysis based control of a multi-DoFunderactuated prosthetic hand," *J. Neuroeng. Rehabil.*, vol. 7, p. 16, 2010.

[56] J. González, Y. Horiuchi, and W. Yu, "Classification of upper limb motions from around-shoulder muscle activities: hand biofeedback," *Open Med. Inform. J.*, vol. 4, pp. 74–80, 2010.

[57] A. Wolczowski and M. Kurzynski, "Human–machine interface in bioprosthesis control using EMG signal classification," *Expert Sys.*, vol. 27, no. 1, pp. 53–70, 2010.

[58] G. Li, A. E. Schultz, and T. A. Kuiken, “Quantifying pattern recognition-based myoelectric control of multifunctional transradial prostheses,” *IEEE Trans. Neural. Syst. Rehabil. Eng*, vol. 18, no. 2, pp. 185–192, Apr. 2010.

[59] J. U. Chu, D. H. Jeong, I. Youn, K. Choi, and Y. J. Lee, “Myoelectric hand prosthesis with novel adaptive grasping and self-locking,” *Int. J. Precis. Eng. Manuf*., vol. 12, no. 6, pp. 1095–1103, Dec. 2011.

[60] N. M. Kakoty and S. M. Hazarika, “Recognition of grasp types through principal components of DWT based EMG features,” in *Proc*. *IEEE International Conference on Rehabilitation Robotics. Robot*, 2011.

[61] Z. Ju, X. Zhu, and H. Liu, “Empirical Copula based templates to recognize surface EMG signals of hand motions,” *Int. J. Human. Robot.*, vol. 08, no. 04, pp. 725–741, Dec. 2011.

[62] G. C. Matrone, C. Cipriani, M. C. Carrozza, and G. Magenes, “Real-time myoelectric control of a multi-fingered hand prosthesis using principal components analysis,” *J. Neuroeng. Rehabil*., vol. 9, p. 40, 2012.

[63] N. Wang, Y. Chen, and X. Zhang, “Realtime recognition of multi-finger prehensile gestures,” *Biomed. Signal Process. Control*, vol. 13, pp. 262–269, 2014.

[64] H. Liu, “Exploring human hand capabilities Into embedded multifingered object manipulation,” *IEEE Trans. Indus. Inf.*, vol. 7, no. 3, pp. 389–398, 2011.

[65] L. A. Jones and S. J. Lederman, *Human Hand Function*. Oxford University Press, 2006.

[66] P. Jenmalm, A. W. Goodwin, and R. S. Johansson, “Control of grasp stability when humans lift objects with different surface curvatures,” *J. Neurophysiol*., vol. 79, no. 4, pp. 1643–1652, Apr. 1998.

[67] M. R. Cutkosky and R. D. Howe, “Human grasp choice and robotic gasp analysis,” *Dextrous Robot Hands*, S. T. Venkataraman and T. Iberall, Eds. Springer New York, 1990, pp. 5–31.

[68] G. Schlesinger. Der MechanischeAufbau der KünstlichenGlieder. In M. Borchardt et al., editors, Ersatzglieder und ArbeitshilfenfürKriegsbeschädigte und Unfallverletzte, pages 321–661. Springer-Verlag: Berlin, Germany, 1919.

[69] J. Kider, “UMCE-FM: Untethered motion capture evaluation for flightline maintenance support,” [Online]. Available: http://www.dtic.mil/cgi-bin/GetTRDoc?AD=ADA487504 [Accessed: July 26, 2013].

[70] R. Merletti, “Standards for reporting EMG data,” International society of electrophysiology and kinesiology,” [Online]. Available: http://educ.ubc.ca/faculty/sanderson/courses/HKIN473/pdf/ISEK_EMG-Standards.pdf [Accessed: July 26, 2013].

[71] M. A. Oskoei and H. Hu, “Support vector machine-based classification scheme for myoelectric control applied to upper limb,” *IEEE Trans Biomed Eng.*, vol. 55, no. 8, pp. 1956–1965, Aug. 2008.

[72] A. Phinyomark, F. Quaine, S. Charbonnier, C. Serviere, F. Tarpin-Bernard, and Y. Laurillau, “EMG feature evaluation for improving myoelectric pattern recognition robustness,” *Expert Sys. Appl.*, vol. 40, no. 12, pp. 4832–4840, Sep. 2013.

[73] K. Englehart, B. Hudgins, and P. A. Parker, “A wavelet-based continuous classification scheme for multifunction myoelectric control,” *IEEE Trans Biomed Eng.*, vol. 48, no. 3, pp. 302–311, Mar. 2001.

[74] M. Zardoshti-Kermani, B. C. Wheeler, K. Badie, and R. M. Hashemi, “EMG feature evaluation for movement control of upper extremity prostheses,” *IEEE Trans. Rehabili. Eng.*, vol. 3, no. 4, pp. 324–333, 1995.

[75] C. Chang and C. Lin, "LIBSVM: A Library for support vector machines," *ACM Trans. on Intel. Systems and Tech*., vol. 2, no. 3, p.27, 2011.

[76] M. I. Ibrahimy, M. R. Ahsan, and O. O. Khalifa, “Design and performance analysis of artificial neural network for hand motion detection from EMG signals,” *World Appl. Sci. J*., vol. 23, no. 6, pp. 751-758, 2013.

[77] A. Phinyomark, P. Phukpattaranont, and C. Limsakul, “Feature reduction and selection for EMG signal classification,” *Expert Sys. Appl.*, vol. 39, no. 8, pp. 7420–7431, Jun. 2012.

[78] N. Wang, Y. Chen, and X. Zhang, “The recognition of multi-finger prehensile postures using LDA,” *Biomed. Signal Process. Control*, vol. 8, no. 6, pp. 706–712, Nov. 2013.

[79] R. Boostani and M. H. Moradi, “Evaluation of the forearm EMG signal features for the control of a prosthetic hand,” *Physiol. Meas.*, vol. 24, no. 2, pp. 309–319, May 2003.

[80] A. Phinyomark, C. Limsakul, and P. Phukpattaranont, “Application of wavelet analysis in EMG feature extraction for pattern classification,” *Measure. Sci. Rev.*, vol. 11, pp. 45–52, Jan. 2011.

[81] M. Zecca, S. Micera, M. C. Carrozza, and P. Dario, “Control of multifunctional prosthetic hands by processing the electromyographic signal,” *Cri.t Rev. Biomed. Eng.*, vol. 30, no. 4–6, pp. 459–485, 2002.

[82] J. U. Chu, I. Moon, and MS. Mun, “A real-time EMG pattern recognition system based on linear-nonlinear feature projection for a multifunction myoelectric hand,” *IEEE Trans. Biomed. Eng.*, vol. 53, no. 11, pp. 2232–2239, Nov. 2006.

[83] R. N. Khushaba, A. Al-Ani, A. Alsukker, and A. Al-Jumaily, “A Combined ant colony and differential evolution feature selection algorithm,” *in Proc. of the 6th international conference on Ant Colony Optimization and Swarm Intelligence*, 2008, pp. 1–12.

[84] M. Hamedi, S.H. Salleh, and T. T., KamarulafizamSwee, “Surface electromyography-based facial expression recognition in bi-polar configuration,” *Jour. Comput. Sc.*, vol. 7, no. 9, pp. 1407–1415, Sep. 2011.

[85] I. Mohammad Rezazadeh, S. M. Firoozabadi, H. Hu, and S. M. R. HashemiGolpayegani, “A novel human--machine interface based on recognition of multi-channel facial bioelectric signals,” *Australas. Phys. Eng. Sci. Med.*, vol. 34, no. 4, pp. 497–513, Dec. 2011.

[86] A. Al-Timemy, R. Khushaba, G. Bugmann, and J. Escudero, “Improving the performance against force variation of EMG controlled multifunctional upper-limb prostheses for transradial amputees,” *IEEE Trans. Neural Syst. Rehabil. Eng.*, vol. PP, no. 99, pp. 1, Jun. 2015.

[87] K. Anam and A. Al-Jumaily. “A novel extreme learning machine for dimensionality reduction on finger movement classification using sEMG,” in *Proc. 7th IEEE conference in Neural Engineering*, 2015, pp. 824-827.

[88] A. Phinyomark, P. Phukpattaranont, and C. Limsakul, “Investigating long-term effects of feature extraction methods for continuous EMG pattern classification,” *Fluctuation Noise Lett.*, vol. 11, no. 4.

[89] A. H. Al-Timemy, G. Bugmann, J. Escudero, and N. Outram, “Classification of finger movements for the dexterous hand prosthesis control with surface electromyography,” *IEEE J. Biomed. Health Inform.*, vol. 17, no. 3 pp. 608-618, May 2013.

[90] R. N. Khushaba, S. Kodagoda, D. Liu, and G. Dissanayake, “Muscle computer interfaces for driver distraction reduction,” *Comput. Methods Programs Biomed.*, vol. 110, no. 2, pp. 137-149, May 2013.

[91] R. N. Khushaba, A. Al-Ani, and A. Al-Jumaily, "Orthogonal fuzzy neighborhood discriminant analysis for multifunction myoelectric hand control", *IEEE Trans. on Biomed. Eng.*, vol. 57, no. 6, pp. 1410-1419, 2010.

[92] K. Anam and A. Al-Jumaily, “Swarm-wavelet based extreme learning machine for finger movement classification on transradial amputees” in *Proc. 36th Annual International Conference of the IEEE Engineering in Medicine and Biology Society*, 2014, pp. 4192-4195.

[93] K. Anam and A. Al-Jumaily, “Adaptive wavelet extreme learning machine (AW-ELM) for index finger recognition using two-channel electromyography,” *Neural. Inf. Process.*, vol. 8834, pp. 471-478, 2014.

[94] D. Cai, X. He, and J. Han, “SRDA: an efficient algorithm for large-scale discriminant analysis,” *IEEE Trans. Knowl. Data Eng.*, vol. 20, no. 1, pp. 1–12, Jan. 2008.

[95] K. S. Kim, H. H. Choi, C. S. Moon, and C. W. Muna, “Comparison of k-nearest neighbor, quadratic discriminant and linear discriminant analysis in classification of electromyogram signals based on the wrist-motion directions,” *Curr. Appl. Phys.*, vol. 11, no. 3, pp. 740-745, May 2011.

[96] G. B. Huang and C. K. Siew, “Extreme learning machine: RBF network case,” in *Proc. 8th Control, Automation, Robotics and Vision Conference*, 2004, pp. 1029-1036.

[97] J. U. Chu, I. Moon, and M. S. Mun, “A supervised feature projection for real-time multifunction myoelectric hand control,” in *Proc. 28th IEEE EMBS Annual International Conference*, 2006, pp. 2417–2420.

[98] A. Al-Timemy, R. N. Khushaba, and J. Escudero, “Selecting the optimal movement subset with different pattern recognition based EMG control algorithms,” in *Proc. 38th IEEE EMBC Annual International Conference*, 2016.

[99] Perotto A.O., Delagi E.F., Iazzetti J., Morrison D. *Anatomical Guide for the Electromyographer: The Limbs and Trunk*, Charles C. Thomas, 4th ed. Springfield, 2005.

[100] Mogk, J. P. M., & Keir, P. J. "Crosstalk in surface electromyography of the proximal forearm during gripping tasks," *Journal of Electromyography and Kinesiology*, vol. 13, no. 1, pp. 63-71.

[101] Kendall F.P., Kendall E. McCreary, H.O. Kendall, G.E. Wadsworth, *Muscles testing and function*, Williams & Wilkins, Baltimore, 1983.

Output จากโครงการวิจัยที่ได้รับทุนจาก สกว.

1 ผลงานตีพิมพ์ในวารสารวิชาการนานาชาติ (ระบุชื่อผู้แต่ง ชื่อเรื่อง ชื่อวารสาร ปี เล่มที่ เลขที่ และหน้า) พร้อมแจ้งสถานะของการตีพิมพ์ เช่น submitted, accepted, in press, published

มีจำนวน 2 เรื่อง ดังรายละเอียดต่อไปนี้

- Pornchai Phukpattaranont, Sirinee Thongpanja, Khairul Anam, Adel Al-Jumaily, and Chusak Limsakul, “Evaluation of feature extraction techniques and classifiers for finger movement recognition using surface electromyography signal,” accepted for publication in *Medical & Biological Eng & Computing (MBEC)* **[impact factor 1.916, Q2 in JCR® Category]**
- Sirinapa Jitaree and Pornchai Phukpattaranont, “Force classification using sEMG from various object lengths and wrist postures,” submitted for publication in *Journal of Mechanical Science and Technology* **[impact factor 1.128, Q3 in JCR® Category]**

2 การนำผลงานวิจัยไปใช้ประโยชน์

- เชิงพาณิชย์ (มีการนำไปผลิต/ขาย/ก่อให้เกิดรายได้ หรือมีการนำไปประยุกต์ใช้โดยภาคธุรกิจ/บุคคลทั่วไป)

-

- เชิงนโยบาย (มีการกำหนดนโยบายอิงงานวิจัย/เกิดมาตรการใหม่/เปลี่ยนแปลงระเบียบข้อบังคับหรือวิธีทำงาน)

-

- เชิงสาธารณะ (มีเครือข่ายความร่วมมือ/สร้างกระแสความสนใจในวงกว้าง)

-

- เชิงวิชาการ (มีการพัฒนาการเรียนการสอน/สร้างนักวิจัยใหม่)

-

3 อื่นๆ (เช่น ผลงานตีพิมพ์ในวารสารวิชาการในประเทศ การเสนอผลงานในที่ประชุมวิชาการ หนังสือ การจดสิทธิบัตร)

-

ภาคผนวก

Pornchai Phukpattaranont, Sirinee Thongpanja, Khairul Anam, Adel Al-Jumaily, and Chusak Limsakul, “Evaluation of feature extraction techniques and classifiers for finger movement recognition using surface electromyography signal,” accepted for publication in *Medical & Biological Eng & Computing (MBEC)* **[impact factor 1.916, Q2 in JCR® Category]**

Your Submission MBEC-D-17-00608R1

Medical & Biological Eng & Computing (MBEC) <em@editorialmanager.com>

CC: sirinee.th@gmail.com, kh.anam.sk@gmail.com, adel.al-jumaily@uts.edu.au, chusak.l@psu.ac.th

Dear Dr. Phukpattaranont,

We are pleased to inform you that your manuscript, "Evaluation of feature extraction techniques and classifiers for finger movement recognition using surface electromyography signal", has been accepted for publication in
Medical & Biological Engineering & Computing.

You will receive an email from Springer in due course with regards to the following items:

1. Offprints
2. Colour figures
3. Transfer of Copyright

Please remember to quote the manuscript number, MBEC-D-17-00608R1, whenever inquiring about your manuscript.

With best regards,
Nitish Thakor
Editor in Chief

Medical & Biological Engineering & Computing

Evaluation of feature extraction techniques and classifiers for finger movement recognition using surface electromyography signal

--Manuscript Draft--

Manuscript Number:	MBEC-D-17-00608R1
Full Title:	Evaluation of feature extraction techniques and classifiers for finger movement recognition using surface electromyography signal
Article Type:	Original article
Keywords:	Electromyography (EMG); Feature extraction; dimensionality reduction; finger movement classification; EMG pattern recognition.
Corresponding Author:	Pornchai Phukpattaranont, Ph.D. Prince of Songkla University Hat Yai, Songkhla, Outside US & Canada THAILAND
Corresponding Author Secondary Information:	
Corresponding Author's Institution:	Prince of Songkla University
Corresponding Author's Secondary Institution:	
First Author:	Pornchai Phukpattaranont
First Author Secondary Information:	
Order of Authors:	Pornchai Phukpattaranont
	Sirinee Thongpanja
	Khairul Anam
	Adel Al-Jumaily
	Chusak Limsakul
Order of Authors Secondary Information:	
Funding Information:	Thailand Research Fund and Faculty of Engineering, Prince of Songkla University (RSA5980049) — Assoc. Prof. Dr. Pornchai Phukpattaranont
	Higher Education Research Promotion and National Research University Project of Thailand, Office of the Higher Education Commission — Assoc. Prof. Dr. Pornchai Phukpattaranont
	UTS International Research Scholarship, University of Technology, Sydney — Dr. Sirinee Thongpanja
Abstract:	Electromyography (EMG) in bio-driven system is used as a control signal, for driving a hand prosthesis or other wearable assistive devices. Processing to get informative drive signals involves three main modules: preprocessing, dimensionality reduction, and classification. This paper proposes a system for classifying a 6-channel EMG signal from 14 finger movements. A feature vector of 66 elements was determined from the 6-channel EMG signal for each finger movement. Subsequently, various feature extraction techniques and classifiers were tested and evaluated. We compared the performance of 6 feature extraction techniques, namely principal component analysis (PCA), linear discriminant analysis (LDA), uncorrelated linear discriminant analysis (ULDA), orthogonal fuzzy neighborhood discriminant analysis (OFNDA), spectral regression linear discriminant analysis (SRDA), and spectral regression extreme learning machine (SRELM). In addition, we also evaluated the performance of 7 classifiers consisting of support vector machine (SVM), linear classifier (LC), Naive Bayes (NB), k-nearest neighbors (KNN), radial basis function extreme learning machine (RBF-ELM), adaptive wavelet extreme learning machine (AW-ELM), and neural network (NN). The results showed that the combination of SRELM as the

Evaluation of feature extraction techniques and classifiers for finger movement recognition using surface electromyography signal

Associate Professor Dr. Pornchai Phukpattaranont*

Department of Electrical Engineering, Faculty of Engineering

Prince of Songkla University, Hat Yai, Songkhla, 90112, Thailand

Phone 0-7428-7045 Fax 0-7445-9395

Email: pornchai.p@psu.ac.th*

Sirinee Thongpanja

Department of Electrical Engineering, Faculty of Engineering,

Prince of Songkla University, Hat Yai, Songkhla, 90112, Thailand

Email: sirinee.th@gmail.com

Khairul Anam

School of Electrical, Mechanical and Mechatronic Systems,

Faculty of Engineering and Information Technology

University of Technology, Sydney (UTS), Broadway, NSW, 2007, Australia

Email: kh.anam.sk@gmail.com

Associate Professor Dr. Adel Al-Jumaily

School of Electrical, Mechanical and Mechatronic Systems

Faculty of Engineering and Information Technology

University of Technology, Sydney (UTS), Broadway, NSW, 2007, Australia

Email: Adel.Al-Jumaily@uts.edu.au

Associate Professor Dr. Chusak Limsakul

Department of Electrical Engineering, Faculty of Engineering

Prince of Songkla University, Hat Yai, Songkhla, 90112, Thailand, Email: chusak.l@psu.ac.th

Abstract

Electromyography (EMG) in bio-driven system is used as a control signal, for driving a hand prosthesis or other wearable assistive devices. Processing to get informative drive signals involves three main modules: preprocessing, dimensionality reduction, and classification. This paper proposes a system for classifying a 6-channel EMG signal from 14 finger movements. A feature vector of 66 elements was determined from the 6-channel EMG signal for each finger movement. Subsequently, various feature extraction techniques and classifiers were tested and evaluated. We compared the performance of 6 feature extraction techniques, namely principal component analysis (PCA), linear discriminant analysis (LDA), uncorrelated linear discriminant analysis (ULDA), orthogonal fuzzy neighborhood discriminant analysis (OFNDA), spectral regression linear discriminant analysis (SRDA), and spectral regression extreme learning machine (SRELM). In addition, we also evaluated the performance of 7 classifiers consisting of support vector machine (SVM), linear classifier (LC), Naive Bayes (NB), *k*-nearest neighbors (KNN), radial basis function extreme learning machine (RBF-ELM), adaptive wavelet extreme learning machine (AW-ELM), and neural network (NN). The results showed that the combination of SRELM as the feature extraction technique and NN as the classifier yielded the best classification accuracy of 99%, which was significantly higher than those from the other combinations tested.

Keywords: Electromyography (EMG), feature extraction, dimensionality reduction, finger movement classification, EMG pattern recognition.

1. Introduction

The loss of finger functions is a major disability that limits everyday capabilities and interactions [1]. Hence, myoelectric control based devices using residual muscles, such as the muscles of the shoulder and/or arm, are used for improving the quality of life for people with physical disabilities [2, 3]. Surface electromyography (EMG) observes electrical activities of the muscles by detection with surface electrodes [4]. The EMG signal contains useful information related to muscular activity, neuromuscular disease, and movements intended [5]. It can be used for controlling a prosthetic arm or hand, as well as with other devices such as a wheelchair, a mouse, and a keyboard. This requires that the pattern of an EMG signal is classified into a predefined class that is matched with the command for controlling the device [6, 7].

A finger movement classification system consists of 3 main modules, namely, preprocessing, dimensionality reduction, and classification. In preprocessing module, a *D*-dimensional vector of numerical features is generated from each segment of EMG data. Then, to increase the classification accuracy and decrease the computational complexity, the dimensionality reduction techniques are

applied in the second module. As a result, a *d*-dimensional vector is obtained. Note that, the dimension of the reduced feature vector is smaller than the dimension of the original feature vector ($d < D$). Finally, the reduced feature vector is used as an input of a classifier for finger movement classification in the last module.

When the number of movements to be classified was small, the dimensionality reduction was not applied because the dimension of the original feature vector was also not high. Classification of 8 finger movements was proposed in [8] using mean absolute value (MAV) and the spectra from Gabor transform as feature values. The number of EMG channels was 2 resulting in the dimension of the feature vector 16. The classification accuracy was 85.10%. Uchida et al. [9] reported that the classification accuracy of 5 finger movements with the feature values based on fast Fourier transform (FFT) was 86% when the feature vector with dimension 20 (10 FFT coefficients × 2-channel EMG) was used.

When the number of movements to be classified increases, the number of elements in the feature vector increases to improve the classification accuracy. The high-dimensional feature vector has been proposed by combining time domain, frequency domain, and/or statistical feature values. However, the increase in the dimension of feature vector can introduce redundancy and add to the computational complexity of classification. Therefore, various dimensionality reduction techniques were proposed to reduce the redundancy and computational complexity [10]. There are two main strategies of dimensionality reduction, i.e., feature extraction and feature selection. While feature extraction tries to determine the best combinations of the original feature vectors to form a new feature vector with smaller dimension, feature selection chooses the best subset of elements from the original feature vector. Previous studies applied various feature extraction methods in EMG classification including principal component analysis (PCA) [11, 12], linear discriminant analysis (LDA) [13, 14], uncorrelated linear discriminant analysis (ULDA) [15], orthogonal fuzzy neighborhood discriminant analysis (OFNDA) [16], and spectral regression linear discriminant analysis (SRDA) [17].

Our previous study [18] proposed a new feature extraction, namely spectral regression extreme learning machine (SRELM), and evaluated its performance along with other feature extraction techniques, including SRDA, ULDA, OFNDA, and PCA. Moreover, in [18] five classifiers including adaptive wavelet ELM (AW-ELM), radial basis function ELM (RBF-ELM), support vector machine (SVM), *k*-nearest neighbors (KNN), and linear classifier (LC) were evaluated for their performances in classifying two channels of EMG signals from 10 hand and finger movements. We reported that SRELM gave the best performance. Moreover, we found that the classification accuracy depended on the classifier. In other words, while SREML provided the best performance when the

KNN classifier was used, ULDA gave the best performance with the SVM classifier. These results indicated that the pairing of a feature extraction technique with a type of classifier affects the classification accuracy. Therefore, another effective classifier, neural network (NN), which was not used in [18], was investigated in this current study.

2. Theory

2.1 Preprocessing methods

In the preprocessing methods, we transform segments of EMG data into an original feature vector. Feature values, which are elements of the original feature vector, are usually determined from the EMG data in the time domain and/or the frequency domain [6]. Recent studies have proposed further feature values based on statistical methods. In this paper, we used Hudgins's feature set [2, 3, 19]: MAV, waveform length (WL), zero crossing (ZC), and slope sign change (SSC), which are popular time domain features used in previous studies. In addition, we also used the fourth order autoregressive coefficient (AR) for representing information on the prediction model [12, 20], mean frequency (MNF) for representing information on the power spectral density [21], kurtosis (KURT) for representing information on peakedness of distribution [22], and skewness (SKW) for representing information on the symmetry of distribution in the EMG signal [13]. As a result, the original feature vector of 11 elements from each segment of EMG data per EMG channel consists of (1) MAV, (2) WL, (3) ZC, (4) SSC (5)-(8) Four AR coefficients, (9) MNF, (10) KURT, and (11) SKW. The detailed mathematical definition of each feature is as follows.

(1) MAV represents the signal energy, which is frequently used for detecting the onset of an EMG signal. MAV feature is the average of absolute value of the EMG signal. It can be defined as [2]

$$\mathrm{MAV} = \frac{1}{N}\sum_{i=1}^{N} | x_i |, \tag{1}$$

where x_i is the amplitude of the EMG signal at sample i and N is the length of the EMG signal.

(2) WL is the cumulative length of the EMG waveform over the segment, and is indicative of the complexity of the EMG signal. It can be expressed as [2]

$$\mathrm{WL} = \sum_{i=1}^{N-1} | x_{i+1} - x_i |. \tag{2}$$

(3) ZC is the number of times that the EMG signal amplitude crosses zero. In other words, it is the number of times that the signal amplitude changes its sign. A threshold must be set to reduce the noise (i.e., threshold was set to 10 μV). It can be defined as [2]

$$\mathrm{ZC} = \sum_{i=1}^{N-1} \left[f(x_i \times x_{i+1}) \cap \left| x_i - x_{i+1} \right| \geq 10 \right], \tag{3}$$

$$f(x) = \begin{cases} 1, & \text{if } x < 0 \\ 0, & \text{otherwise} \end{cases}. \tag{4}$$

(4) SSC is the number of times that the slope of the EMG signal changes sign. It is defined as [2]

$$\mathrm{SSC} = \sum_{i=2}^{N} \left[s\left\{ (x_i - x_{i-1})(x_i - x_{i+1}) \right\} \cap \left\{ \left| x_i - x_{i-1} \right| \geq 10 \cup \left| x_i - x_{i+1} \right| \geq 10 \right\} \right], \tag{5}$$

$$s(x) = \begin{cases} 1, & \text{if } x > 0 \\ 0, & \text{otherwise} \end{cases}. \tag{6}$$

(5) AR describes each sample of the EMG signal as a linear combination of the previous sample plus a white noise error term, which can be defined as [20]

$$x_i = \sum_{p=1}^{P} a_p x_{i-p} + w_i \,, \tag{7}$$

where a_p is the coefficient in the AR model. P is the order of the AR model and w_i is white noise or error sequence. In this paper, P is set to four. As a result, the number of feature values from the AR model is 4.

(6) MNF is the average frequency. It is defined as the sum of product of power spectrum and frequency divided by the total spectrum intensity, which can be expressed as [21]

$$\mathrm{MNF} = \sum_{j=1}^{M} f_j P_j \Big/ \sum_{j=1}^{M} P_j \,, \tag{8}$$

where f_j is the frequency of spectrum at frequency bin j. P_j is the EMG power spectrum at frequency bin j and M is the number of bins.

(7) KURT is a classical higher-order statistical characteristic indicating non-Gaussianity, and is used to quantify the peakedness of a distribution. It is the fourth-order cumulant of the data, which can be defined as [22]

$$\mathrm{KURT} = \left[\frac{1}{N} \sum_{i=1}^{N} y_i^4 \Big/ \left(\frac{1}{N} \sum_{i=1}^{N} y_i^2 \right)^2 \right] - 3, \tag{9}$$

where y_i represents the ith normalized EMG amplitude, which has zero mean and unit variance. N denotes the total number of the normalized EMG samples. Kurtosis can be either positive or negative.

(8) SKW is a measure used for characterizing the degree of asymmetry of the distribution of a random variable y. It is the third-order cumulant of the data, which can be defined as [13]

$$\mathrm{SKW} = \frac{1}{N} \sum_{i=1}^{N} (y_i - \bar{y})^3 \Big/ \left(\sqrt{\frac{1}{N} \sum_{i=1}^{N} (y_i - \bar{y})^2} \right)^3 . \tag{10}$$

2.2 Feature extraction

Six feature extraction techniques are evaluated in this paper including PCA, LDA, ULDA, OFNDA, SRDA, and SRELM. It should be noted that the dimension of the reduced feature vector from each feature extraction technique except PCA was 13, matching the total number of movements minus one. On the other hand, the dimension of the reduced feature vector from PCA was 14. The brief details on each technique are as follows.

- PCA tries to find a set of orthogonal basis vectors that captures maximum information from the original dimensions. PCA decomposes the covariance structure of the original dimensions by calculating the eigenvalues and eigenvectors of the data. The components, i.e., eigenvalues and eigenvectors, are ranked according to their variance to the principal axes ranging from the highest contribution to the lowest.

- LDA tries to find an optimal transformation vector by maximizing the ratio of the between-class distance to the within-class distance, so that the maximum class discrimination is achieved.

- ULDA is an extension of classical LDA, such that the features in the transformed space are uncorrelated, so the redundancy in the transformed space could be reduced. The objective of ULDA is to find the optimal discriminant vectors.

- OFNDA minimizes the distances within the classes and maximizes the distances between the centers of different classes, while taking into account the contribution of the samples to the different classes and to efficiently overcome the singularity problems of classical LDA by employing the QR-decomposition.

- SRDA combines the spectral analysis of the graph matrix and regression techniques, and is essentially developed from LC [23]. A set of linear regression problems is solved to obtain the transformation vectors.

- SRELM was proposed in our previous study [18]. It is integrated from extreme learning machine (ELM) and spectral regression (SR), which utilizes the obtained eigenvector to project the hidden layer output to the output layer. The hidden layer weights are determined randomly. The output weight is computed using SR. There are two parameters in optimizing SRELM performance: number of hidden nodes and alpha. In order to evaluate the optimal parameters in this paper, the number of hidden nodes was varied from 100 to 1,500 nodes with an increment of 100 nodes and alpha was varied from 1 to 20 with an increment of 1.

2.3 Feature evaluation

In this paper, we applied the statistical criteria, namely, the ratio of a Euclidean distance to a standard deviation (RES) index, to evaluate class separation performance of the reduced feature vector obtained from each feature extraction technique. The advantage of the RES index is that its result is independent of any classifier. The RES index can be defined as [24]

$$\text{RES index} = \frac{\overline{ED}}{\overline{\sigma}}. \tag{11}$$

$\overline{ED}$ is the distance between coordinates of a pair of clusters p and q in n-dimensional Euclidean space, which can be defined as

$$\overline{ED} = \frac{2}{K(K-1)} \sum_{p=1}^{K-1} \sum_{q=p+1}^{K} \sqrt{(\overline{m}_1^p - \overline{m}_1^q)^2 + (\overline{m}_2^p - \overline{m}_2^q)^2}, \tag{12}$$

where m is the average value of feature. p and q are indexes representing the movements. K is the total number of movements. ($1 \le k \le K$, $K = 14$)

$\overline{\sigma}$ is dispersion of clusters p and q, which can be expressed as

$$\overline{\sigma_i} = \frac{1}{IK}\sum_{i=1}^{I}\sum_{k=1}^{K} s_{ik}\,, \tag{13}$$

where s is a standard deviation of a feature and I is the length of feature vector ($1 \le i \le I$, I = 13 or 14). The RES index increases when the class separation performance of EMG features increases.

2.4 Classification

Seven classifiers are tested and compared in this paper, i.e., SVM, LC, NB, KNN, RBF-ELM, AW-ELM, and NN. Brief details of each classifier and its corresponding parameters used are as follows.

- SVM uses a discriminant hyperplane to separate the classes [25]. SVM aims to find the optimal hyperplane that maximizes the margins between the points of different classes. The margins are the distances between the hyperplane and the nearest training points. In this study, SVM type was *C*-support vector classification. Kernel type was radial basis function. Gamma in kernel function was set to 1/number of features and cost was set to 1.

- LC was implemented using a simple max gate function as a classification rule [26]. It is assumed that the feature vectors have multivariate normal distribution with mean vector and common covariance matrix.

- NB classifier aims to reach the best hypothesis through a given training data set [27]. Bayes theorem provides a way to calculate the probability of a hypothesis based on its prior probability of both the data found and the total data. NB often performs well although independence assumptions between data are violated.

- KNN is a process to assign a new feature vector to a class in all available cases using a similarity measure such as distance functions [26]. After the distances between the feature vector and all the training samples are determined, the new case is assigned to the class with the largest probability. In other words, it is classified by a majority vote of its *k* neighbors. In this paper, *k* was set to 14.

- RBF-ELM is a variant of ELM classifier, which is single layer feed-forward network with radial basis function [28]. It employs randomized method to initialize the centers and widths of RBF kernels and the output weights of RBF network are calculated analytically. In order to select the optimal parameters, a grid search method was used. From the step sizes at 0.1, 0.5, 1, 5, 10, 15, and 20, we can obtain 49 combinations of cost and kernel parameters under test.

The optimal parameters were selected from the combination that gave the maximum accuracy.

- AW-ELM proposed by Anam and Al-Jumaily [29] is the combination of ELM with wavelet neural network. It utilizes a wavelet function as the activation function in the hidden node. The function is adjusted according to changes in the input. In order to select the optimal parameter, the number of hidden nodes was varied from 25 to 500 nodes with an increment of 25 nodes

- NN is a multilayer perceptron, which is composed of several layers: one input layer, one or several hidden layers and one output layer [30]. Each neuron in each layer is connected with the output of the previous one. In this paper, we designed three layered feed-forward back-propagation neural networks consisting of input layer, tan-sigmoid hidden layer and linear output layer. The number of neurons in input layer was either 13 for PCA or 14 for other feature extraction techniques. The number of neurons in hidden layer was 10, 20, or 30, with the best alternative selected for obtaining maximal accuracy. The number of neurons in output layer was 14, i.e., one neuron per movement type. In addition, NN was trained using scaled gradient descent algorithm.

3. Materials and methods

3.1 EMG data acquisition and experimental setup

A commercial EMG measurement system (Mobi6-6b, TMS International B.V.) with built-in band-pass filter (20-500 Hz) and amplifier with a gain factor of 19.5 was used for recoding EMG signals at a sampling rate of 1024 Hz. The EMG signals from 6 forearm muscles were recorded using 12 pairs of bipolar disposable Ag/AgCl electrodes (H124SG, Kendel ARBO) with an inter-electrode distance of 20 mm. In addition, a Ag/AgCl electrode was placed on the wrist to provide a common ground reference. Fig. 1 (Left) shows the electrode placements on the 6 forearm muscles used for EMG data acquisition. While the first group of muscles, namely, extensor carpi ulnaris (CH6), extensor carpi radialis longus (CH5), and extensor digitorum (CH4), are located on the posterior compartment of the forearm to perform extension at the fingers, the second group of muscles, namely, flexor carpi ulnaris (CH3), palmaris longus (CH2), and flexor carpi radialis (CH1) are located on the anterior compartment of the forearm to produce flexion at the fingers.

Ten able-bodied subjects (7 males and 3 females) with ages ranging from 20 to 23 years participated in the experiments. Each subject performed 14 different finger movements in a ramdom sequence for a trial consisting of thumb flexion (M1), index flexion (M2), middle flexion (M3), ring

flexion (M4), little flexion (M5), hand close (M6), index-middle-ring-little flexion (M7), middle-ring-little flexion (M8), ring-little fingers flexion (M9), middle-ring flexion (M10), index-middle-ring flexion (M11), thumb-little flexion (M12), thumb-ring-little flexion (M13), and thumb-middle-ring-little flexion (M14), as shown in Fig. 1 (Right). Within the trial, the beginning of each movement activity is triggered by an auditory clue. Following the clue, the subject performed the movement and held the contraction for 5 s in duration until a rest cue was given. A one-minute period rest state was taken between each movement in the trial. The trial was repeated five times with a ten-minute period rest state. As a result, each movement was performed 5 times.

Fig. 2 shows an example of EMG signals obtained from six muscles during thumb flexion (M1). The EMG signals with 5 s in duration (5,120 samples) from CH1 to CH6 were shown in the top to bottom rows, respectively. The differences in amplitudes of EMG signals from different muscles are clearly seen. While the amplitudes of EMG signals from CH6 are largest, the amplitudes of EMG signals from CH1 are smallest.

3.2 Methods

Fig. 3 shows the method for evaluating feature extraction techniques and classifiers used in recognizing the EMG signals from finger movements in this paper. After 6 channels of EMG signals from 14 hand and finger movements were acquired, they were processed using the analytical method consisting of 5 steps, i.e., (1) Segmentation, (2) Feature generation, (3) Feature extraction, (4) Performance evaluation with RES index, and (5) Performance evaluation with classifiers. The details on each step are as follows.

Step 1) Segmentation: In this step, the collected EMG data with a length of 5120 samples was segmented by the disjoint windowing technique with a window length of 256 samples (250 ms) resulting in 20 segmented EMG data for each EMG channel of each movement.

Step 2) Feature generation: In this step, the eleven feature values described in Section 2.1 including MAV, WL, ZC, SSC, MNF, KURT, SKW, and 4 coefficients from AR were calculated for each EMG segment. The feature values from 6 EMG channels were formed as an original feature vector. As a result, the dimension of the original feature vector was 66 for each movement (11 feature values per EMG channel × 6 EMG channels).

Step 3) Feature extraction: In this step, the six feature extraction techniques described in Section 2.2 including PCA, LDA, ULDA, OFNDA, SRDA, and SRELM were applied to the original

feature vector in Step 2). As a result, the dimension of the original feature vector, which was 66 from Step 2), was reduced to 14 for PCA and 13 for the others in this step.

Step 4) Performance evaluation with RES index: In this step, the performance on class separation ability of all reduced feature vectors from each feature extraction technique resulting from Step 3) was evaluated with the RES index described in Section 2.3. As a result, six RES index from 6 feature extraction techniques were obtained and compared.

Step 5) Performance evaluation with classifiers: In this step, all reduced feature vectors from each feature extraction technique in Step 3) were used as the inputs of 7 classifiers, which were briefly described in Section 2.4. Therefore, there are 42 combinations of the reduced feature vector with the classifier under test. The performance based on classification accuracy from each combination was evaluated and compared.

Note that, the reduced feature vectors were classified with a 10-fold cross-validation. In other words, the reduced feature vectors were randomly partitioned into 10 subsets. The classifier training was performed using 9 subsets and the remaining subset was used for classifier testing. This process was repeated 10 times such that each of the 10 subsets was used as the testing data. Finally, the performance of each pairing of the reduced feature vector with the classifier was evaluated and compared using mean and standard deviation of classification accuracies. The classification accuracy can be expressed as

$$\text{classification accuracy} = \frac{\text{Number of correct classifications}}{\text{Total number of finger movements under test}} \times 100\% . \quad (14)$$

4. Results

4.1 Characteristics of the reduced feature vectors

Fig. 4 shows as an example the scatter plot between the first two elements of the reduced feature vectors from each feature extraction technique. The result shows that the first two elements of the reduced feature vectors by SRELM provided better separation than those from other feature extraction techniques, while the first two elements of the reduced feature vectors from LDA, ULDA, OFNDA, and SRDA are quite overlapped. In addition, PCA provided results that had the worst performance in separating finger movements.

Fig. 5 shows the RES index calculated from all reduced feature vectors by each feature extraction technique. The RES index of reduced feature vectors by SRELM is higher than that of

other feature extraction techniques. In other words, SRELM provides the reduced feature vectors that have the best performance in separating finger movements. The RES indexes of reduced feature vectors from SRDA, OFNDA, LDA, and ULDA are quite similar, while the reduced feature vectors from PCA give the lowest RES index. We can clearly see that the RES index of reduced feature vectors in Fig. 5 is consistent with the scatter plot of reduced feature vectors in Fig. 4**.**

4.2 Classification accuracy

Table I presents the classification accuracy using various feature extraction techniques paired with different classifiers. While the best classification accuracies from LC, KNN, AW-ELM, and NN are obtained with the reduced feature vectors from SRELM, the best classification accuracies from SVM and RBF-ELM are obtained with the reduced feature vectors from SRDA. However, for each feature extraction technique, we can observe that NN with 10 nodes in the hidden layer provides the highest classification accuracy. Moreover, the combination of SRELM and NN gives the maximum classification accuracy at 99.09%.

Table II presents the classification accuracies for 14 movements obtained from the NN classifier with different numbers of nodes in hidden layer, i.e. 10, 20, or 30 neurons. When we increase the number of neurons in hidden layer from 10 to 20 and to 30, the classification accuracy changes slightly for each feature extraction technique. Results show that 20 neurons in hidden layer gives the best accuracy at 99.57% among all combinations of feature extraction techniques and classifiers, when the reduced feature vectors from SRELM are used.

Table III presents classification accuracies with channel reduction. The subset of channels was optimized by considering the classification accuracies obtained from all combinations of each channel set. Firstly, all possible combinations of five channels out of the six total were trialed for classification. Only the set of five channels providing the highest classification accuracy was selected. Secondly, all possible combinations of four channels out of the five total from the first step, were trialed for classification. For instance, the accuracies from all combinations of five channels are shown in the second row to the seventh row in Table III. We can see that the combination of CH2, CH3, CH4, CH5, and CH6 provides the highest classification accuracy, so this channel set was selected as the best combination of five channels. Then, all possible combinations of four channels out of the five selected channels from the first step were trialed. As a result, the combination of CH2, CH3, CH5, and CH6 provides the best classification accuracy and it was chosen as the optimal set of four channels. The procedure was repeated for three, two and one channels, respectively. The results show that the classification accuracy decreases from 99.57 to 58.95% when the number of channels decreases from 6 to 1. Moreover, to obtain a high classification accuracy, EMG signals from the

muscles located on the anterior and posterior compartments of the forearm are needed. For example, the maximum classification accuracy from two EMG channels at 85.38% can be obtained from the combination of flexor carpi radialis (CH3) and extensor carpi ulnaris (CH6), which are located on the anterior and posterior compartments of the forearm, respectively.

Table IV presents classification accuracies from movement reduction using 2 channels of EMG signals, namely, CH3 and CH6. The selection of these two EMG channels was guided by Table III. The subset of finger movements was optimized by considering classification accuracy of each movement. All EMG signals from 14 finger movements were firstly classified, and then the classification accuracy was individually investigated for each movement from the confusion matrix [32]. The movement providing the lowest classification accuracy was removed from the movement set. The procedure was repeated until the number of movements decreased to two movements. The results show that the classification accuracy increases from 85.38% to 100% when the number of movements decreases from 14 to 10 movements. In other words, the reduction in the number of movements decreases the complexity of classification, resulting in better classification accuracy.

5. Discussion

Results of the scatter plot shown in Fig. 4 and the RES index shown in Fig. 5 show that the reduced feature vectors from SRELM provides the best performance in separating finger movements. Anam and Al-Jumaily [18] reported that SRELM is an extreme learning machine (ELM) for supervised feature extraction with consideration of the class label. The aim of the training is to produce output that is very close to the output target. In other words, the training tries to minimize the error between the actual output and target. As a result, the reduced feature vectors from SRELM show better performance in separating fourteen finger movements than those from other feature extractions. In addition, LDA considers also class label in the extraction step (i.e., supervised feature extraction) and ULDA is developed to solve the limitation of LDA by producing a set of uncorrelated discriminant features employing the singular value decomposition [14]. In contrast, as Chu et al. [31] reported the PCA does not consider the class labels in the extraction process (i.e., it performs unsupervised feature extraction). Therefore, the output is another representation of the reduced feature vectors and its performance is lower than with other feature extraction techniques.

Table V presents the performance comparisons of the proposed method with those from previous publications. The classification performance can be divided into two groups. In the first group, the number of EMG channels used is 2 [8, 9, 13, 18, A]. The dimensions of feature vectors from [8] and [9] are 16 and 20, respectively. The classifier used in is NN. The classification accuracy is 85%-86%. It is important to note that there is no application of feature extraction for classifying

movements from both individual and combined fingers in [8] and [9]. This may be the cause of poor classification accuracy. However, feature extraction is applied for reducing a dimension of the feature vector in [13, 18, A]. The classification accuracy of the proposed technique for classifying 10 movements from 2-channel EMG signals achieves 100% [A] compared to 86.72% and 92.00% in [18] and [13], respectively. Note that, in [18], the feature vectors were generated from two EMG channels plus one channel formed from summation of the two channels. Moreover, Bayesian fusion was applied as a post processing in [13]. Comparison between [A] and [18] indicates that the pairing of a feature extraction technique with a type of classifier affects classification accuracy. Another way to increase classification accuracy when the number of movement increases is to increase in the number of EMG channels as shown in [11-12, 19-20, B]. Results show that the proposed technique achieves good accuracy in classifying 14 movements from 6-channel EMG signals at 99.57% [B]. The results of this study clearly illustrate that using high dimensional feature vectors with feature extraction could improve the classification performance.

6. Conclusions

This paper proposed a system for classifying 14 finger movements, involving individual and combined finger flexion observed by 6 channels of EMG signals. Six feature extraction techniques were evaluated including principal component analysis (PCA), linear discriminant analysis (LDA), uncorrelated linear discriminant analysis (ULDA), orthogonal fuzzy neighborhood discriminant analysis (OFNDA), spectral regression linear discriminant analysis (SRDA), and spectral regression extreme learning machine (SRELM). The results show that the reduced feature vectors from SRELM give the best performance in terms of feature separation among these feature extraction techniques. In addition, the best feature separation ability obtained with SRELM was confirmed by a quantitative measure, namely the RES index. Subsequently, seven classifiers were validated, namely, support vector machine (SVM), linear classifier (LC), Naive Bayes (NB), *k*-nearest neighbors (KNN), radial basis function extreme learning machine (RBF-ELM), adaptive wavelet extreme learning machine (AW-ELM), and neural network (NN). The results show that NN provides the best performance in separating 6-channel EMG signals to identify 14 finger movements. Classification accuracy of up to 99% was reached when using SRELM and NN in combination.

Acknowledgement

This work was jointly funded by the Thailand Research Fund and Faculty of Engineering, Prince of Songkla University through Contract No. RSA5980049, in part by the Higher Education Research Promotion and National Research University Project of Thailand, Office of the Higher Education Commission and UTS International Research Scholarship, University of Technology, Sydney. In addition, the authors would like to thank the Research and Development Office (RDO),

Prince of Songkla University, and Associate Professor Dr. Seppo Karrila, Faculty of Science and Industrial Technology, Prince of Songkla University, for commenting on the manuscript.

References

1. Kuiken TA, Li G, Lock BA, Lipschutz RD, Miller LA, Stubblefield KA, Englehart K (2009) Targeted muscle reinnervation for real-time myoelectric control of multifunction artificial arms. J Am Med Assoc 301(6): 619–628
2. Englehart K, Hudgins B (2003) A robust, real-time control scheme for multifunction myoelectric control. IEEE Trans Biomed Eng 50(7): 848–854
3. Hudgins B, Parker P, Scott RN (1993) A new strategy for multifunction myoelectric control. IEEE Trans Biomed Eng 40(1): 82–94
4. De Luca CJ (1979) Physiology and mathematics of myoelectric signals. IEEE Trans Biomed Eng 26(6): 313–325
5. Orosco EC, Lopez NM, Di Sciascio F (2013) Bispectrum-based features classification for myoelectric control. Biomed Signal Process Control 8(2): 153–168
6. Oskoei MA, Hu H (2007) Myoelectric control systems—A survey. Biomed Signal Process Control 2(4): 275–294
7. Parker P, Englehart K, Hudgins B (2006) Myoelectric signal processing for control of powered limb prostheses. J Electromyogr Kinesiol, 16(6): 541–548
8. Nishikawa D, Yu W, Yokoi H, Kakazu Y (1999) EMG prosthetic hand controller using real-time learning method. In: Proc IEEE International Conference on Systems, Man and Cybernetics, pp. 153–158
9. Uchida N, Hiraiwa A, Sonehara N, Shimohara K (1992) EMG pattern recognition by neural networks for multi fingers control. In: Proc 14th Annual International Conference of the IEEE Engineering in Medicine and Biology, 1992, pp. 1016–1018
10. Zecca M, Micera S, Carrozza MC, Dario P (2002) Control of multifunctional prosthetic hands by processing the electromyographic signal. Crit Rev Biomed Eng 30(4–6): 459–485
11. Tenore FVG, Ramos A, Fahmy A, Acharya S, Cummings RE, Thakor NV (2009) Decoding of individuated finger movements using surface electromyography. IEEE Trans Biomed Eng 56(5): 1427 –1434
12. Al-Timemy AH, Bugmann G, Escudero J, Outram N (2013) Classification of finger movements for the dexterous hand prosthesis control with surface electromyography. IEEE J. Biomed. Health Inform 17(3): 608-618

13. Khushaba RN, Kodagoda S, Takruri M, Dissanayake G (2012) Toward improved control of prosthetic fingers using surface electromyogram (EMG) signals. Expert Sys Appl 39(12): 10731–10738

14. Khushaba RN, Kodagoda S, Liu D, Dissanayake G (2013) Muscle computer interfaces for driver distraction reduction. Comput Methods Programs Biomed 110(2): 137-149

15. Phinyomark A, Phukpattaranont P, Limsakul C (2012) Investigating long-term effects of feature extraction methods for continuous EMG pattern classification. Fluctuation Noise Lett 11(4)

16. Khushaba RN, Al-Ani A, Al-Jumaily A (2010) Orthogonal fuzzy neighborhood discriminant analysis for multifunction myoelectric hand control. IEEE Trans on Biomed Eng 57(6): 1410-1419

17. Anam K, Al-Jumaily A (2014) Swarm-wavelet based extreme learning machine for finger movement classification on transradial amputees. In: Proc 36th Annual International Conference of the IEEE Engineering in Medicine and Biology Society, 2014, pp. 4192-4195

18. Anam K, Al-Jumaily A (2015) A novel extreme learning machine for dimensionality reduction on finger movement classification using sEMG. In: Proc 7th International IEEE/EMBS Conference on Neural Engineering (NER), pp. 824-827

19. Du YC, Lin CH, Shyu LY, Chen T (2010) Portable hand motion classifier for multi-channel surface electromyography recognition using grey relational analysis. Expert Sys Appl 37(6): 4283–4291

20. Tavakolan M, Xiao ZG, Menon, C (2011) A preliminary investigation assessing the viability of classifying hand postures in seniors. Biomed Eng Online 10: 79

21. Phinyomark A, Phukpattaranont P, Limsakul C (2012) Feature reduction and selection for EMG signal classification. Expert Syst Appl 39: 7420-7431

22. Al-Timemy A, Khushaba R, Bugmann G, Escudero J (2016) Improving the performance against force variation of EMG controlled multifunctional upper-limb prostheses for transradial amputees. IEEE Trans Neural Syst Rehabil Eng 24(6): 650-661

23. Cai D, He X, Han J (2008) SRDA: an efficient algorithm for large-scale discriminant analysis. IEEE Trans Knowl Data Eng 20(1): 1–12

24. Phinyomark A, Limsakul C, Phukpattaranont P (2011) Application of wavelet analysis in EMG feature extraction for pattern classification. Measure Sci Rev 11: 45–52

478 25. Chang CC, Lin CJ (2011) LIBSVM: a Library for support vector machines. ACM Trans Intel
479 Syst Technol 2(3): 27:1-27:27

480 26. Kim KS, Choi HH, Moon CS, Muna CW (2011) Comparison of k-nearest neighbor, quadratic
481 discriminant and linear discriminant analysis in classification of electromyogram signals
482 based on the wrist-motion directions. Curr Appl Phys 11(3): 740-745

483 27. Domingos, P., & Pazzani, M. (1996). Beyond independence: conditions for the optimality of
484 the simple Bayesian classifier. In: Proc International Conference on Machine Learning, pp.
485 105-112

486 28. Huang GB, Siew CK (2004) Extreme learning machine: RBF network case. In: Proc 8th
487 Control, Automation, Robotics and Vision Conference, pp. 1029-1036

488 29. Anam K, Al-Jumaily A (2014) Adaptive wavelet extreme learning machine (AW-ELM) for
489 index finger recognition using two-channel electromyography. In: Proc International
490 Conference on Neural Information Processing (ICONIP 2014), pp. 471-478

491 30. Ibrahimy MI, Ahsan MR, Khalifa OO (2013) Design and performance analysis of artificial
492 neural network for hand motion detection from EMG signals. World Appl Sci J 23(6): 751-
493 758

494 31. Chu JU, Moon I, Mun MS (2006) A supervised feature extraction for real-time multifunction
495 myoelectric hand control. In Proc 28th IEEE EMBS Annual International Conference, pp.
496 2417–2420

497 32. Al-Timemy A, Khushaba RN, Escudero J (2016) Selecting the optimal movement subset with
498 different pattern recognition based EMG control algorithms. In: Proc 38th IEEE EMBC
499 Annual International Conference

500

Pornchai Phukpattaranont received the B.Eng. (Hons.) and M.Eng. degrees in electrical engineering from the Prince of Songkla University, Songkhla, Thailand, in 1993 and 1997, respectively, and the Ph.D. degree in electrical and computer engineering from the University of Minnesota, Minneapolis, MN, USA, in 2004.

He is currently an Associate Professor of Electrical Engineering with the Prince of Songkla University. Examples of his ongoing research include the pattern recognition system based on electromyographic signal, electrocardiographic signal, and microscopic images of breast cancer cells. His current research interests include signal and image analysis for medical applications and ultrasound signal processing.

Dr. Phukpattaranont is a member of the ECTI Association and Thai Biomedical Engineering Research Societies.

Sirinee Thongpanja was born in Songkhla, Thailand. She received the B.Eng. degree in biomedical engineering and the M.Eng. degree in electrical engineering from the Prince of Songkla University, Songkhla, Thailand, in 2011 and 2012, respectively, and the Ph.D. degree in electrical engineering from the Prince of Songkla University, Songkhla, Thailand, in 2016.

Her current research interests include surface electromyography signal processing and pattern recognition.

Chusak Limsakul received the B.Eng. degree in electrical engineering from the King Mongkut's Institute of Technology Ladkrabang, Bangkok, Thailand, in 1978, and the D.E.A. and Dr.Ing. degrees from the Institute National des Sciences Appliquees de Toulouse, Toulouse, France, in 1982 and 1985, respectively.

He was a Lecturer with the Department of Electrical Engineering, Prince of Songkla University, Songkhla, Thailand, in 1978, where he is currently an Associate Professor of Electrical Engineering and the President. His current research interests include biomedical signal processing, biomedical instrumentation, and neural network.

Khairul Anam was born in Buleleng-Bali on 5th of April 1978. He received his B. Eng from Dept. of Electrical Engineering, Universitas Brawijaya in 2002, M.Eng from Institut Teknologi Sepuluh Nopember (ITS) Surabaya in 2008, and PhD from University of Technology, Sydney, Australia in 2016.

He is currently a senior lecturer in Dept. Of Electrical Engineering, Universitas Jember, Indonesia. His main interest is artificial intelligence and its application in electrical engineering, biomedical engineering and other fields.

544

Dr Adel Al-Jumaily received his B.SC. (Eng.) in Electrical Engineering & Education, UT Bagdad and M.SC. in Engineering Management, UT-Bagdad and Ph.D. in Electrical Engineering, UTM Malaysia.

Currently, he is an associate professor in the University of Technology Sydney. His research interest is in the fields of Computational Intelligence, Bio-Mechatronics Systems, Health Technology and Biomedical, Vision based cancer diagnosing, and Artificial Intelligent Systems.

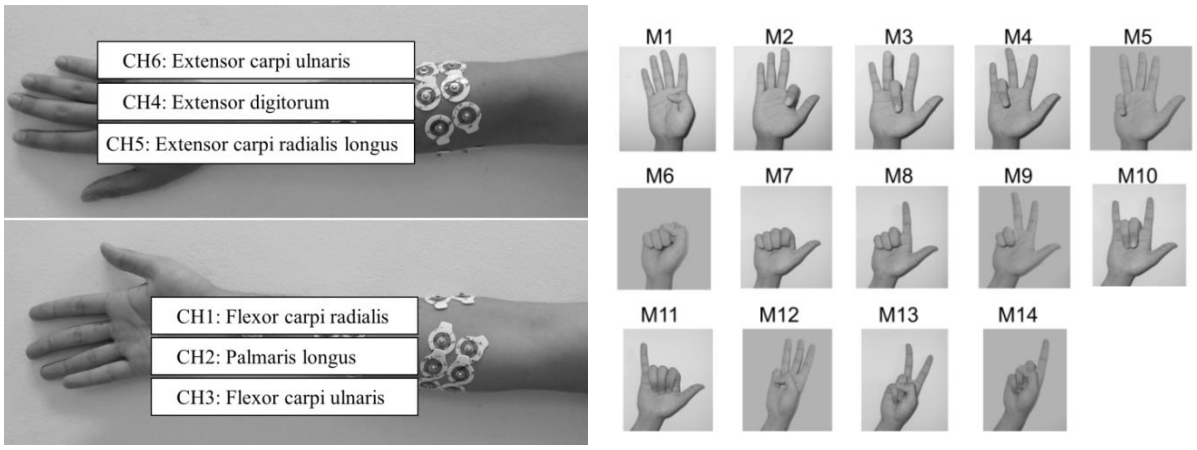

Fig. 1. Left: The electrode locations on forearm muscles. Right: The fourteen finger movements.

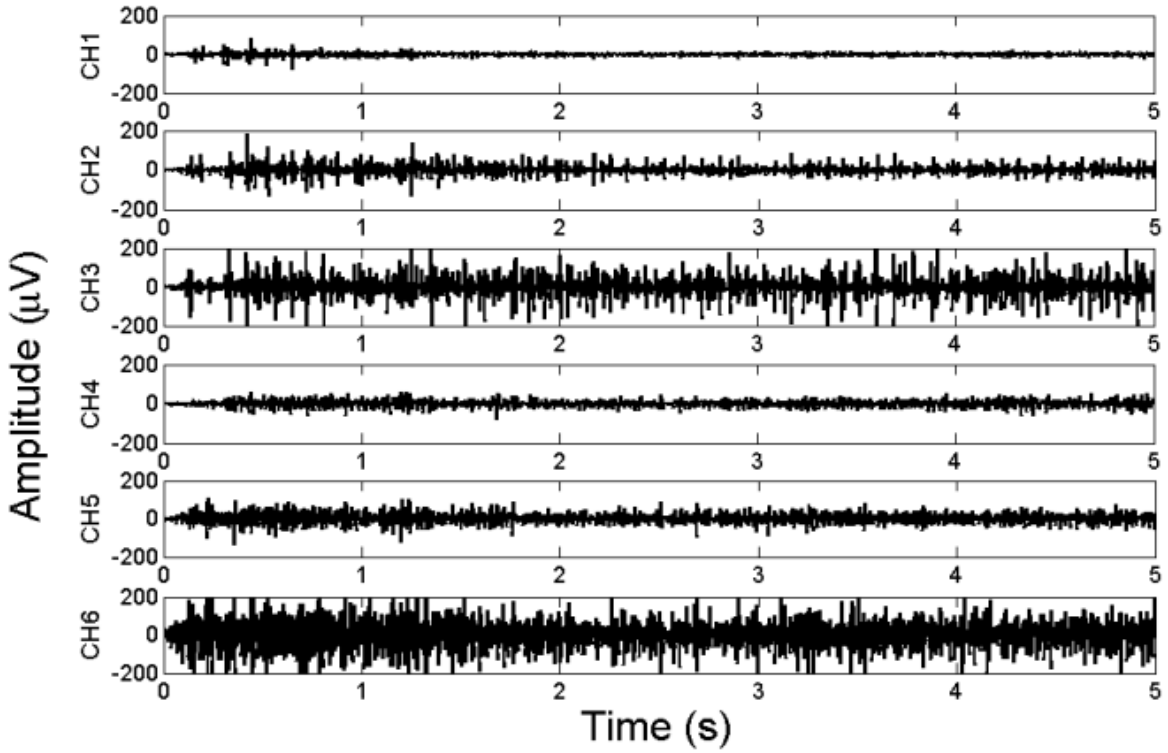

Fig. 2. Example of the 6-channel EMG signal from thumb flexion (M1).

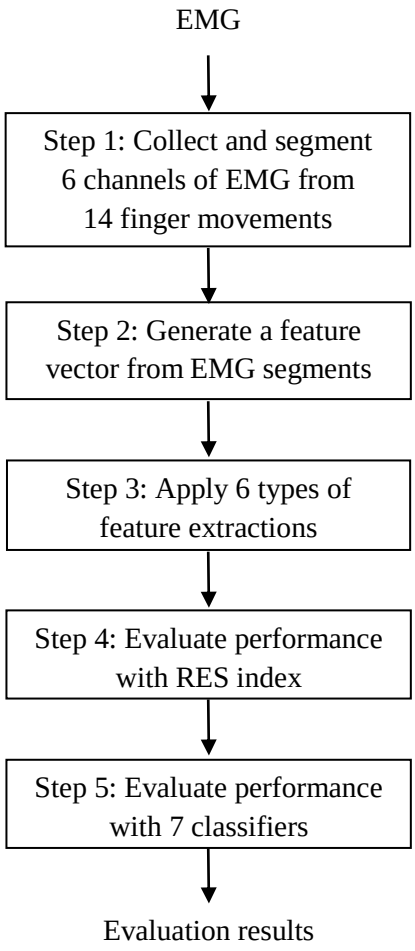

Fig. 3. EMG acquisition and analytical method.

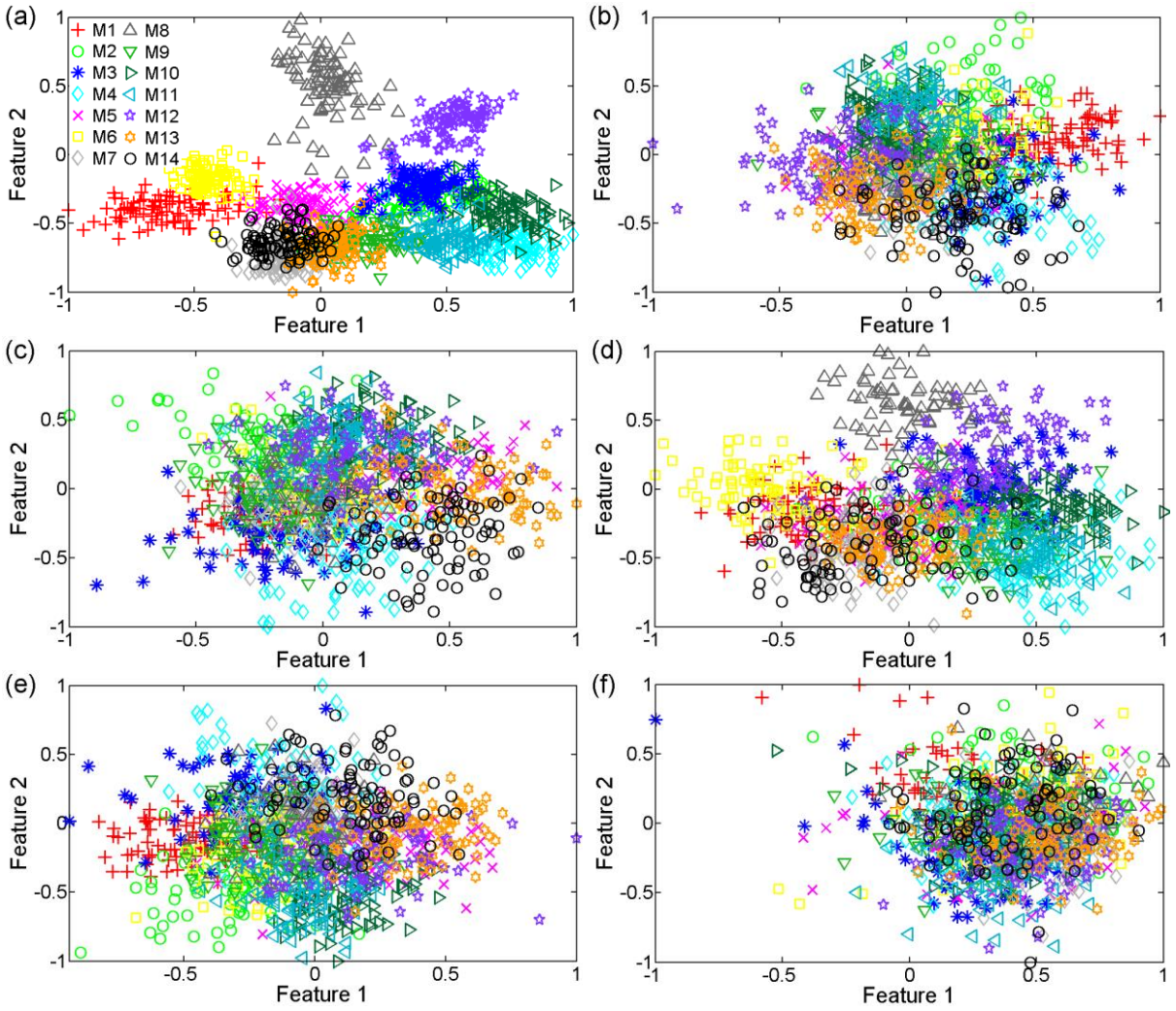

Fig. 4. Scatter plots of the first two elements of the reduced feature vectors when using (a) SRELM, (b) LDA, (c) ULDA, (d) SRDA, (e) OFNDA, and (f) PCA.

.

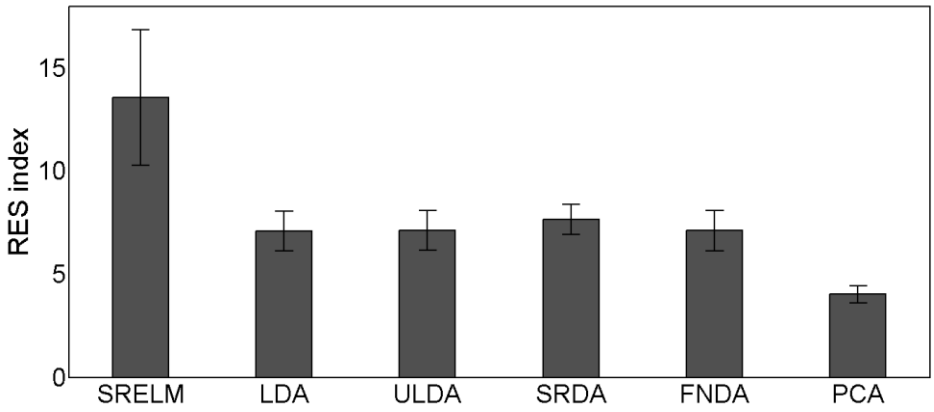

Fig. 5. RES index determined using all reduced feature vectors from 6 feature extraction techniques.

Table I Mean and standard deviation of classification accuracies for 14 movements obtained with various pairs of feature extraction (FE) and classifier.

FE	SVM	LC	NB	KNN	RBF-ELM	AW-ELM	NN
SRELM	92.92±4.35	***93.64±4.00***	90.04±4.57	***93.04±4.09***	93.24±3.88	***92.12±4.34***	***99.09±0.83***
LDA	93.30±3.91	92.42±3.69	***90.39±4.41***	92.29±4.37	93.33±4.11	91.08±4.55	95.51±2.74
ULDA	93.01±3.97	92.34±3.77	90.01±4.30	92.15±4.46	93.12±4.06	90.76±4.98	95.58±2.82
SRDA	***93.70±3.55***	92.13±3.89	89.81±4.39	93.01±3.65	***93.89±3.54***	92.07±4.17	95.12±3.08
OFNDA	93.09±3.98	92.31±3.84	90.30±4.21	92.06±4.30	93.31±3.90	90.84±4.68	95.59±2.76
PCA	83.96±6.93	83.23±6.46	72.61±7.26	79.51±7.76	81.91±8.27	75.46±7.67	85.59±6.58

Table II Mean and standard deviation of classification accuracies for 14 movements obtained from the NN classifier with three alternative sizes of the hidden layer.

FE	10 neurons	20 neurons	30 neurons
SRELM	***99.09±0.83***	***99.57±0.42***	***99.54±0.46***
LDA	95.51±2.74	96.61±2.45	96.84±2.25
ULDA	95.58±2.82	96.68±2.34	96.83±2.21
SRDA	95.12±3.08	96.37±2.33	96.49±2.40
OFNDA	95.59±2.76	96.47±2.56	96.86±2.25
PCA	85.59±6.58	87.87±6.21	88.47±6.01

Table III Mean and standard deviation (SD) of classification accuracies for 14 movements obtained from the SRELM feature extraction and the NN classifier as the number of available EMG channels is reduced step by step.

Channel combination	Mean±SD	Note
CH1-CH2-CH3-CH4-CH5-CH6	***99.57±0.52***	6 channels
CH2-CH3-CH4-CH5-CH6	***99.24±0.51***	Remove CH1
CH1-CH2-CH3-CH4-CH5	98.71±1.12	
CH1-CH2-CH3-CH4-CH6	98.90±0.90	
CH1-CH2-CH3-CH5-CH6	99.05±1.00	
CH1-CH2-CH4-CH5-CH6	98.90±1.60	
CH1-CH3-CH4-CH5-CH6	98.86±1.31	
CH2-CH3-CH5-CH6	***97.95±1.52***	Remove CH1 and CH4
CH2-CH3-CH4-CH5	97.33±1.70	
CH2-CH3-CH4-CH6	97.90±1.06	
CH2-CH4-CH5-CH6	96.95±2.24	
CH3-CH4-CH5-CH6	97.90±1.29	
CH3-CH5-CH6	***93.71±3.94***	Remove CH1, CH4, and CH2
CH2-CH3-CH5	93.38±2.68	
CH2-CH3-CH6	92.81±3.79	
CH2-CH5-CH6	92.90±3.32	
CH3-CH6	***85.38±4.55***	Remove CH1, CH4, CH2, and CH5
CH3-CH5	84.76±4.92	
CH5-CH6	80.19±5.67	
CH3	***58.95±8.49***	Remove CH1, CH4, CH2, CH5, and CH6
CH6	56.24±9.45	

Table IV Mean and standard deviation of classification accuracies for movement reduction obtained from the SRELM feature extraction and the NN classifier using the EMG signals from CH3 and CH6**.**

# movements	Mean±SD	Movement removal
14	85.38±4.55	-
13	99.08±0.68	M7
12	99.28±0.59	M7 and M13
11	99.94±0.19	M7, M13, and M6
10	100.00±0.00	M7, M13, M6, and M14

Table V Performance comparisons with other techniques from previous publications.

Ref.	#M	#Ch	Features in each EMG channel	#DF	FE	Classifiers	Acc. (%)
[8]	8	2	MAV, SGT	16	-	NN	85.10
[9]	5	2	FFT	20	-	NN	86.00
[13]	10	2	7^{th}-order AR, SSC, ZC, WL, SKW, HTD	28	LDA	SVM	≈92.00
[18]	10	2+1	6^{th}-order AR, SSC, ZC, WL, SKW, MAV, HTD	42	SRELM	AW-ELM	86.73
[A]	10	2	4^{th}-order AR, SSC, ZC, WL, SKW, MAV, MNF, KURT	22	SRELM	NN	100.00
[11]	12	32	WL	32	PCA	NN	94.30
[12]	15	6	6^{th}-order AR, RMS, WL, ZC, IEMG, SSC	66	OFNDA	LDA	98.25
[19]	11	7	IEMG, WL, VAR, ZC, SSC, WAMP	42	-	NN	93.90
[20]	15	4	4^{th}-order AR, WL, RMS	24	-	SVM	97.60
[B]	14	6	4^{th}-order AR, MAV, WL, ZC, SSC, MNF, KURT, SKW	66	SRELM	NN	99.57

#M: The number of movements, #Ch: The number of EMG channels used, #DF: The dimension of the feature vector before applying feature extraction, FE: Feature extraction, Acc: Accuracy, SGT: the spectra from Gabor transform, FFT: fast Fourier transform, HTD: Hjorth time domain, IEMG: Integrated EMG, VAR: Variance of EMG, RMS: Root mean square, [A]: The proposed method when using 2-EMG channels for classifying 10 finger movements, [B]: The proposed method when using 6-EMG channels for classifying 14 finger movements.

Sirinapa Jitaree and Pornchai Phukpattaranont, “Force classification using sEMG from various object lengths and wrist postures,” submitted for publication in *Journal of Mechanical Science and Technology* **[impact factor 1.128, Q3 in JCR® Category]**

Journal of Mechanical Science and Technology

Force classification using sEMG from various object lengths and wrist postures

--Manuscript Draft--

Manuscript Number:	
Full Title:	Force classification using sEMG from various object lengths and wrist postures
Article Type:	Original Paper
Order of Authors:	Sirinapa Jitaree, Ph.D.
	Pornchai Phukpattaranont
Keywords:	EMG signal processing; pinch; classification; prosthetic devices; SFFS; k-nearest neighbor; neural network; proportional myoelectric control
Corresponding Author:	Pornchai Phukpattaranont THAILAND
Corresponding Author Secondary Information:	
Corresponding Author's Institution:	
Corresponding Author's Secondary Institution:	
First Author:	Sirinapa Jitaree, Ph.D.
First Author Secondary Information:	
Order of Authors Secondary Information:	
Funding Information:	Thailand Research Fund and Faculty of Engineering, Prince of Songkla University (No. RSA5980049) — Dr. Sirinapa Jitaree Higher Education Research Promotion and National Research University Project of Thailand, Office of the Higher Education Commission — Assoc. Dr. Pornchai Phukpattaranont
Abstract:	Pattern recognition in myoelectric control of upper-limb prosthetic devices is important to restore functions of an amputee. In this study, we classify 5 force levels of thumb-index pinch in 3 wrist postures and 5 object lengths using the surface electromyography (sEMG), which can be applied in proportional myoelectric control. Twelve channels of sEMG from muscles in 3 regions, i.e., hand, lower forearm, and upper forearm were recorded. Twelve traditional time-domain features were determined from each sEMG segment. Then, the optimal feature subset was obtained by the sequential forward floating selection (SFFS) method. Seven classifiers consisting of linear and non-linear classifiers were compared. Results show that k-nearest neighbor can outperform other classifiers with the average classification error 1%. However, the error from the muscles in upper forearm region only is about 10%. These muscles can be used in the prosthetic design for the wrist disarticulation amputee and the transradial amputee.
Suggested Reviewers:	

Springer

KSME

Journal of Mechanical Science and Technology 00 (2010) 0000~0000

www.springerlink.com/content/1738-494x
submitted manuscript under review

Force classification using sEMG from various object lengths and wrist postures

Sirinapa Jitaree[1] and Pornchai Phukpattaranont[1]

[1] *Department of Electrical Engineering, Faculty of Engineering, Prince of Songkla University, Songkhla, 90110, Thailand*

(Manuscript Received 000 0, 2009; Revised 000 0, 2009; Accepted 000 0, 2009)

Abstract

Pattern recognition in myoelectric control of upper-limb prosthetic devices is important to restore functions of an amputee. In this study, we classify 5 force levels of thumb-index pinch in 3 wrist postures and 5 object lengths using the surface electromyography (sEMG), which can be applied in proportional myoelectric control. Twelve channels of sEMG from muscles in 3 regions, i.e., hand, lower forearm, and upper forearm were recorded. Twelve traditional time-domain features were determined from each sEMG segment. Then, the optimal feature subset was obtained by the sequential forward floating selection (SFFS) method. Seven classifiers consisting of linear and non-linear classifiers were compared. Results show that k-nearest neighbor can outperform other classifiers with the average classification error 1%. However, the error from the muscles in upper forearm region only is about 10%. These muscles can be used in the prosthetic design for the wrist disarticulation amputee and the transradial amputee.

Keywords: EMG signal processing; Pinch; Classification; Prosthetic devices; SFFS; K-nearest neighbor; Neural network; Proportional myoelectric control

1. Introduction

Recently, the loss of hand or finger is a major disability of human that limits the capabilities and interactions in daily life of a person. The myoelectric control using the residual muscles, the arm or the shoulder, is used to help amputees for improving their quality of life. The surface electromyography (sEMG) signal is widely applied to control prosthetic devices [1]. However, there are many limitations about a small fixed set of gestures. The motions cannot be freely controlled by users' intentions. Therefore, the more natural, creative and intuitive motions in hand gesture recognition should be developed. However, identifying force level and/or motions in hand gestures remains a difficult task.

Kamavuako et al. [2] studied the correlation between force profiles and single-channel intramuscular EMG (iEMG). The correlation coefficient between the iEMG and force was approximately 0.9, which was quite similar to that from the sEMG and force. He et al. [3] proposed the novel features based on discrete Fourier transform to classify 9 grasp and wrist motions under 3 muscle contraction levels (20%, 50%, and 80% of maximal voluntary contraction) with linear discriminant analysis (LDA). Results showed that the proposed features provided better classification accuracy compared to that from the traditional time-domain features because of their robust property, which can be against varying contraction levels. In [4], well-known time-domain features from sEMG, such as root mean square (RMS), mean absolute value (MAV), were used as the inputs of time-delayed artificial neural network to predict forearm muscle forces during the extension and flexion wrist movements in real time.

In [5], a novel set of features based on Fourier transform relations, the Parseval's theorem, and power spectrum moments, which was able to be against force variation, was developed. It was used to classify 6 motions including different grip and finger movements under 3 force levels (low, moderate, high). Four classifiers including LDA, Naïve Bayes (NB), random forest, and k-nearest neighbor (KNN) were compared. Results showed that the proposed set of features could improve the classification performance (6%−8%) in comparison to other methods of feature extraction and LDA gave the best performance compared to other classifiers.

Celadon et al. [6] estimated force profiles and force levels from individual finger movements (flexion and extension) using high density sEMG. RMS was used as the feature. Three methods including LDA, common spatial patterns proportional estimator (CSP-PE), and thresholding algorithm were evaluated and compared. Results showed that the performance from the CSP-PE is the best when the number of electrodes was less than 24. However, for higher resolution of the recording, the performance from CSP-PE was comparable to that from LDA.

† This paper was recommended for publication in revised form by Associate Editor 000 000-please leave blank.

*Corresponding author. Tel.: +6674287045, Fax.: +6674459395
E-mail address: pornchai.p@psu.ac.th.

Effective features are essential in pattern recognition for myoelectric control. Dimensionality reduction is usually applied when the number of channels used to record sEMG signals is large to reduce redundancy and increase relevance of the features [7-14]. Adewuyi et al. [7] studied 5 sEMG feature sets for classifying 4 hand motions in different wrist positions from 16 non-amputees and 4 partial-hand amputees. Results showed that the feature subset from LDA combined with a feature selection algorithm based on the sequential forward searching (SFS) method gave the lowest classification error. However, the main drawback of SFS method is the nesting effect [15], i.e., inability to remove the added feature.

In this paper, the sequential forward floating selection (SFFS), which is a suboptimal search strategy to solve the nesting effect [16], is applied to select the optimal feature subset for classification of 5 force levels. Twelve channels of sEMG signals from the muscles in 3 upper-limb regions including region of hand (RH), region of lower forearm (RLF) and region of upper forearm (RUF), were recorded from thumb-index pinch with 3 wrist postures, 5 length objects, and 5 force levels. The classification errors from the muscles in RH, RLF, and RUF would be evaluated and compared so that the muscles can be appropriately chosen and used.

2. Materials and Methods

2.1 EMG data acquisition

Twelve channels of sEMG signals were recorded from 3 regions on the right arm including RH, RLF and RUF as shown in Fig. 1. The list of related muscles in each region is shown in Table 1. The muscles in RH, RLF, and RUF are shown in Fig. 2, Fig. 3, and Fig. 4, respectively. Details of muscles in each region are as follows.

RH: The sEMG data from 3 muscles in RH consisting of the adductor pollicis (AP), the abductor pollicis brevis (APB), and the first dorsal interosseous (FDI) were collected from bipolar Ag/AgCl electrodes (EL254S, BIOPAC) at an inter-electrode distance 10 mm.

RLF: The sEMG data from 2 muscles in RLF including the flexor pollicis longus (FPL) and the extensor pollicis longus (EPL) were recorded using bipolar Ag/AgCl electrodes (H124SG, Kendel ARBO) at an inter-electrode distance 20 mm.

RUF: Seven pair of electrodes were placed in RUF without specific muscle positions at approximately one third of the forearm length from the head of the ulna. The type and configuration of electrodes used were the same as in RLF. The distances between adjacent electrodes (d) were approximately equal. For each subject, d was calculated from the distance around the forearm circumference divided by seven. The first pair of electrode was placed at a distance of $d/2$ from the ulnar.

Table 1. List of related muscles in each region.

Regions	Channels	Muscles
RH	3	AP, APB, FDI (c1-c3)
RLF	2	FPL, EPL (c4-c5)
RUF	7	ECU, EDC, EDM, ECRL, ECRB, BR, FCR, PL, FDS, FCU, FDP (c6-c12)

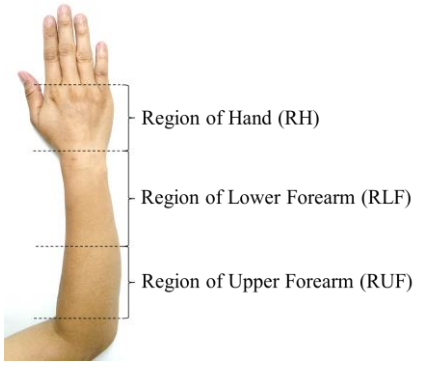

Fig. 1. Three regions of the forearm used in sEMG data acquisition.

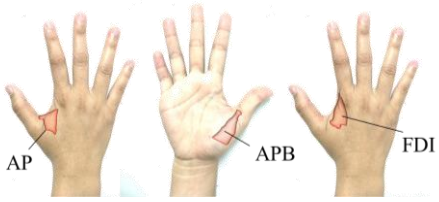

Fig. 2. Three muscles in RH including the AP (left), the APB (Middle), and the FDI (right).

Fig. 3. Two muscles in RLF including the FPL (left) and the EPL (right).

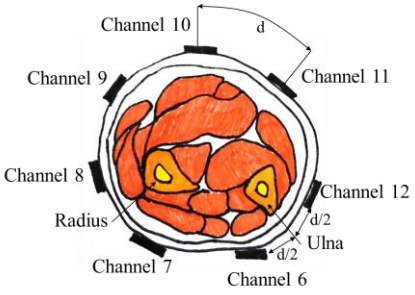

Fig. 4. Cross-section of the RUF indicating approximate electrode locations.

All sEMG data were acquired by a commercial measurement system (MP150, BIOPAC system). A band-pass filter of 10 Hz to 500 Hz and an amplifier gain of 1000 times were set. The sEMG data were sampled at a rate of 1000 Hz. Force data were measured using a force sensor (KISTLER 9017B) and recorded synchronously with sEMG data by the BIOPAC MP150 acquisition system with a sample rate of 1000 Hz.

Ten healthy subjects (6 males and 4 females) participated in this study. Mean and standard deviation of subjects' age were 29.9 ± 6.9 years. They were asked to maintain 5 object lengths (i.e., 45, 60, 75, 90, and 105 mm as shown in Fig. 5) with thumb-index pinch at 3 wrist postures (i.e., flexion, neutral, and extension as shown in Fig. 6). For each length and each wrist posture, they performed 5 levels of contraction force: 10, 30, 50, 70, and 100% of maximal pinch force. The order of posture combinations was randomized. The sEMG from each contraction was recorded for an 8 s duration and repeated 3 times. For each subject, a total of 225 data sets were collected (3 wrist postures × 5 object lengths × 5 force levels × 3 trials).

In experiment, the subjects seated in a chair with the elbow flexed at 90° and the lower forearm resting in the horizontal plane (i.e., rest state). They were asked to pinch force from the rest state to the specific force level (which produces an sEMG ramp period), and then maintained the force with static contraction for 4 s in duration (which produces an sEMG steady-state period), and released the force (which also produces an sEMG ramp period) to the rest state. The sEMG signals in the steady-state period from time 3 s to 5 s were further used in force classification. Figure 7 shows an example of the sEMG signals obtained from the AP muscle (c1) with the wrist flexion posture used in force classification.

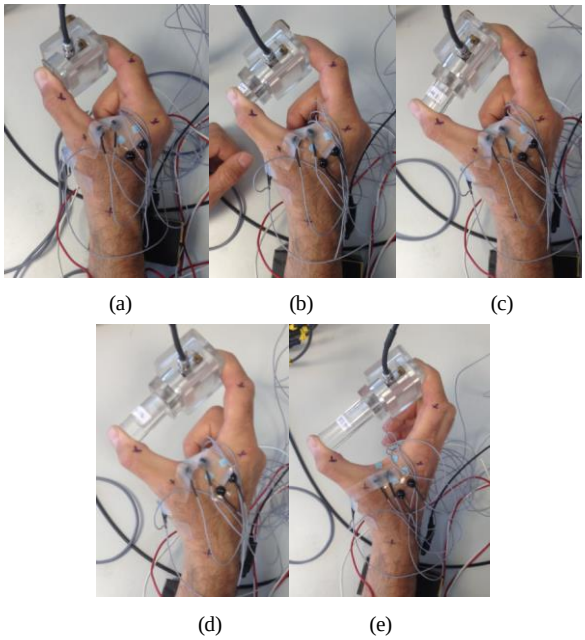

Fig. 5. Thumb-index pinch on the boxes with 5 lengths (a) 45 mm (b) 60 mm (c) 75 mm (d) 90 mm (e) 105 mm.

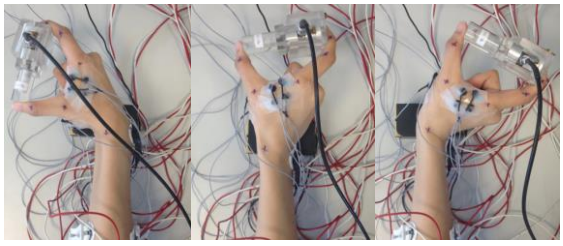

Fig. 6. Thumb-index pinch at 3 wrist postures, flexion (left), neutral (middle), and extension (right).

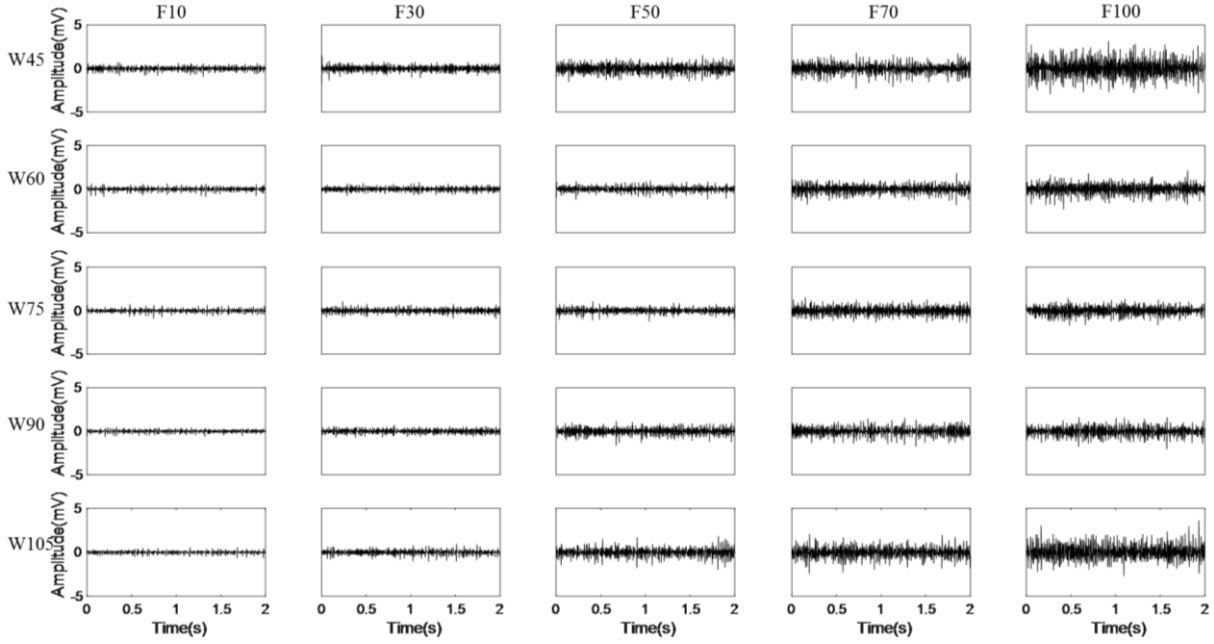

Fig. 7. Example of the sEMG signals from the AP muscles (c1) with wrist flexion posture in 5 force levels (column) and 5 object lengths (row).

2.2 Methods

Figure 8 shows the proposed method for force classification from thumb-index pinch using sEMG consisting of 3 stages, i.e., (1) Preprocessing, (2) Feature selection, (3) Classification. The details on each analytical stage are as follows.

1) Preprocessing

There are 4 main steps in preprocessing. The first step is noise removal using a notch filter. Then, the filtered sEMG with the length of 2 s (3-5 s) is segmented using the 256 ms analysis window with 50% overlap [17]. As a result, fourteen sEMG segments are obtained for each sEMG channel. Next, in the feature calculation step, twelve frequently used time-domain features described in Table 2 are determined from each sEMG segment. In total, the feature vector with dimension 144 (12 features per channel × 12 channels) is obtained for each force level of each subject. Finally, the values from each channel and feature pair in all force levels are normalized so that their values are in the range of -1 to 1.

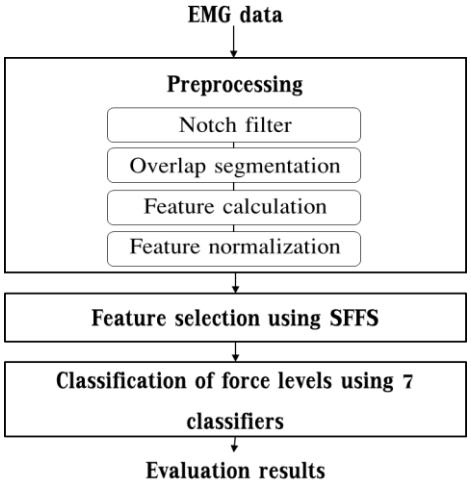

Fig. 8. Method for force classification from thumb-index pinch using sEMG.

Table 2. List of time domain features used in this study.

Feature name	**Equation**	**Feature name**	**Equation**
f1: Difference Absolute Standard Deviation Value (DASDV)	$\mathrm{DASDV}=\sqrt{\frac{1}{N-1}\sum_{n=1}^{N-1}\left(x_{n+1}-x_n\right)^2}$	f7: Root Mean Square (RMS)	$\mathrm{RMS}=\sqrt{\frac{1}{N}\sum_{n=1}^{N}x_n^2}$
f2: Log Detector (LOG)	$\mathrm{LOG}=e^{\frac{1}{N}\sum_{n=1}^{N}\log\left(\lvert x_n\rvert\right)}$	f8: Third Temporal Moment (TM3)	$\mathrm{TM3}=\left\lvert\frac{1}{N}\sum_{n=1}^{N}x_n^3\right\rvert$
f3: Modified MAV 1 (MAV1)	$\mathrm{MAV1}=\frac{1}{N}\sum_{n=1}^{N}w_n\lvert x_n\rvert$, $w_n=\begin{cases}1, & \text{if } 0.25N\le n\le 0.75N\\ 0.5, & \text{otherwise}\end{cases}$	f9: Forth Temporal Moment (TM4)	$\mathrm{TM4}=\left\lvert\frac{1}{N}\sum_{n=1}^{N}x_n^4\right\rvert$
f4: Modified MAV 2 (MAV2)	$\mathrm{MAV2}=\frac{1}{N}\sum_{n=1}^{N}w_n\lvert x_n\rvert$, $w_n=\begin{cases}1, & \text{if } 0.25\mathrm{N}\le n\le 0.75N\\ 4n/N, & \text{elseif } \mathrm{n}<0.25N\\ 4(n-N)/N, & \text{otherwise}\end{cases}$	f10: Fifth Temporal Moment (TM5)	$\mathrm{TM5}=\left\lvert\frac{1}{N}\sum_{n=1}^{N}x_n^5\right\rvert$
		f11: Variance (VAR)	$\mathrm{VAR}=\frac{1}{N-1}\sum_{n=1}^{N}x_n^2$
f5: Mean Absolute Value (MAV)	$\mathrm{MAV}=\frac{1}{N}\sum_{n=1}^{N}\lvert x_n\rvert$	f12: Waveform Length (WL)	$\mathrm{WL}=\sum_{n=1}^{N-1}\lvert x_{n+1}-x_n\rvert$
f6: Maximum Fractal Length (MFL) [18]	$\mathrm{MFL}=\frac{\left\{\left(\sum_{n=1}^{\left[\frac{N-m}{k}\right]}\lvert x(m+nk)-x(m+(n-1).k)\rvert\right)\frac{N-1}{\left[\frac{N-m}{k}\right].k}\right\}}{k}$, $(m=1,2,...,k)$		
where N denotes the window length, x_n is the nth EMG sample within current window. In MFL, k = 128 and m integers represent time interval and in itial time, respectively.			

2) Feature selection

To reduce the computational complexity and processing time, a smaller dimension of features can be obtained by feature selection techniques. Given a set of feature *Y*, the method will select a smaller subset of feature *X* that performs the best performance for the criterion function, *J*(*X*). Normally, a subset $X \subseteq Y$ can be found by

$$J(Y) = \max_{X \subseteq Y, |X| = f} J(X), \tag{1}$$

where *f* is the desired number of selected features. However, the exhaustive search is exponential and impractical for even moderate values of *Y* [19]. In this study, the feature selection using the correlation forward selection based on SFFS method is used. The SFFS proposed by Pudil et al [16] is defined by floating up and down during the search. It starts from the empty set that evaluates all possible single-feature expansions of the current subset.

The SFFS was applied to select the optimal feature subset from each feature vector for force classification. To find the optimum distance for SFFS, six criteria were tested including (1) inter-intra distance (inin), (2) sum of estimated Mahalanobis distances (mahas), (3) minimum of estimated Mahalanobis distances (maham), (4) sum of squared Euclidean distances (eucls), (5) minimum of squared Euclidean distances (euclm), and (6) 1-nearest neighbor. Figure 9 shows an example of normalized distances as a function of feature subset dimension. Results show that 1-nearest neighbor is able to reach the maximum distance at the feature dimension of 10, which is faster than other criteria. Therefore, the feature subset obtained from 1-nearest neighbor is used as the input of classifiers in the next stage.

3) Classification

In this study, seven classifiers, namely DT, LDA, quadratic discriminant analysis (QDA), SVM, KNN, NB, and NN were tested and compared. For each subject, the cross-validation was applied for the performance evaluation of each classifier. The 10-fold cross validation was used. In other words, data were divided into 10 subsets. In each round, one of them was testing data, while others were training data. In total, ten classification errors were obtained with different subsets of testing data. The performance from each classifier was measured by means and standard deviation of classification errors from 10 subjects. Brief descriptions and the parameters used for each classifier are described as follows.

a. DT classifier is based on hierarchy. Its model is constructed in the form of tree structure including node, branch and leaf. Nodes are the features, branches are the possible outcome of the test, and leaves are the class labels. The DT structure is constructed based on a top-down technique by starting with selection of the best feature to be a root node and then picking branches to the leaves at each step [20]. In this study, the splitting criterion was defined as purity and pruning was not used.

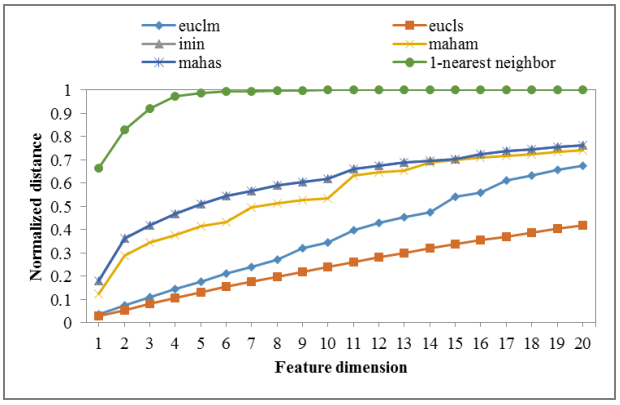

Fig. 9. Example of normalized distances as a function of feature subset dimension.

b. LDA classifier is a linear and binary supervised algorithm that considers a probability distribution between two classes to assign the class of unknown data. In multi-class classification problem, a one versus all approach is applied to this binary classifier. The aim of LDA is to solve the following problem:

$$y = \omega^T x + \omega_0. \tag{2}$$

Vector *x* is the feature vector. Vectors ω and ω_0 are identified by spreading interclass means and reducing interclass variance [21]. In this study, LDA was computed without regularization. Because of no manually specified internal parameters in this classifier, the trial-and-error approach using cross-validation of training set was applied.

c. QDA produces a quadratic line for separation of two classes based on their Gaussian densities with unequal variances [22]. The purpose is to calculate the decision boundary as denoted in:

$$y = x^T \omega x + \omega^T x + \omega_0. \tag{3}$$

Parameter tuning of QDA in this study was the same as LDA.

d. SVM is a supervised algorithm proposed by Vapnik [23]. The general concept of SVM is to operate a discriminant hyper-plane to separate the classes of data set, especially in non-linearly separable problems [24]. It aims to find the optimal hyper-plane that maximizes the margins between the data set. In this study, the radial basis function was selected as the kernel function because the feature dimension was not large. The cost parameter was 1.0 and the kernel parameter (γ) was $1/n$ (*n* is the dimension of feature vector from SFFS). Moreover, multiple SVM was set for multi-class problem using one-against-rest approach.

e. KNN classifier known as the lazy learning algorithm is simple and efficient in machine learning [25]. Its process starts with calculations of distances between testing data and training data. The distance values among the test sample to other

samples would be measured by various methods such as Euclidean distance and Minkowski distance. Then, they are sorted in descending order and the class of testing data is designated by the majority vote among the k largest distances. The selecting of k value is very important. If k is too small, the algorithm is sensitive to noise. On the other hand, if it is too large, the nearest neighbor may include points from other classes. In this study, the Euclidean distance was used and the number of the nearest neighbors, k, was optimized based on the leave-one-out error on dataset.

f. NB classifier is a simple probabilistic classifier based on Bayes rule. It aims to reach the best hypothesis through a given training data set. Bayes theorem provides a way to calculate the probability of a hypothesis based on its prior probability of both the data found and the total data [26]. The main advantage of this classifier is that it only needs mean and standard deviation of the features to estimate the parameters for classification. In this study, the number of bins 49 was used to find the class based maximum posterior probability.

g. NN classifier is a common nonlinear classifier that is the multilayer perceptron learning a mapping between inputs and outputs. In this study, the architecture of NN was the feed-forward network consisting of one input layer, one hidden layer and one output layer. The number of neurons in the input layer is same as the number of features selected by SFFS, whereas the number of neurons in the output layer is equal to the number of classes, which is 5 force levels. The number of neurons in the hidden layer under this study is 10, 20, and 30. The training algorithm was the Levenberg-Marquardt. A hyperbolic tangent sigmoid function was used as the transfer function in all layers. The maximum error during the training was defined as 0.02/m (m is the size of training data).

3. Results

3.1 Feature selection

Figure 10 (Top) shows the average and standard deviation of probability of feature selection in percent by SFFS accumulated from 10 subjects. The most frequently selected features are f1 (DASDV) and f6 (MFL) at approximately 16%. On the other hand, f10 (TM5) is the least frequently chosen feature (1.9%). The average and standard deviation of probability of the selected channels in percent are shown in Fig. 10 (Bottom). Two most frequently selected channels are c3 in RH and c12 in RUF, whereas the EPL muscle (c5) in RLF is scanty in selection.

Table 3 shows the number of selections in each feature and channel pair accumulated from 10 subjects. The f1c1 and f1c4 are the highest frequently selected pairs (5 subjects). On the other hand, while the 3 lowest frequently selected features are f4, f9, and f10 (the number of selections $\leq$ 5), the 5 lowest frequently selected channels are c5, c8, c9, c10, and c11 (the number of selections $\leq$ 15). These results agree with the average and standard deviation of probability of feature selection and channel selection shown in Fig. 10.

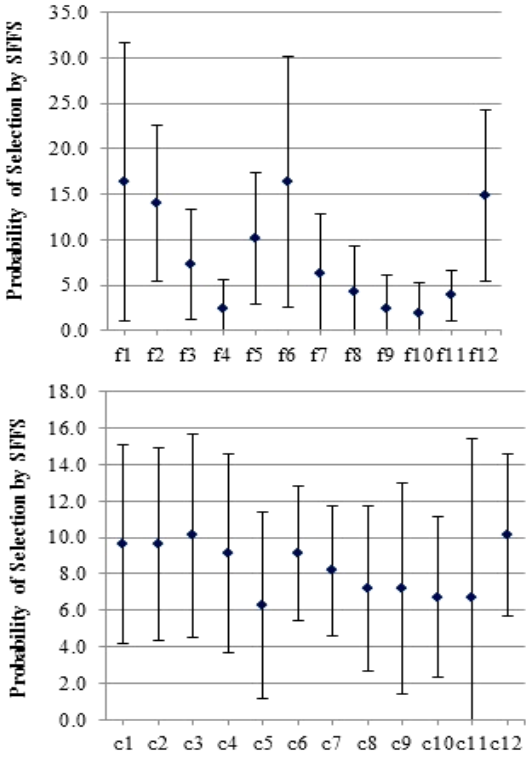

Fig. 10. Probability of selection in percent by SFFS accumulated from 10 subjects. (Top) Features. (Bottom) Channels.

Table 3. The number of selections in each feature and channel pair accumulated from 10 subjects.

Channel	*f1*	f2	f3	f4	f5	*f6*	f7	f8	f9	f10	f11	f12	Sum
c1	*5*	2	0	1	1	4	1	0	2	1	1	2	20
c2	4	2	2	1	2	4	2	1	1	0	0	1	20
c3	1	4	3	0	3	4	0	0	0	0	4	2	*21*
c4	*5*	*4*	2	0	1	2	1	2	0	1	0	1	19
c5	2	2	1	1	1	3	0	0	0	0	0	3	13
c6	3	2	0	1	2	3	1	1	0	1	2	3	19
c7	3	3	1	0	1	2	2	2	0	0	0	3	17
c8	1	2	2	0	1	3	1	0	1	0	0	4	15
c9	2	2	1	1	2	2	1	2	0	0	0	2	15
c10	2	3	0	0	3	2	1	0	0	0	1	2	14
c11	2	1	1	0	2	1	2	1	0	0	0	4	14
c12	4	2	2	0	2	4	1	0	1	1	0	4	*21*
Sum	*34*	29	15	5	21	*34*	13	9	5	4	8	31	208

Table 4 and Table 5 show the number of selected features and the number of selected channels from each subject, respectively. While the features selected in all subjects are f1 and f6, the channels selected in all subjects are c2, c6, and c12. Subject 2 is the only one who does not have selected channels in RFL. Subject 9 and subject 10 have the maximum (44 pairs) and minimum (6 pairs) number of feature and channel pairs selected by SFFS, respectively.

3.2 Classification

Figure 11 shows the classification errors averaged from 10 subjects from all feature inputs (dark) compared with those from SFFS feature inputs (gray). The errors from the all feature inputs are comparable to those from the SFFS feature inputs in all classifiers except for LDA and SVM. The errors from DT, LDA, QDA, and NB classifiers are greater than 10%. In SVM, the classification error from the SFFS inputs reaches 13%, which is almost 3 times greater than the errors from all feature inputs. The KNN classifier gives the best performance at 0.8% for all feature inputs and 0.2% for SFFS feature inputs. NN classifiers perform better when the number of neurons in the hidden layer increases from 10, to 20 and 30 at the expense of computational complexity. The errors from NN-30 with all and SFFS feature inputs are 2.5% and 3%, respectively. These results indicate that the feature set selected from SFFS can be used as the inputs of KNN and NN classifiers for classification of force levels.

Figure 12 shows the classification errors categorized by 5 muscle regions when the SFFS features are used as the inputs of LDA, KNN, and NN-30. While KNN and NN-30 are used in comparisons because they give high classification performance, LDA is chosen because it is widely used in previous studies of sEMG classification. Results show that the minimum errors are obtained when all muscle regions are used. The errors increase when only some muscle regions are used. For example, in KNN classifier, the error from RLF+RUF (c4-c12) increases to 6.9% compared to that from RH+RLF+RUF (c1-c12), which is only 0.2%. Moreover, when considering only a single muscle region, RUF gives better performance than the others.

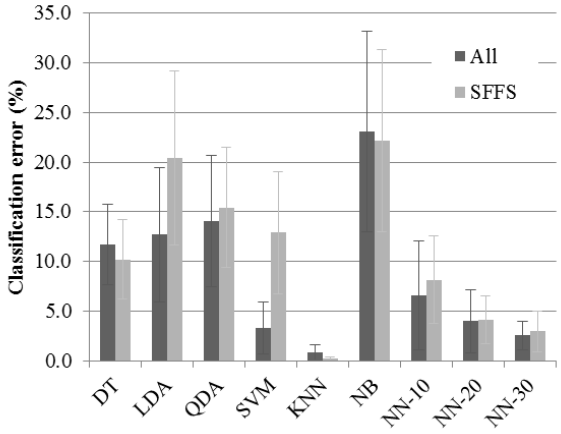

Fig. 11. Classification errors averaged from 10 subjects from all feature inputs (dark) compared with those from SFFS feature inputs (gray).

Table 4. The number of selected features from each subject.

Subject	f1	f2	f3	f4	f5	f6	f7	f8	f9	f10	f11	f12	Sum
sj1	3	4	4	2	4	1	1	1	0	0	1	0	21
sj2	1	2	1	0	1	1	2	0	0	0	0	2	10
sj3	4	2	0	0	0	3	0	0	0	0	0	2	11
sj4	3	7	2	2	2	5	4	2	2	1	1	6	37
sj5	4	1	1	0	2	2	2	3	0	0	1	3	19
sj6	7	1	1	0	2	3	0	0	0	0	0	0	14
sj7	1	5	0	0	2	6	1	0	0	0	1	2	18
sj8	1	2	1	0	0	6	0	1	3	3	2	9	28
sj9	8	5	5	1	8	4	3	2	0	0	2	6	44
sj10	2	0	0	0	0	3	0	0	0	0	0	1	6
Sum	34	29	15	5	21	34	13	9	5	4	8	31	208

Table 5. The number of selected channels from each subject.

Subject	c1	c2	c3	c4	c5	c6	c7	c8	c9	c10	c11	c12	Sum
sj1	0	4	2	2	2	1	2	3	2	1	0	2	21
sj2	1	1	0	0	0	1	1	1	1	0	3	1	10
sj3	1	1	1	0	1	1	1	1	2	1	0	1	11
sj4	5	3	1	3	2	2	3	3	5	3	3	4	37
sj5	1	3	2	2	1	2	2	0	1	1	1	3	19
sj6	1	2	1	1	0	2	1	1	0	2	1	2	14
sj7	1	1	3	1	2	2	1	1	1	1	1	3	18
sj8	5	3	4	4	1	2	1	1	1	1	2	3	28
sj9	4	1	6	6	3	5	5	4	2	4	3	1	44
sj10	1	1	1	0	1	1	0	0	0	0	0	1	6
Sum	20	20	21	19	13	19	17	15	15	14	14	21	208

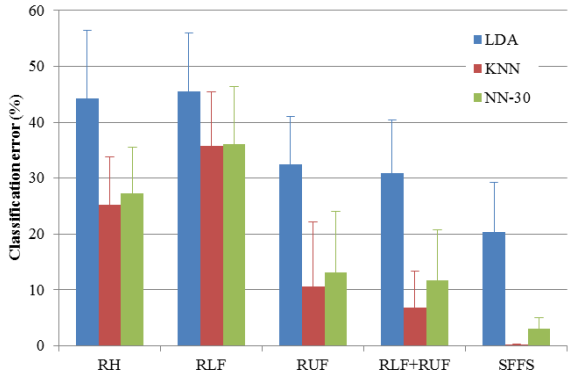

Fig. 12. Classification errors categorized by 5 muscle regions when the SFFS features are used as the inputs of LDA, KNN, and NN-30.

4. Discussion

Results from SFFS indicate that some features and channels are not necessary for force classification. The features f1, f6, and f12, which are DASDV, MFL, and WL, respectively, are useful for classifying force levels. They would be applied to the real-time EMG recognition system as a single feature. Instead of using RMS [6], [27] or MAV [28], which is used as the single feature in previous studies, the use of one among 3 features, i.e., DASDV, MFL, and WL, may provide better accuracy.

In channel selection, the muscles in RH are more important than other groups because they are directly responsible for thumb-index pinch, especially the AP muscle (c1) [29]. In RLF, the FPL muscle (c4) is more important than the EPL muscle (c5) causing from the adduction effect [29]. Although there is no specific muscle position in RUF, the electrode placements of c9 and c10 could be removed. However, c12 in RUF is the most frequently selected channel meaning that it should be included in the prosthetic design applications.

As shown in Fig. 12, when comparing classification errors among 3 muscle regions, i.e. RH, RLF, and RUF, results indicate that the muscles in RUF provide lower errors than the muscles in other regions. Although the muscles in RLF were usually found in sEMG classifications of finger movements in previous studies [5], [22], [30], [31], they gave the highest errors in this study. However, when using the muscles in RLF combined with the muscles in RUF, the classification errors slightly decrease. Therefore, the muscles in RLF and RUF are helpful for prosthetic design applications, especially in the wrist disarticulation amputee and the transradial amputee.

5. Conclusions

This paper presents the selection of sEMG channels and features for the classification of force levels in thumb-index pinch, which can be applied in proportional myoelectric control. The sEMG data were recorded from 3 muscle regions (12 channels) of 10 non-amputee subjects when they performed 5 force levels of thumb-index pinch with 3 wrist positions (flexion, neutral, extension) and 5 object lengths (45, 60, 75, 90, 105 mm). Twelve traditional time-domain features were extracted. The SFFS was applied for searching the best subset of channels and features that yielded the lowest classification error. Each force level signal was trained and classified using 7 classifiers including DT, LDA, QDA, SVM, NB, KNN, and NN. Results show that KNN and NN can give higher performance than others. The group of muscles and feature set selected by SFFS method can perform to comparable the set of all muscle channels and features. Three features consisting of DASDV, MFL, and WL are primarily selected in the classification. The most frequently selected group of muscles is RH, especially the AP muscle. However, the combination of RLF and RUF can perform high performance. This is helpful for prosthetic design applications, especially in the wrist disarticulation amputee and transradial amputee.

Acknowledgment

This work was jointly funded by the Thailand Research Fund and Faculty of Engineering, Prince of Songkla University through Contract No. RSA5980049, in part by the Higher Education Research Promotion and National Research University Project of Thailand, Office of the Higher Education Commission. We are very grateful to Dr. Sirinee Thongpanja for supplying us with the sEMG dataset.

References

[1] P. Geethanjali, Myoelectric control of prosthetic hands: state-of-the-art review, *Med. Devices (Auckl)*, 9 (2016) 247–255.
[2] K. E. Kamavuako et al., Relationship between grasping force and features of single-channel intramuscular EMG signals, *J. Neurosci. Methods*, 185 (2009) 143–150.
[3] J. He et al., Invariant surface EMG feature against varying contraction level for myoelectric control based on muscle coordination, *IEEE J. Biomed. Health Inform.* 19 (3) (2015) 874–882.
[4] E. Kilic, EMG based neural network and admittance control of an active wrist orthosis, *J. Mech. Sci. Technol.* 31 (12) (2017) 6093–6106.
[5] A. H. Al-Timemy et al., Improving the performance against force variation of EMG controlled multifunctional upper-limb prostheses for transradial amputees, *IEEE Trans. Neural Syst. Rehabil. Eng.* 24 (6) (2016) 650–661.
[6] N. Celadon et al., Proportional estimation of finger movements from high-density surface electromyography, *J. Neuroengineering Rehabil.* 13 (2016) 73.
[7] A. A. Adewuyi, L. J. Hargrove, T. A. Kuiken, Evaluating EMG feature and classifier selection for application to partial-hand prosthesis control, *Front. Neurorobot.* 19 (2016) 10–15.
[8] G. R. Naik, A. H. Al-Timemy, and H. T. Nguyen, Transradial amputee gesture classification using an optimal number of sEMG sensors: an approach using ICA clustering, *IEEE Trans. Neural Syst. Rehabil. Eng.* 24 (8) (2016) 837–846.
[9] H. Huang et al., Ant colony optimization-based feature selection method for surface electromyography signals classification, *Comput. Biol. Med.* 42 (2012) 30–38.
[10] I. Mesa et al., Channel and feature selection for a surface

electromyographic pattern recognition task, *Expert Syst. Appl.* 41 (11) (2014) 5190–5200.
[11] R. N. Khushaba et al., A framework of temporal-spatial descriptors-based feature extraction for improved myoelectric pattern recognition, *IEEE Trans. Neural Syst. Rehabil. Eng.* 25 (10) (2017) 1821–1831.
[12] J. Liu, Feature dimensionality reduction for myoelectric pattern recognition: a comparison study of feature selection and feature projection methods, *Med. Eng. Phys.* 36 (12) (2014) 1716–1720.
[13] M. A. Oskoei and H. Hu, Support vector machine-based classification scheme for myoelectric control applied to upper limb, *IEEE Trans. Biomed. Eng.* 55 (8) (2008) 1956–1965.
[14] Y. Na et al., Ranking hand movements for myoelectric pattern recognition considering forearm muscle structure, *Med. Biol. Eng. Comput.* 55 (8) (2017) 1507–1518.
[15] S. Theodoridis and K. Koutroumbas, *Pattern Recognition (Third Edition), Academic Press*, London, UK, (2006).
[16] P. Pudil, J. Novovičová, and J. Kittler, Floating search methods in feature selection, *Pattern Recogn. Lett.* 15 (11) (1994) 1119–1125.
[17] M. A. Oskoei and H. Hu, Myoelectric control systems–A survey, *Biomed. Signal Process. Control*, 2 (4) (2007) 275–294.
[18] S. P. Arjunan and D. K. Kumar, Decoding subtle forearm flexions using fractal features of surface electromyogram from single and multiple sensors, *J. NeuroEngineering Rehabil.* 7 (2010) 53.
[19] A. K. Jain, R. P. W. Duin, and J. Mao, Statistical pattern recognition: a review, *IEEE Trans. Pattern Anal. Mach. Intell.* 22 (2000) 4–37.
[20] L. Rokach and O. Maimon, Top-down induction of decision trees classifiers - a survey, *IEEE Trans. Syst. Man Cybern. Part C Appl. Rev.* 35 (4) (2005) 476–487.
[21] ¨O. Aydemir and T. Kayikcioglu, Investigation of the most appropriate mother wavelet for characterizing imaginary EEG signals used in BCI systems, *Turk. J. Elec. Eng. & Comp. Sci.* 24 (2016) 38–49.
[22] C. Altin and O. Er, Designing wearable joystick and performance comparison of EMG classification methods for thumb finger gestures of joystick control, *Biomed. Res.* 28 (11) (2017) 4730–4736.
[23] V. N. Vapnik, *Statistical Learning Theory, John Wiley & Sons*, New York, USA, (1998).
[24] R. Mccue, A comparison of the accuracy of support vector machine and Naïve Bayes algorithms in spam classification, *University of California at Santa Cruz Nov, CA*, (2009).
[25] T. Cover and P. Hart, Nearest neighbor pattern classification, *IEEE Trans. Inf. Theory*, 13 (1967) 21–27.
[26] C. Borgelt, H. Timm, and R. Kruse, Probalistic networks and fuzzy clustering as generalizations of Naive Bayes classifiers, *Computational Intelligence in Theory and Practice (Advances in Soft Computing), Bernd Reusch and Karl-Heinz Temme, eds.* Heidelberg, Germany (2001) 121–138.
[27] Z. Tang, H. Yu, and S. Cang, Impact of load variation on joint angle estimation from surface EMG signals, *IEEE Trans. Neural Syst. Rehabil. Eng.* 24 (12) (2016) 1342–1350.
[28] C. Choi et al., Real-time pinch force estimation by surface electromyography using an artificial neural network, *Med. Eng. Phys.* 32 (5) (2010) 429–436.
[29] S. K. Lee and J. R. Wisser, Restoration of pinch in intrinsic muscles of the hand, *Hand Clinics*, 28 (1) (2012) 45–51.
[30] F. Riillo et al., Optimization of EMG-based hand gesture recognition: Supervised vs. unsupervised data preprocessing on healthy subjects and transradial amputees, *Biomed. Signal Process. Control*, 14 (2014) 117–125.
[31] N. Malešević et al., Vector autoregressive hierarchical hidden Markov models for extracting finger movements using multichannel surface EMG signals, *Complexity*, 1 (2018) 1–12.

Sirinapa Jitaree received the B.Eng. degree in Biomedical Engineering in 2011, and the Ph.D. degree in Department of Electrical Engineering in 2016. Both degrees are from Prince of Songkla University, Thailand. She is recently a postdoctoral fellowship of Electrical Engineering at Prince of Songkla University. Her research interests include breast cancer microscopic image, texture analysis, image analysis and pattern recognition.

Pornchai Phukpattaranont received the B.Eng. (Hons.) and M.Eng. degrees in electrical engineering from the Prince of Songkla University, Songkhla, Thailand, in 1993 and 1997, respectively, and the Ph.D. degree in electrical and computer engineering from the University of Minnesota, Minneapolis, MN, USA, in 2004.

He is currently an Associate Professor of Electrical Engineering with the Prince of Songkla University. Examples of his ongoing research include the pattern recognition system based on electromyographic signal, electrocardiographic signal, and microscopic images of breast cancer cells. His current research interests include signal and image analysis for medical applications and ultrasound signal processing.

Dr. Phukpattaranont is a member of the ECTI Association and Thai Biomedical Engineering Research Societies.